NOAA Technical Report NESDIS 142-5

Regional Climate Trends and Scenarios for the U.S. National Climate Assessment

Part 5. Climate of the Southwest U.S.

Washington, D.C.
January 2013

U.S. DEPARTMENT OF COMMERCE
National Oceanic and Atmospheric Administration
National Environmental Satellite, Data, and Information Service

NOAA TECHNICAL REPORTS

National Environmental Satellite, Data, and Information Service

The National Environmental Satellite, Data, and Information Service (NESDIS) manages the Nation's civil Earth-observing satellite systems, as well as global national data bases for meteorology, oceanography, geophysics, and solar-terrestrial sciences. From these sources, it develops and disseminates environmental data and information products critical to the protection of life and property, national defense, the national economy, energy development and distribution, global food supplies, and the development of natural resources.

Publication in the NOAA Technical Report series does not preclude later publication in scientific journals in expanded or modified form. The NESDIS series of NOAA Technical Reports is a continuation of the former NESS and EDIS series of NOAA Technical Reports and the NESC and EDS series of Environmental Science Services Administration (ESSA) Technical Reports.

Copies of earlier reports may be available by contacting NESDIS Chief of Staff, NOAA/ NESDIS, 1335 East-West Highway, SSMC1, Silver Spring, MD 20910, (301) 713-3578.

NOAA Technical Report NESDIS 142-5

Regional Climate Trends and Scenarios for the U.S. National Climate Assessment

Part 5. Climate of the Southwest U.S.

Kenneth E. Kunkel, Laura E. Stevens, Scott E. Stevens, and Liqiang Sun
Cooperative Institute for Climate and Satellites (CICS), North Carolina State University and NOAA's National Climatic Data Center (NCDC)
Asheville, NC

Emily Janssen and Donald Wuebbles
University of Illinois at Urbana-Champaign
Champaign, IL

Kelly T. Redmond
Western Regional Climate Center, Desert Research Institute
Reno, NV

J. Greg Dobson
National Environmental Modeling and Analysis Center
University of North Carolina at Asheville
Asheville, NC

U.S. DEPARTMENT OF COMMERCE
Rebecca Blank, Acting Secretary

National Oceanic and Atmospheric Administration
Dr. Jane Lubchenco, Under Secretary of Commerce for Oceans and Atmosphere and NOAA Administrator

National Environmental Satellite, Data, and Information Service
Mary Kicza, Assistant Administrator

PREFACE

This document is one of series of regional climate descriptions designed to provide input that can be used in the development of the National Climate Assessment (NCA). As part of a sustained assessment approach, it is intended that these documents will be updated as new and well-vetted model results are available and as new climate scenario needs become clear. It is also hoped that these documents (and associated data and resources) are of direct benefit to decision makers and communities seeking to use this information in developing adaptation plans.

There are nine reports in this series, one each for eight regions defined by the NCA, and one for the contiguous U.S. The eight NCA regions are the Northeast, Southeast, Midwest, Great Plains, Northwest, Southwest, Alaska, and Hawai‘i/Pacific Islands.

These documents include a description of the observed historical climate conditions for each region and a set of climate scenarios as plausible futures – these components are described in more detail below.

While the datasets and simulations in these regional climate documents are not, by themselves, new, (they have been previously published in various sources), these documents represent a more complete and targeted synthesis of historical and plausible future climate conditions around the specific regions of the NCA.

There are two components of these descriptions. One component is a description of the historical climate conditions in the region. The other component is a description of the climate conditions associated with two future pathways of greenhouse gas emissions.

Historical Climate

The description of the historical climate conditions was based on an analysis of core climate data (the data sources are available and described in each document). However, to help understand, prioritize, and describe the importance and significance of different climate conditions, additional input was derived from climate experts in each region, some of whom are authors on these reports. In particular, input was sought from the NOAA Regional Climate Centers and from the American Association of State Climatologists. The historical climate conditions are meant to provide a perspective on what has been happening in each region and what types of extreme events have historically been noteworthy, to provide a context for assessment of future impacts.

Future Scenarios

The future climate scenarios are intended to provide an internally consistent set of climate conditions that can serve as inputs to analyses of potential impacts of climate change. The scenarios are not intended as projections as there are no established probabilities for their future realization. They simply represent an internally consistent climate picture using certain assumptions about the future pathway of greenhouse gas emissions. By “consistent” we mean that the relationships among different climate variables and the spatial patterns of these variables are derived directly from the same set of climate model simulations and are therefore physically plausible.

These future climate scenarios are based on well-established sources of information. No new climate model simulations or downscaled data sets were produced for use in these regional climate reports.

The use of the climate scenario information should take into account the following considerations:

1. All of the maps of climate variables contain information related to statistical significance of changes and model agreement. This information is crucial to appropriate application of the information. Three types of conditions are illustrated in these maps:
    a. The first condition is where most or all of the models simulate statistically significant changes and agree on the direction (whether increasing or decreasing) of the change. If this condition is present, then analyses of future impacts and vulnerabilities can more confidently incorporate this direction of change. It should be noted that the models may still produce a significant range of magnitude associated with the change, so the manner of incorporating these results into decision models will still depend to a large degree on the risk tolerance of the impacted system.
    b. The second condition is where the most or all of the models simulate changes that are too small to be statistically significant. If this condition is present, then assessment of impacts should be conducted on the basis that the future conditions could represent a small change from present or could be similar to current conditions and that the normal year-to-year fluctuations in climate dominate over any underlying long-term changes.
    c. The third condition is where most or all of the models simulate statistically significant changes but do not agree on the direction of the change, i.e. a sizeable fraction of the models simulate increases while another sizeable fraction simulate decreases. If this condition is present, there is little basis for a definitive assessment of impacts, and, separate assessments of potential impacts under an increasing scenario and under a decreasing scenario would be most prudent.
2. The range of conditions produced in climate model simulations is quite large. Several figures and tables provide quantification for this range. Impacts assessments should consider not only the mean changes, but also the range of these changes.
3. Several graphics compare historical observed mean temperature and total precipitation with model simulations for the same historical period. These should be examined since they provide one basis for assessing confidence in the model simulated future changes in climate.
    a. Temperature Changes: Magnitude. In most regions, the model simulations of the past century simulate the magnitude of change in temperature from observations; the southeast region being an exception where the lack of century-scale observed warming is not simulated in any model.
    b. Temperature Changes: Rate. The *rate* of warming over the last 40 years is well simulated in all regions.
    c. Precipitation Changes: Magnitude. Model simulations of precipitation generally simulate the overall observed trend but the observed decade-to-decade variations are greater than the model observations.

In general, for impacts assessments, this information suggests that the model simulations of temperature conditions for these scenarios are likely reliable, but users of precipitation simulations may want to consider the likelihood of decadal-scale variations larger than simulated by the models. It should also be noted that accompanying these documents will be a web-based resource with downloadable graphics, metadata about each, and more information and links to the datasets and overall descriptions of the process.

1. INTRODUCTION

The Global Change Research Act of 1990[1] mandated that national assessments of climate change be prepared not less frequently than every four years. The last national assessment was published in 2009 (Karl et al. 2009). To meet the requirements of the act, the Third National Climate Assessment (NCA) report is now being prepared. The National Climate Assessment Development and Advisory Committee (NCADAC), a federal advisory committee established in the spring of 2011, will produce the report. The NCADAC Scenarios Working Group (SWG) developed a set of specifications with regard to scenarios to provide a uniform framework for the chapter authors of the NCA report.

This climate document was prepared to provide a resource for authors of the Third National Climate Assessment report, pertinent to the states of California, Nevada, Utah, Arizona, Colorado, and New Mexico; hereafter referred to collectively as the Southwest. The specifications of the NCADAC SWG, along with anticipated needs for historical information, guided the choices of information included in this description of Southwest climate. While guided by these specifications, the material herein is solely the responsibility of the authors and usage of this material is at the discretion of the 2013 NCA report authors.

This document has two main sections: one on historical conditions and trends, and the other on future conditions as simulated by climate models. The historical section concentrates on temperature and precipitation, primarily based on analyses of data from the National Weather Service's (NWS) Cooperative Observer Network, which has been in operation since the late 19th century. Additional climate features are discussed based on the availability of information. The future simulations section is exclusively focused on temperature and precipitation.

With regard to the future, the NCADAC, at its May 20, 2011 meeting, decided that scenarios should be prepared to provide an overall context for assessment of impacts, adaptation, and mitigation, and to coordinate any additional modeling used in synthesizing or analyzing the literature. Scenario information for climate, sea-level change, changes in other environmental factors (such as land cover), and changes in socioeconomic conditions (such as population growth and migration) have been prepared. This document provides an overall description of the climate information.

In order to complete this document in time for use by the NCA report authors, it was necessary to restrict its scope in the following ways. Firstly, this document does not include a comprehensive description of all climate aspects of relevance and interest to a national assessment. We restricted our discussion to climate conditions for which data were readily available. Secondly, the choice of climate model simulations was also restricted to readily available sources. Lastly, the document does not provide a comprehensive analysis of climate model performance for historical climate conditions, although a few selected analyses are included.

The NCADAC directed the "use of simulations forced by the A2 emissions scenario as the primary basis for the high climate future and by the B1 emissions scenario as the primary basis for the low climate future for the 2013 report" for climate scenarios. These emissions scenarios were generated by the Intergovernmental Panel on Climate Change (IPCC) and are described in the IPCC Special Report on Emissions Scenarios (SRES) (IPCC 2000). These scenarios were selected because they

[1] http://thomas.loc.gov/cgi-bin/bdquery/z?d101:SN00169:|TOM:/bss/d101query.html

incorporate much of the range of potential future human impacts on the climate system and because there is a large body of literature that uses climate and other scenarios based on them to evaluate potential impacts and adaptation options. These scenarios represent different narrative storylines about possible future social, economic, technological, and demographic developments. These SRES scenarios have internally consistent relationships that were used to describe future pathways of greenhouse gas emissions. The A2 scenario "describes a very heterogeneous world. The underlying theme is self-reliance and preservation of local identities. Fertility patterns across regions converge very slowly, which results in continuously increasing global population. Economic development is primarily regionally oriented and per capita economic growth and technological change are more fragmented and slower than in the other storylines" (IPCC 2000). The B1 scenario describes "a convergent world with…global population that peaks in mid-century and declines thereafter…but with rapid changes in economic structures toward a service and information economy, with reductions in material intensity, and the introduction of clean and resource-efficient technologies. The emphasis is on global solutions to economic, social, and environmental sustainability, including improved equity, but without additional climate initiatives" (IPCC 2000).

The temporal changes of emissions under these two scenarios are illustrated in Fig. 1 (left panel). Emissions under the A2 scenario continually rise during the 21st century from about 40 gigatons (Gt) CO_2-equivalent per year in the year 2000 to about 140 Gt CO_2-equivalent per year by 2100. By contrast, under the B1 scenario, emissions rise from about 40 Gt CO_2-equivalent per year in the year 2000 to a maximum of slightly more than 50 Gt CO_2-equivalent per year by mid-century, then falling to less than 30 Gt CO_2-equivalent per year by 2100. Under both scenarios, CO_2 concentrations rise throughout the 21st century. However, under the A2 scenario, there is an acceleration in concentration trends, and by 2100 the estimated concentration is above 800 ppm. Under the B1 scenario, the rate of increase gradually slows and concentrations level off at about 500 ppm by 2100. An increase of 1 ppm is equivalent to about 8 Gt of CO_2. The increase in concentration is considerably smaller than the rate of emissions because a sizeable fraction of the emitted CO_2 is absorbed by the oceans.

The projected CO_2 concentrations are used to estimate the effects on the earth's radiative energy budget, and this is the key forcing input used in global climate model simulations of the future. These simulations provide the primary source of information about how the future climate could evolve in response to the changing composition of the earth's atmosphere. A large number of modeling groups performed simulations of the 21st century in support of the IPCC's Fourth Assessment Report (AR4), using these two scenarios. The associated changes in global mean temperature by the year 2100 (relative to the average temperature during the late 20th century) are about +6.5°F (3.6°C) under the A2 scenario and +3.2°F (1.8°C) under the B1 scenario with considerable variations among models (Fig. 1, right panel).

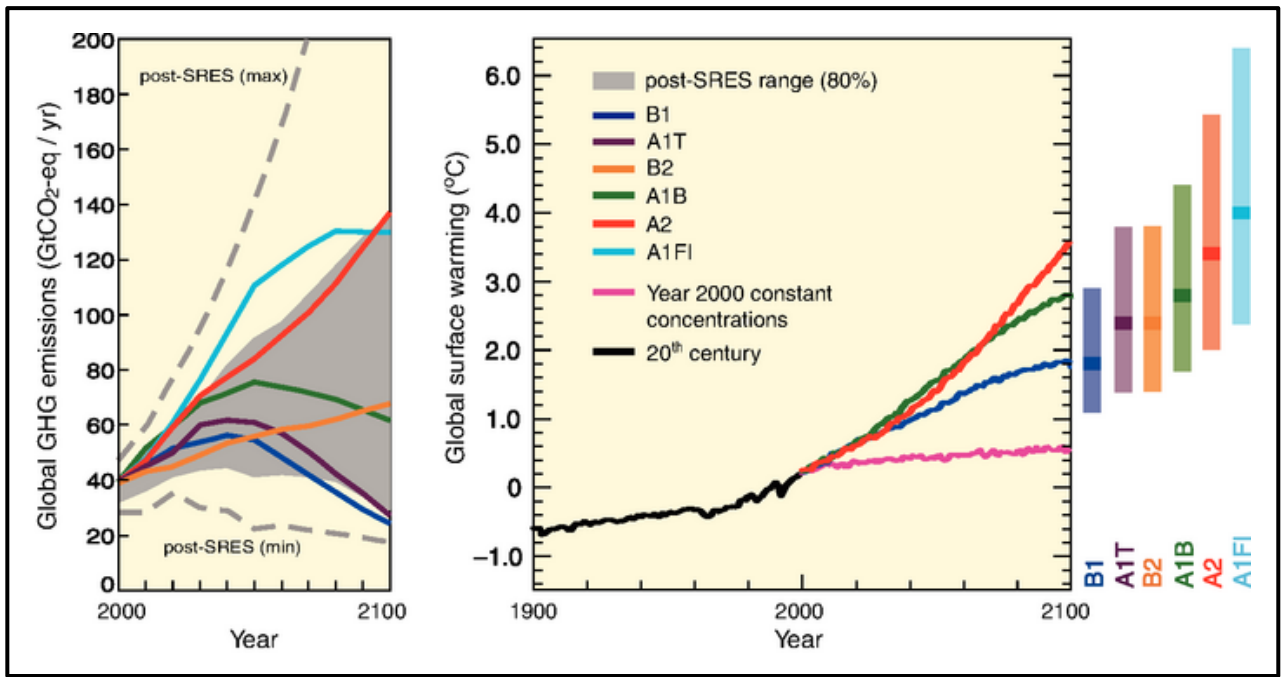

Figure 1. Left Panel: Global GHG emissions (in $GtCO_2$-eq) in the absence of climate policies: six illustrative SRES marker scenarios (colored lines) and the 80th percentile range of recent scenarios published since SRES (post-SRES) (gray shaded area). Dashed lines show the full range of post-SRES scenarios. The emissions include CO_2, CH_4, N_2O and F-gases. Right Panel: Solid lines are multi-model global averages of surface warming for scenarios A2, A1B and B1, shown as continuations of the 20th-century simulations. These projections also take into account emissions of short-lived GHGs and aerosols. The pink line is not a scenario, but is for Atmosphere-Ocean General Circulation Model (AOGCM) simulations where atmospheric concentrations are held constant at year 2000 values. The bars at the right of the figure indicate the best estimate (solid line within each bar) and the likely range assessed for the six SRES marker scenarios at 2090-2099. All temperatures are relative to the period 1980-1999. From IPCC AR4, Sections 3.1 and 3.2, Figures 3.1 and 3.2, IPCC (2007).

In addition to the direct output of the global climate model simulations, the NCADAC approved "the use of both statistically- and dynamically-downscaled data sets". "Downscaling" refers to the process of producing higher-resolution simulations of climate from the low-resolution outputs of the global models. The motivation for use of these types of data sets is the spatial resolution of global climate models. While the spatial resolution of available global climate model simulations varies widely, many models have resolutions in the range of 100-200 km (~60-120 miles). Such scales are very large compared to local and regional features important to many applications. For example, at these scales mountain ranges are not resolved sufficiently to provide a reasonably accurate representation of the sharp gradients in temperature, precipitation, and wind that typically exist in these areas.

Statistical downscaling achieves higher-resolution simulations through the development of statistical relationships between large-scale atmospheric features that are well-resolved by global models and the local climate conditions that are not well-resolved. The statistical relationships are developed by comparing observed local climate data with model simulations of the recent historical climate. These relationships are then applied to the simulations of the future to obtain local high-

resolution projections. Statistical downscaling approaches are relatively economical from a computational perspective, and thus they can be easily applied to many global climate model simulations. One underlying assumption is that the relationships between large-scale features and local climate conditions in the present climate will not change in the future (Wilby and Wigley 1997). Careful consideration must also be given when deciding how to choose the appropriate predictors because statistical downscaling is extremely sensitive to the choice of predictors (Norton et al. 2011).

Dynamical downscaling is much more computationally intensive but avoids assumptions about constant relationships between present and future. Dynamical downscaling uses a climate model, similar in most respects to the global climate models. However, the climate model is run at a much higher resolution but only for a small region of the earth (such as North America) and is termed a "regional climate model (RCM)". A global climate model simulation is needed to provide the boundary conditions (e.g., temperature, wind, pressure, and humidity) on the lateral boundaries of the region. Typically, the spatial resolution of an RCM is 3 or more times higher than the global model used to provide the boundary conditions. With this higher resolution, topographic features and smaller-scale weather phenomena are better represented. The major downside of dynamical downscaling is that a simulation for a region can take as much computer time as a global climate model simulation for the entire globe. As a result, the availability of such simulations is limited, both in terms of global models used for boundary conditions and time periods of the simulations (Hayhoe 2010).

Section 3 of this document (Future Regional Climate Scenarios) responds to the NCADAC directives by incorporating analyses from multiple sources. The core source is the set of global climate model simulations performed for the IPCC AR4, also referred to as the Climate Model Intercomparison Project phase 3 (CMIP3) suite. These have undergone extensive evaluation and analysis by many research groups. A second source is a set of statistically-downscaled data sets based on the CMIP3 simulations. A third source is a set of dynamically-downscaled simulations, driven by CMIP3 models. A new set of global climate model simulations is being generated for the IPCC Fifth Assessment Report (AR5). This new set of simulations is referred to as the Climate Model Intercomparison Project phase 5 (CMIP5). These scenarios do not incorporate any CMIP5 simulations as relatively few were available at the time the data analyses were initiated.
As noted earlier, the information included in this document is primarily concentrated around analyses of temperature and precipitation. This is explicitly the case for the future scenarios sections; due in large part to the short time frame and limited resources, we capitalized on the work of other groups on future climate simulations, and these groups have devoted a greater effort to the analysis of temperature and precipitation than other surface climate variables.

Climate models have generally exhibited a high level of ability to simulate the large-scale circulation patterns of the atmosphere. These include the seasonal progression of the position of the jet stream and associated storm tracks, the overall patterns of temperature and precipitation, the occasional occurrence of droughts and extreme temperature events, and the influence of geography on climatic patterns. There are also important processes that are less successfully simulated by models, as noted by the following selected examples.

Climate model simulation of clouds is problematic. Probably the greatest uncertainty in model simulations arises from clouds and their interactions with radiative energy fluxes (Dufresne and Bony 2008). Uncertainties related to clouds are largely responsible for the substantial range of

global temperature change in response to specified greenhouse gas forcing (Randall et al. 2007). Climate model simulation of precipitation shows considerable sensitivities to cloud parameterization schemes (Arakawa 2004). Cloud parameterizations remain inadequate in current GCMs. Consequently, climate models have large biases in simulating precipitation, particularly in the tropics. Models typically simulate too much light precipitation and too little heavy precipitation in both the tropics and middle latitudes, creating potential biases when studying extreme events (Bader et al. 2008).

Climate models also have biases in simulation of some important climate modes of variability. The El Niño-Southern Oscillation (ENSO) is a prominent example. In some parts of the U.S., El Niño and La Niña events make important contributions to year-to-year variations in conditions. Climate models have difficulty capturing the correct phase locking between the annual cycle and ENSO (AchutaRao and Sperber 2002). Some climate models also fail to represent the spatial and temporal structure of the El Niño - La Niña asymmetry (Monahan and Dai 2004). Climate simulations over the U.S. are affected adversely by these deficiencies in ENSO simulations.

The model biases listed above add additional layers of uncertainty to the information presented herein and should be kept in mind when using the climate information in this document.

The representation of the results of the suite of climate model simulations has been a subject of active discussion in the scientific literature. In many recent assessments, including AR4, the results of climate model simulations have been shown as multi-model mean maps (e.g., Figs. 10.8 and 10.9 in Meehl et al. 2007). Such maps give equal weight to all models, which is thought to better represent the present-day climate than any single model (Overland et al. 2011). However, models do not represent the current climate with equal fidelity. Knutti (2010) raises several issues about the multi-model mean approach. These include: (a) some model parameterizations may be tuned to observations, which reduces the spread of the results and may lead to underestimation of the true uncertainty; (b) many models share code and expertise and thus are not independent, leading to a reduction in the true number of independent simulations of the future climate; (c) all models have some processes that are not accurately simulated, and thus a greater number of models does not necessarily lead to a better projection of the future; and (d) there is no consensus on how to define a metric of model fidelity, and this is likely to depend on the application. Despite these issues, there is no clear superior alternative to the multi-model mean map presentation for general use. Tebaldi et al. (2011) propose a method for incorporating information about model variability and consensus. This method is adopted here where data availability make it possible. In this method, multi-model mean values at a grid point are put into one of three categories: (1) models agree on the statistical significance of changes and the sign of the changes; (2) models agree that the changes are not statistically significant; and (3) models agree that the changes are statistically significant but disagree on the sign of the changes. The details on specifying the categories are included in Section 3.

2. REGIONAL CLIMATE TRENDS AND IMPORTANT CLIMATE FACTORS

2.1. Description of Data Sources

One of the core data sets used in the United States for climate analysis is the National Weather Service's Cooperative Observer Network (COOP), which has been in operation since the late 19th century. The resulting data can be used to examine long-term trends. The typical COOP observer takes daily observations of various climate elements that might include precipitation, maximum temperature, minimum temperature, snowfall, and snow depth. While most observers are volunteers, standard equipment is provided by the National Weather Service (NWS), as well as training in standard observational practices. Diligent efforts are made by the NWS to find replacement volunteers when needed to ensure the continuity of stations whenever possible. Over a thousand of these stations have been in operation continuously for many decades (NOAA 2012a).

For examination of U.S. long-term trends in temperature and precipitation, COOP data is the best available resource. Its central purpose is climate description (although it has many other applications as well); the number of stations is large, there have been relatively few changes in instrumentation and procedures, and it has been in existence for over 100 years. However, there are some sources of temporal inhomogeneities in station records, described as follows:

- One instrumental change is important. For much of the COOP history, the standard temperature system was a pair of liquid-in-glass (LIG) thermometers placed in a radiation shield known as the Cotton Region Shelter (CRS). In the 1980s, the NWS began replacing this system with an electronic maximum-minimum temperature system (MMTS). Inter-comparison experiments indicated that there is a systematic difference between these two instrument systems, with the newer electronic system recording lower daily maximum temperatures (T_{max}) and higher daily minimum temperatures (T_{min}) (Quayle et al. 1991; Hubbard and Lin 2006; Menne et al. 2009). Menne et al. (2009) estimate that the mean shift (going from CRS/LIG to MMTS) is -0.52K for T_{max} and +0.37K for T_{min}. Adjustments for these differences can be applied to monthly mean temperature to create homogeneous time series.
- Changes in the characteristics and/or locations of sites can introduce artificial shifts or trends in the data. In the COOP network, a station is generally not given a new name or identifier unless it moves at least 5 miles and/or changes elevation by at least 100 feet (NWS 1993). Site characteristics can change over time and affect a station's record, even if no move is involved (and even small moves << 5 miles can have substantial impacts). A common source of such changes is urbanization around the station, which will generally cause artificial warming, primarily in T_{min} (Karl et al. 1988), the magnitude of which can be several degrees in the largest urban areas. Most research suggests that the overall effect on national and global temperature trends is rather small because of the large number of rural stations included in such analyses (Karl et al. 1988; Jones et al. 1990) and because homogenization procedures reduce the urban signal (Menne et al. 2009).
- Station siting can cause biases. Recent research by Menne et al. (2010) and Fall et al. (2011) examined this issue in great detail. The effects on mean trends was found to be small in both studies, but Fall et al. (2011) found that stations with poor siting overestimate (underestimate) minimum (maximum) temperature trends.

- Changes in the time that observations are taken can also introduce artificial shifts or trends in the data (Karl et al. 1986; Vose et al. 2003). In the COOP network, typical observation times are early morning or late afternoon, near the usual times of the daily minimum and maximum temperatures. Because observations occur near the times of the daily extremes, a change in observation time can have a measurable effect on averages, irrespective of real changes. The study by Karl et al. (1986) indicates that the difference in monthly mean temperatures between early morning and late afternoon observers can be in excess of 2°C. There has, in fact, been a major shift from a preponderance of afternoon observers in the early and middle part of the 20th century to a preponderance of morning observers at the present time. In the 1930s, nearly 80% of the COOP stations were afternoon observers (Karl et al. 1986). By the early 2000s, the number of early morning observers was more than double the number of late afternoon observers (Menne et al. 2009). This shift tends to introduce an artificial cooling trend in the data.

A recent study by Williams et al. (2011) found that correction of known and estimated inhomogeneities lead to a larger warming trend in average temperature, principally arising from correction of the biases introduced by the changeover to the MMTS and from the biases introduced by the shift from mostly afternoon observers to mostly morning observers.

Much of the following analysis on temperature, precipitation, and snow is based on COOP data. For some of these analyses, a subset of COOP stations with long periods of record was used, specifically less than 10% missing data for the period of 1895-2011. The use of a consistent network is important when examining trends in order to minimize artificial shifts arising from a changing mix of stations.

2.2. General Description of Southwest Climate

The Southwest region is highly varied topographically with mountain ranges and coastlines having substantial impacts on climate conditions. There are large horizontal variations in climate in some areas caused by elevation differences and by the blockage of air masses by mountain ranges. The region straddles mid and subtropical latitudes. Far western parts of the region have a Mediterranean-like climate, which is characteristic of northern subtropical latitudes on the western sides of continents. Such climates have cool and wet winters and warm to hot, dry summers. The interior, southern, low elevation parts of the region are the hottest and driest locations in the U.S., a result of persistent subtropical high pressure. During the winter, the mid-latitude storm track is often located over the region, resulting in frequent storm systems that bring precipitation to the region. The Pacific coastal ranges and the Sierra Nevada typically receive very large amounts of cold season precipitation by virtue of their position as the first mountain ranges in the path of Pacific storms. Interior ranges generally receive smaller but considerable amounts of precipitation that are essential as a source of water for the region. A notable feature of the climate of the interior Southwest is a summer peak in precipitation caused by a continental-scale shift in wind flow known as the North American Monsoon. This feature is most prominent in Arizona and New Mexico; in some areas half of the annual precipitation falls in July and August as a result of this phenomenon.

The average annual temperature (Fig. 2) varies widely across the region, partly as a result of latitudinal variations, but mostly because of elevation differences. The average annual temperature is greater than 70°F in southwestern Arizona and southeastern California and is greater than 60°F

over a swath ranging from central California to southeastern New Mexico. By contrast, the average annual temperature is less than 50°F across the northern portions of the region from northeastern California to northeastern Colorado. At the highest mountain locations, the average temperature is less than 40°F. The total range across the region exceeds 40°F, leading to very large variations in ecosystem types. Average annual precipitation at these spatial scales varies widely (Fig. 3) from less than 5 inches in the lower Colorado River valley to more than 60 inches along the northwestern California coast. Amounts range locally from less than 2 inches in Death Valley, CA, to over 100 inches near Crescent City CA. Large local spatial gradients arise from the large variations in topography. In general, winter is the wettest time of year. Even though the region contains the driest locations in North America, water is the main agent of geomorphic change in the most arid landscapes.

A large fraction of the water available in the region falls as snow. Agriculture relies heavily on irrigation (about 80-85 percent of all water used), mostly supplied by snowmelt. Another agricultural sector, ranching, relies on natural precipitation. This region includes California, the single most productive agricultural state in the United States.

The reliability of high mountain snowfall has led to an abundance of ski resorts, many of them world-class. The Southwest is a tourism mecca, many attracted by the climate. Major urban centers in the region, ranked in the top 30 by population (U.S. Census Bureau 2011), include Los Angeles (rank #2), San Francisco (#11), Riverside (#12), Phoenix (#14), San Diego (#17), Denver (#21), Sacramento (#25), and Las Vegas (#30). These urban centers are in arid settings and depend on non-local water. Among major U.S. cities, Las Vegas and Phoenix have the hottest summertime climate. Air pollution is a major challenge in several cities, most notably in Los Angeles, where the combination of blocking mountains and persistent summertime high pressure leads to ideal conditions for adverse air quality. Some interior cities experience adverse air quality in the winter when high pressure aloft traps cold air near the surface.

The region‘s relatively benign winter climate has led to a large migration of population from northern and eastern regions of the United States, a trend expected to continue.

Human health and safety are affected by climate conditions, although the number of hazards is less than in other regions. Some of the principal hazards are temperature extremes, lightning, flash floods, wind events, and snow storms.

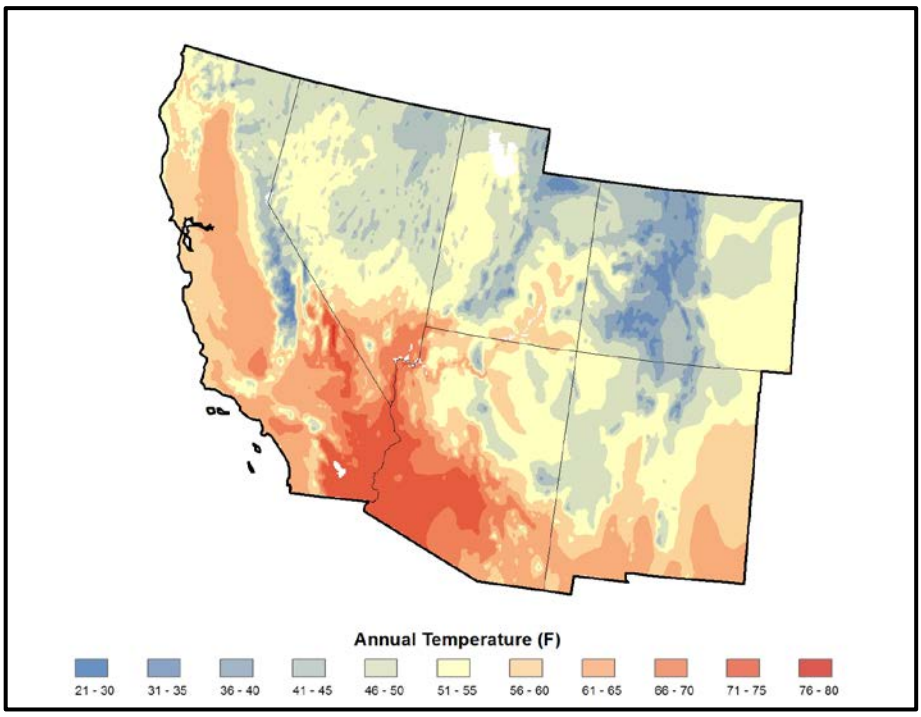

Figure 2. Average (1981-2010) annual temperature (°F) for the Southwest region. Based on a new gridded version of COOP data from the National Climatic Data Center, the CDDv2 data set (R. Vose, personal communication, July 27, 2012).

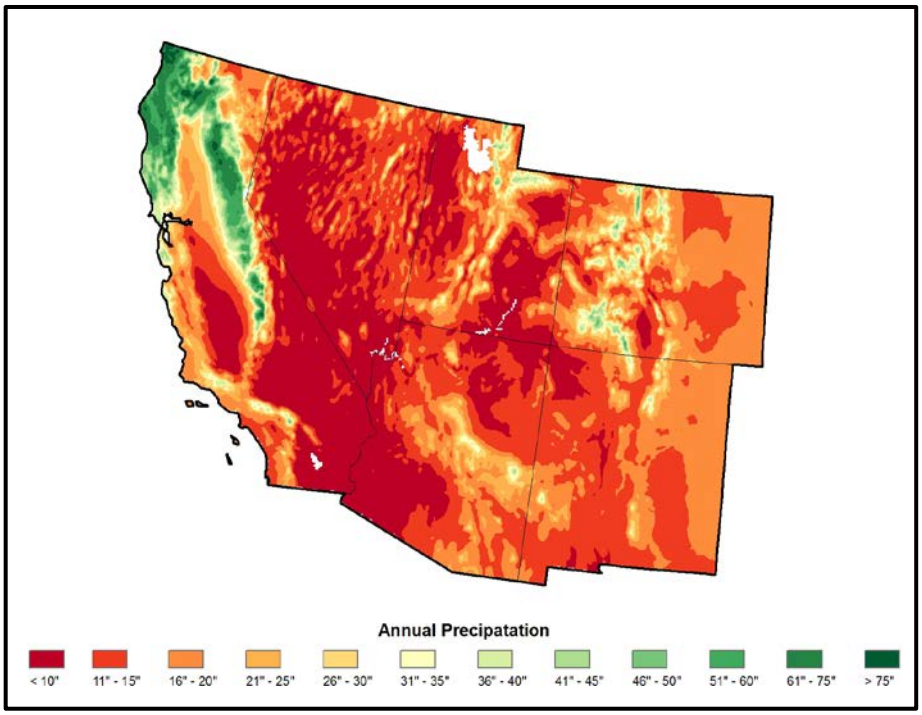

Figure 3. Average (1981-2010) annual precipitation (inches) for the Southwest region. Based on a new gridded version of COOP data from the National Climatic Data Center, the CDDv2 data set (R. Vose, personal communication, July 27, 2012).

2.3. Important Climate Factors

The Southwest region experiences a wide range of extreme weather and climate events that affect human society, ecosystems, and infrastructure. This discussion is meant to provide general information about these types of weather and climate phenomena. These include:

2.3.1. Drought

Drought represents an accumulated imbalance between the supply of water and the demand for water by plants, animals, the atmosphere, the soil column, and humans.

The Southwest has experienced numerous dry periods during the observational record. The most significant droughts are those that affect the primary season of hydrologic recharge (winter). In areas affected by the monsoon, which can bring up to 40-50 percent of the annual total, summer precipitation deficits can also have ecological impacts.

Temperature affects evaporation and transpiration, as well as the demand for water by the human population. In all seasons, as temperature rises, the conversion of precipitation (as snow or in liquid form) to soil moisture and then to streamflow proceeds less efficiently. As temperature rises, precipitation must increase as well to maintain a given level of hydrologic recharge.

The Southwest has experienced two significant dry periods since the middle 20th century, one in the mid 1950s, and the other near and after the turn of the millennium. The second of these was warmer than the first, increasing overall water loss. Furthermore, the decades of the 1980s and 1990s were relatively wet, and vigorous vegetative growth took place. This combination set the stage 10-20 years afterwards for fires of unprecedented ferocity and size, with at least four of the states exceeding their largest fires on record during the last decade.

With its arid climate, the Southwest preserves paleoclimate records exceptionally well. For example, close scrutiny of climate reconstructions based on tree rings has shown that major droughts in the Colorado River Basin have occurred approximately once or twice per century for the last 500-1000 years (Grissino-Mayer and Swetnam 2000; Woodhouse 2003; Meko et al. 2007). These can last up to several decades, far outside of modern experience, a vulnerability not fully appreciated until the last 10-15 years.

Drought characteristics are not uniform within the six states. Colorado, for example, has multiple sources and mechanisms for precipitation, and thus appears to be somewhat more “protected” from lengthy droughts (Redmond 2003). Tree ring records from California spanning the last 400-600 years show spectral peaks near 8 and 15 years (Redmond et al. 2002), and less evidence of very long droughts seen farther to the east. Drought has been less completely characterized in the central Great Basin, but it is noteworthy that the severe Sierra drought of 1987-1992 was barely noticeable in eastern Nevada. The dust-bowl-type droughts of the Great Plains have mostly affected the far eastern portions of the region, where precipitation has a summer maximum.

Southwest drought is clearly tied to the ENSO cycle, especially all along the US-Mexico border (Redmond and Koch 1991; Cayan et al. 1999). More tentative ties to the Pacific Decadal Oscillation (Mantua et al. 1997) have been uncovered in parts of the region (Biondi et al. 2001; Brown and Comrie 2002), and there are suggestions of ties in the Colorado River Basin to the Atlantic Multidecadal Oscillation (McCabe et al. 2004). The physical mechanisms and chain of causality behind ENSO ties to Southwest drought are much better understood than those to other global climate patterns.

2.3.2. Heat Waves

In parts of the Southwest, life is near the upper physical limitation for temperature, and it is vulnerable to even minor upward fluctuations. Other areas, such as the coast and high mountains, are comfortably away from such limits. In all areas, extended high temperatures that are unusual for the locale can impact ecosystems, hydrologic processes, and human comfort, health, and mortality. Among these effects are insect infestations, rapid snowmelt in spring, heat stroke, dehydration, and exacerbation of existing health issues, particular in the young and elderly. Consecutive hot days and nights can create cumulative stress, so that the consequences of a single warm day are not as great as episodes of a few days or longer.

In most of the Southwest atmospheric humidity is usually quite low, and most of the population is not exposed to the humid conditions of the East. Exceptions occur during the monsoon season at low elevations, and more rarely in other, lower parts of the region. The lack of humidity promotes evaporative cooling, so that tolerance for heat is improved to some extent. Water vapor is a strong greenhouse gas, and low humidity promotes more rapid surface cooling at night. Increases in other absorbers (such as CO_2) would be expected to help reduce radiative cooling at night. The region has seen a steady increase in average overnight minima and in extremely warm nights (see following section 2.4).

In much of the region, summer temperatures have not shown appreciable trends up to the early 1990s (see section 2.4). Since that time many summers have been considerably warmer than usual. The most recent notable heat wave was experienced in California in 2006 (Gershunov et al. 2009; Knowlton et al. 2009; Ostro et al. 2009).

2.3.3. Winter Storms

Large-scale cyclonic storms occur primarily in winter and its shoulder seasons, decreasing in frequency from north to south over the Southwest. The Sierra Nevada, for example, typically experiences 20-25 storms of at least moderate intensity at the latitude of Lake Tahoe. The effects of such storms are greatly enhanced by mountains, especially for precipitation and snowfall amount, and by wind. The storm track associated with the main jet stream meanders greatly during a typical winter, but can remain at lower or higher latitudes for extended periods, particularly if ENSO is in a strong warm (southern storm track) or cold (northern storm track) phase.

With its close proximity to the Pacific Ocean, the Sierra Nevada is subject to precipitation episodes as large as any in the U.S. (Dettinger et al. 2011). Recent research has uncovered the role of “atmospheric rivers” as drivers of nearly all major precipitation events (Neiman et al. 2008) along the West Coast. Their interior effects can be likewise significant, and are the subject of ongoing investigations. Like hurricanes, major winter storms are a mixed blessing, delivering both disruption

and precious water. Especially in lower latitudes a few large storms can make the difference between adequate and deficient snow pack and thus affect water supplies for the summer.

In the normal annual cycle, the main storm track shifts southward during winter, reaching the latitude of central California most often in January and into February and thereafter shifting back northward. Strong winds are sometimes experienced along the coast, and often as severe mountain downslope winds in the lee of all major north-south mountain chains. Low pressure systems develop just east of the Rocky Mountains, more commonly in late spring, and lead to significant upslope air flow, and to a spring maximum in snowfall in the western High Plains and Rocky Mountain Front.

Unlike the Great Plains and much of the eastern United States, the presence of about a thousand mountain ranges in the West disrupts the classic storm development commonly portrayed in meteorology textbooks. Mountains alter frontal progress, and lead to strong local enhancements of precipitation, snowfall, and wind. The rain-snow level in the atmosphere determines whether precipitation will remain as snow or run off as liquid. Temporary upward excursions in the freezing level can lead to rain-on-snow events, one source of large floods in elevated terrain. Tools to track the annual mean freezing level show that it has been rising over the past several decades, typically by 100-150 meters (Fig. 4). This has occurred mostly in seasons other than winter (Dec-Jan-Feb).

2.3.4. Floods

Floods have several different sources in the Southwest (Hirschboeck 1988; Michaud et al. 2001). As with other parts of the country, large-scale synoptic storms, more common in winter, can bring widespread heavy precipitation. These can either be deep, rapidly moving atmospheric waves associated with an active jet stream, or slower moving “cut-off” systems tapping tropical and subtropical moisture, which, by lingering, produce large precipitation totals. The floods in Arizona in the winter of 1992-1993 were a noteworthy example, causing floods on the largest regional rivers. The presence of the nearby Pacific Ocean provides a source region for moisture.

Mountains can greatly enhance precipitation, whether from large low pressure systems, regional mesoscale features, or local thunderstorms. Mountains also reduce precipitation in leeward “rain shadows” where widespread subsidence is present. Complex interactions between atmospheric flow and mountain chain orientation can lead to strong events in the interior portions of the Southwest away from the ocean. Timing and sequencing of events are critical to the formation of some floods. A week or two of cool weather, with extensive low elevation snowpack, followed by a warm system with high freezing levels and tropical moisture, can produce large and destructive floods. The same two events in the opposite order in time would not produce nearly the same effect.

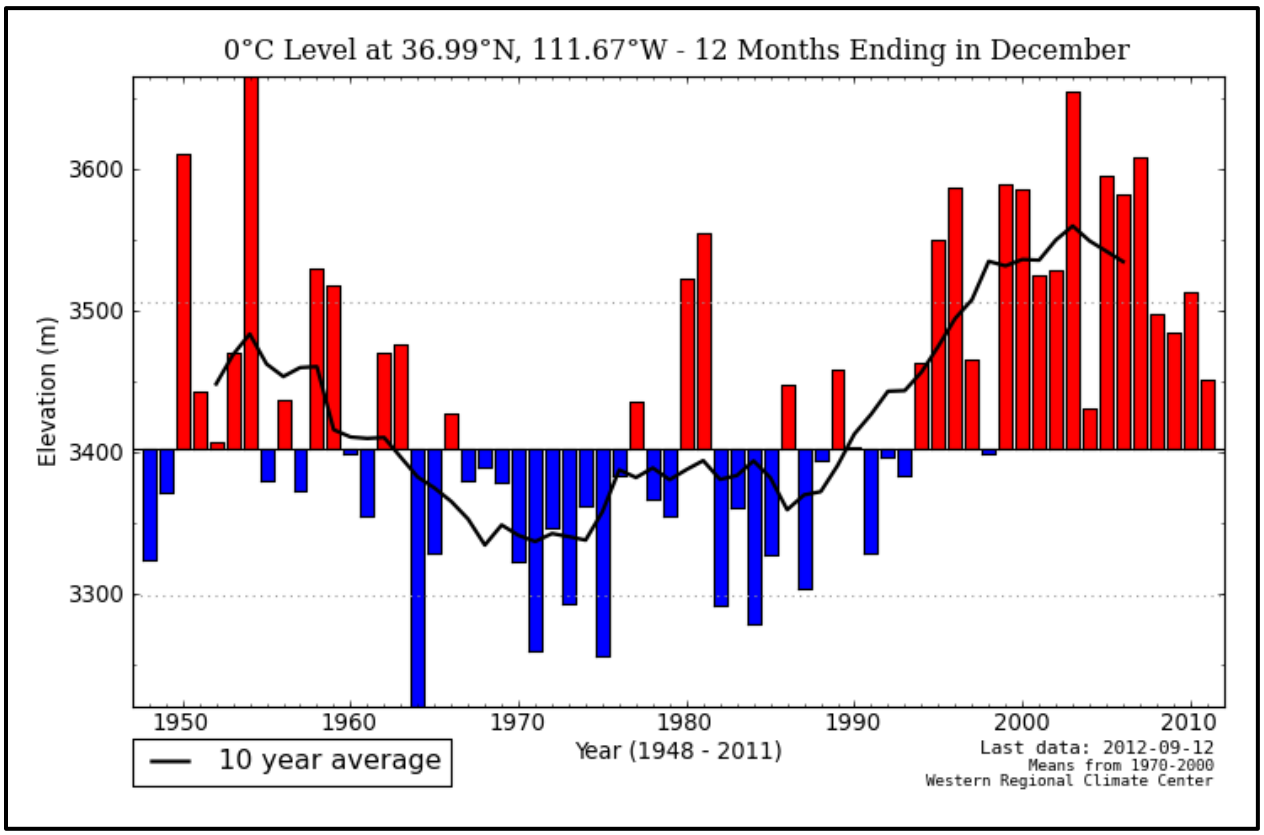

Figure 4. Mean annual freezing level in the center of the Southwest (over Glen Canyon Dam). Red: above period average. Blue: below period average. Black: Ten-year running mean. From the North American Freezing Level Tracker, based on Global Reanalysis data (WRCC 2012).

Of note, in many ways California seems almost designed to produce very large floods in very short times. Long plumes of moisture impinging perpendicularly on a high mountain range within a relatively narrow band nearly fixed in place, in essence a fire hose aimed at the Sierra, can produce tremendous floods. The travel time on the American River from Sierra crest (10,000 ft) to Sacramento (sea level) is only about 18 hours, and exceptional amounts of runoff can arrive nearly simultaneously from three distinct river forks that converge just above Folsom Reservoir (National Research Council 1999), which protects Sacramento.

A second major source of floods is the North American monsoon, which usually pushes out of Mexico into southern Arizona and New Mexico in early July (Higgins and Gochis 2007; Gutzler et al. 2009). Very humid air and abundant solar heating lead to very heavy rains on localized scales, and numerous flash floods in normally dry deserts. The monsoon flow typically spreads northward into eastern Nevada (and sometimes to the California deserts), and then curves into Utah and Colorado, and sometimes farther north. Summer floods associated with the monsoon can be severe in small watersheds, the dominant flood at those scales, but are seldom widespread enough to cause flooding in larger drainage basins such as the Salt or Verde Rivers.

Another type of flood can result from decaying tropical storms and hurricanes in the Eastern Pacific west of Mexico. That area experiences nearly twice as many such storms as the Atlantic, but most

of them wander westward to die over cool ocean waters. On occasion these storms follow a northward trajectory that takes them toward the Desert Southwest or even southern California. The moisture plumes from these dying systems (such as Paul in 1982) can generate intense, lasting, and slow-moving systems of thunderstorms capable of dumping very heavy precipitation over wide areas. These are most likely to occur in late summer and early autumn. On other occasions, moist easterly winds over the western High Plains rise up as they confront the Rocky Mountain Front, sometimes leading to extensive complexes of nearly stationary heavy thunderstorms, copious rain, and very destructive flash floods (Maddox et al. 1978; Weaver et al. 2000). These are, in part, a result of favorable dynamics and as well of very moist air.

Another type of flood, seen particularly in spring and summer of 2011, involves large snow packs developing over winter, cool springs with little melting and perhaps added precipitation as rain or snow, followed by early and mid-summer heat waves. This combination can combine to produce extended periods of flood flow, at times exceeding all-time maximums, with or without the addition of early summer precipitation. Snowmelt floods usually have extended high peaks, and mostly fall in the realm of "nuisance" floods, but these can occasionally cause large losses because of their duration and disruption.

Climatologists have recently recognized that gigantic events such as the California Flood of 1861-62 (Null and Hulbert 2007) can be seen in paleoclimate evidence, with an approximate return interval of 300 years. The state was sparsely populated during that winter, and recent exercises of the emergency response community (Dettinger et al. 2012) show that modern damage from a now-very-plausible several-week sequence of major storms could quite readily reach $0.5 to 1.0 trillion.

2.3.5. Warm Downslope Winds

In areas of high topographic relief, strong downslope winds often occur during favored portions of the annual cycle. Though regional in scale (30-200 miles), such episodes can have very significant consequences, particularly in combination with other weather phenomena. Notable among these are the Santa Ana winds of coastal southern California (Raphael 2003), their counterpart ("Sundowners") along the east-west oriented coastline around Santa Barbara, and easterly flow around San Francisco Bay ("Diablo" winds).

These winds occur when high pressure develops over the southern Great Basin, setting up a strong pressure gradient from inland to the coast. Because of the complex topography and friction, air moves almost directly down this gradient at speeds that can readily reach 45-80 miles/hr, with higher gusts. Compressional heating of this already dry air leads to elevated temperature and very low absolute and relative humidity. Organic material is thus susceptible to rapid drying. Furthermore, these winds are more common after the annual summer dry season, when vegetation and soil are greatly depleted in moisture. Under such circumstances, any small fire can quickly put tens of thousands of homes and structures in immediate jeopardy, many in places with difficult access, as well as those mobilized to respond. Over the recent decade, large, destructive, and disruptive fires, particularly in 2003 and 2007, have burned about 6,000 residences and led to mass evacuations of up to a third of a million people (Kailes 2008). Even with no effects arising from changes in climate, vulnerability to fire is a topic of high priority for all of California, especially southern California (Krawchuk and Morris 2012).

2.4. Climatic Trends

The temperature and precipitation data sets used to examine trends were obtained from NOAA's National Climatic Data Center (NCDC). The NCDC data is based on NWS Cooperative Observer Network (COOP) observations, as descibed in Section 2.1. Some analyses use daily observations for selected stations from the COOP network. Other analyses use a new national gridded monthly data set at a resolution of 5 x 5 km, for the time period of 1895-2011. This gridded data set is derived from bias-corrected monthly station data and is named the "Climate Division Database version 2 beta" (CDDv2) and is scheduled for public release in January 2013 (R. Vose, NCDC, personal communication, July 27, 2012).

The COOP data were processed using 1901-1960 as the reference period to calculate anomalies. In Section 3, this period is used for comparing net warming between model simulations and observations. There were two considerations in choosing this period for this purpose. Firstly, while some gradually-increasing anthropogenic forcing was present in the early and middle part of the 20th century, there is a pronounced acceleration of the forcing after 1960 (Meehl et al. 2003). Thus, there is an expectation that the effects of that forcing on surface climate conditions should accelerate after 1960. This year was therefore chosen as the ending year of the reference period. Secondly, in order to average out the natural fluctuations in climate as much as possible, it is desirable to use the longest practical reference period. Both observational and climate model data are generally available starting around the turn of the 20th century, thus motivating the use of 1901 as the beginning year of the reference period. We use this period as the reference for historical time series appearing in this section in order to be consistent with related figures in Section 3.

2.4.1. Temperature

Figure 5 shows annual and seasonal time series of temperature anomalies for the period of 1895-2011. Annual temperature (Fig. 5, top) has generally increased over the past 115 years, with a rise in the 1920s and 1930s, a prolonged level period, and a second rise from the mid 1970s to around 2000. Temperatures have leveled since then, and the past three years have cooled from recent averages. The warmest year is 1934. Of significant note, the daytime history is considerably different from that at night (Fig. 6). Daytime temperatures show less overall trend, and resemble the mean temperature time series, with much more cooling in the last five years. At night, by contrast, the temperature increase is somewhat steadier, and shows little evidence of the cool mean temperatures seen in this region and in the entire West during the last five years. For maximum, minimum, and mean temperatures, the recent 10-year averages all surpass any previous decadal value. Seasonal time series (Fig. 5, middle and bottom) are similar to the annual time series. The recent period of elevated temperatures is most prominent in the spring (middle right) and summer (bottom left).

Table 1 shows temperature trends for the period of 1895-2011, calculated using the CDDv2 data set. Values are only displayed for trends that are statistically significant at the 95% confidence level. Temperature trends are upward and statistically significant for each season, as well as the year as a whole, with magnitudes ranging from +0.16 to +0.21°F/decade.

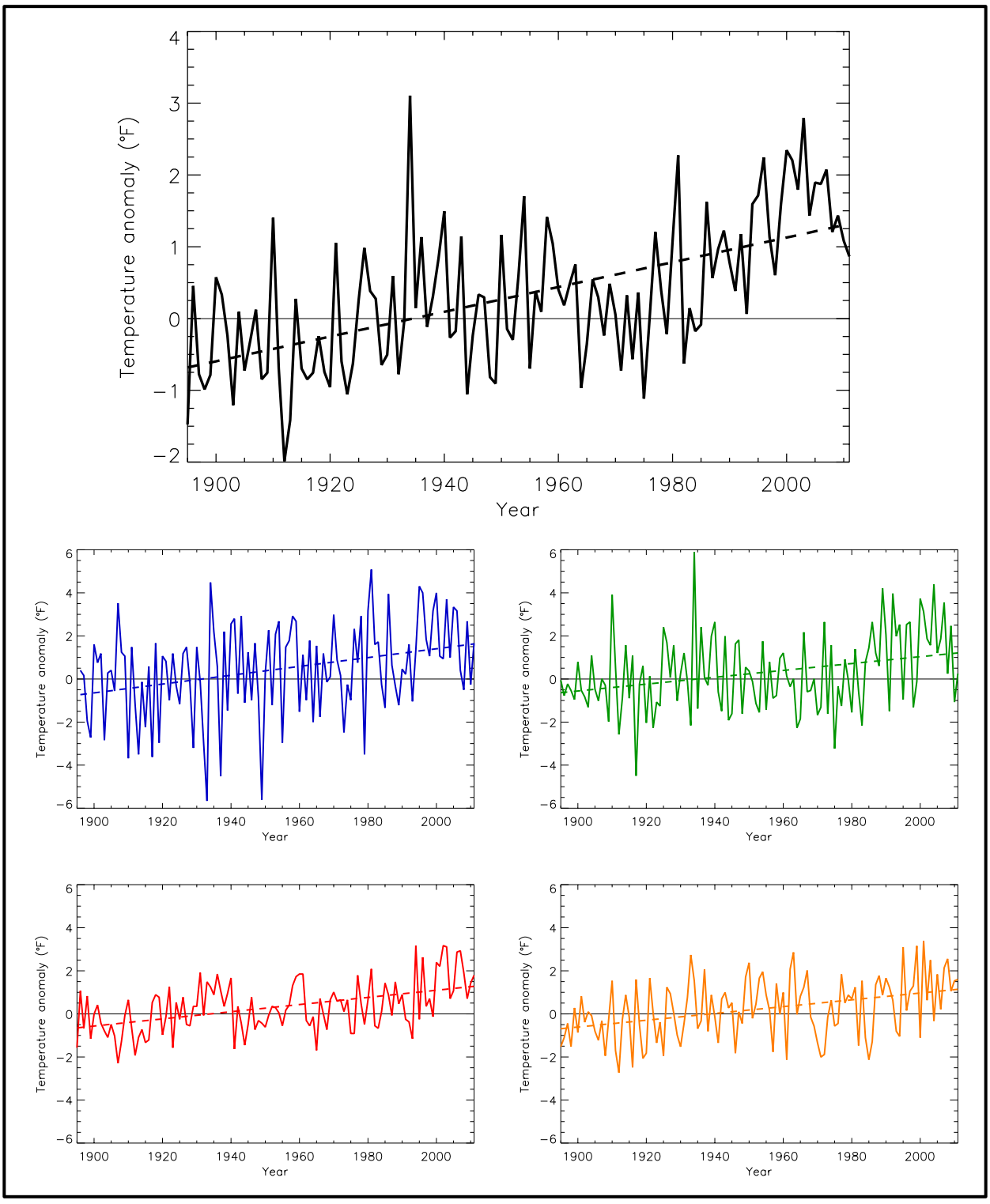

Figure 5. Temperature anomaly (deviations from the 1901-1960 average, °F) for annual (black), winter (blue), spring (green), summer (red), and fall (orange), for the Southwest U.S. Dashed lines indicate the best fit by minimizing the chi-square error statistic. Based on a new gridded version of COOP data from the National Climatic Data Center, the CDDv2 data set (R. Vose, personal communication, July 27, 2012). Note that the annual time series is on a unique scale. Trends are upward and statistically significant annually and for all seasons.

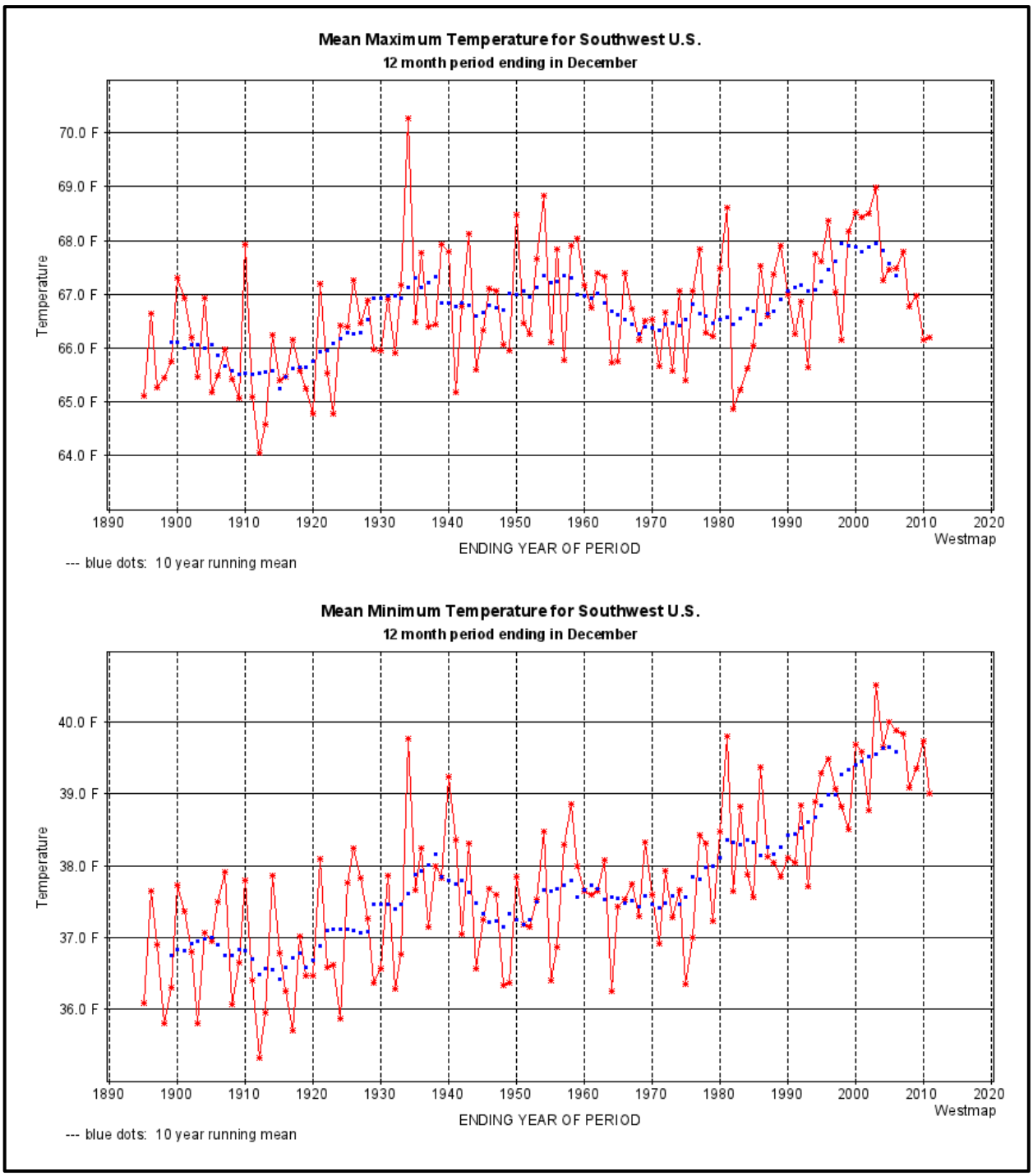

Figure 6. Annual mean maximum temperature for the six states, 1895-2011 (top). Annual mean minimum temperature for the six states, 1895-2011 (bottom). Annual values in red, 10-year running means in blue. Parameter-elevation Regressions on Independent Slopes Model (PRISM) data from WestMap (DRI 2012).

Table 1. 1895-2011 trends in temperature anomaly (°F/decade) and precipitation anomaly (inches/decade) based on a new gridded version of COOP data from the National Climatic Data Center, the CDDv2 data set (R. Vose, personal communication, July 27, 2012) for the Southwest U.S., for each season as well as the year as a whole. Only values statistically significant at the 95% confidence level are displayed. Statistical significance of trends was assessed using Kendall's tau coefficient. The test using tau is a non-parametric hypothesis test.

Season	Temperature (°F/decade)	Precipitation (inches/decade)
Winter	+0.21	—
Spring	+0.16	—
Summer	+0.17	—
Fall	+0.16	—
Annual	+0.17	—

2.4.2. Precipitation

Annual water year precipitation (Fig. 7) averages 15.4 inches over the period of record, and shows no long-term trend. The Southwest has exhibited exceptional and protracted variability during the last 30 years. The region experienced its wettest conditions in the 1980s and 1990s but has dried in the last decade. This wet period start coincides with the shift in Pacific climate in 1976 after which El Nino became much more frequent (Ebbesmeyer et al. 1991). El Nino generally causes wet winters in the border states. The wettest year is 1940-41 (a major El Nino) and four years are nearly tied for driest, the latest being 2001-2002. Major droughts were noted around 1900, in the mid 1950s, and the early 2000s.

Winter is the wettest season and contributes the most to annual hydrologic recharge, with a much smaller contribution from warm summer precipitation. Summer contributions to annual totals vary from little in CA to considerable in the southern Rockies and much of Arizona. Colorado precipitation seasonality varies considerably within the state.

Figure 8 shows annual (for the calendar year) and seasonal time series of precipitation anomalies for the period of 1895-2011, again calculated using the CDDv2 data set. The annual time series is qualitatively similar to the water year time series (Fig. 7). Seasonal time series do not exhibit any obvious long-term trends, except for fall, which shows a slight upward trend, although this is not statistically significant. The recent tendency toward drier years is most apparent in the spring time series.

Trends in precipitation for the period of 1895-2011 can be seen in Table 1. Precipitation trends are not statistically significant for any season. The nominal upward trend in fall (as seen in Fig. 8) is not statistically significant.

See http://charts.srcc.lsu.edu/trends/ (LSU 2012) for a comparative seasonal or annual climate trend analysis of a specified state from the Southwest region, using National Climate Data Center (NCDC) monthly and annual temperature and precipitation datasets.

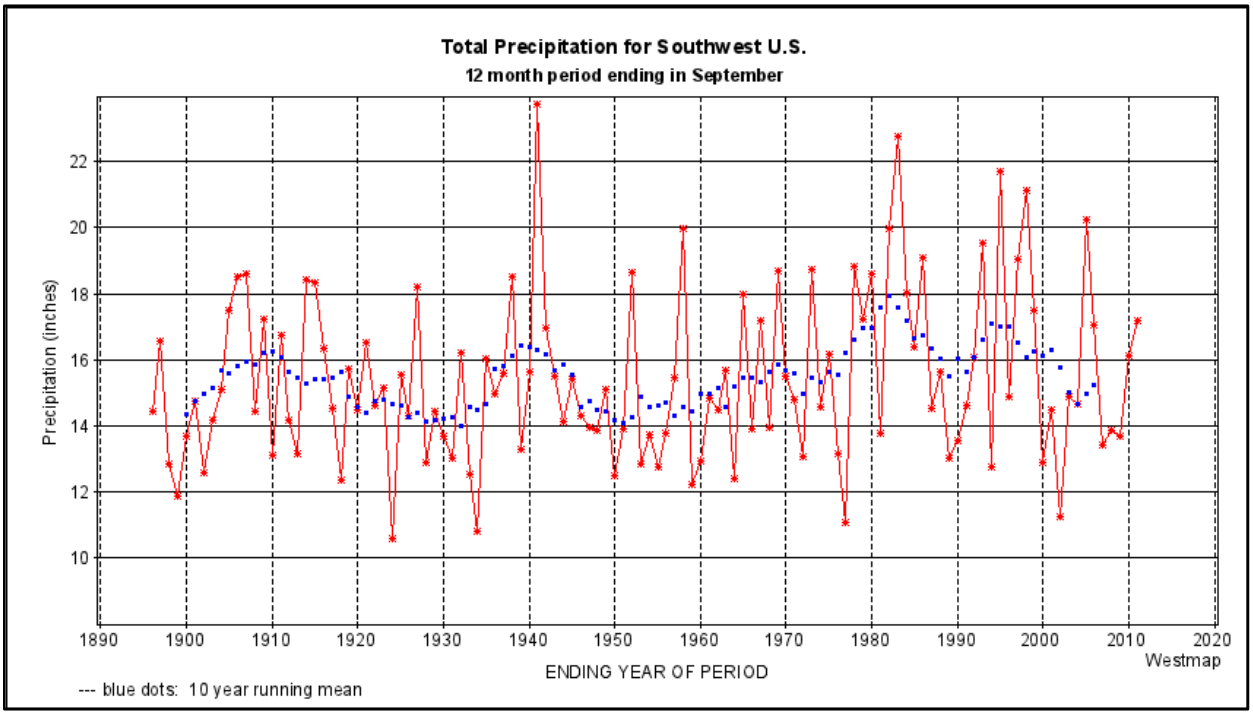

Figure 7. Annual water year (Oct-Sep) precipitation (inches/month) for the six states of the Southwest U.S., 1895/96-2010/11. Annual values in red, 10-year running means in blue. PRISM data from WestMap (DRI 2012).

2.4.3. Extreme Heat and Cold

Large spatial variations in the temperature climatology of this region result in analogous spatial variations in the definition of "extreme temperature". We define here extremes as relative to a location's overall temperature climatology, in terms of local frequency of occurrence.

Figure 9 shows time series of an index intended to represent heat and cold wave events. This index specifically reflects the number of 4-day duration episodes with extreme hot and cold temperatures, exceeding a threshold for a 1 in 5-year recurrence interval, calculated using daily COOP data from long-term stations. Extreme events are first identified for each individual climate observing station. Then, annual values of the index are gridding the station values and averaging the grid box values.

There is a large amount of interannual variability in extreme cold periods and extreme hot periods, reflecting the fact that, when they occur, such events affect large areas and thus large numbers of stations in the region simultaneously experience an extreme event exceeding the 1 in 5-year threshold.

The frequency of extreme heat waves has generally been increasing (Fig. 9, top) in recent decades. There is an overall upward trend that is statistically significant. The largest number of occurrences (during the entire period of record since 1895) was in 2003, with 2006 also a very high year. The 1930s "Dust Bowl" era also experienced a high number of heat waves, particularly 1931. By contrast, the frequency of extreme cold periods has been very low since the early 1990s (Fig. 9, bottom). There is an overall downward trend that is statistically significant.

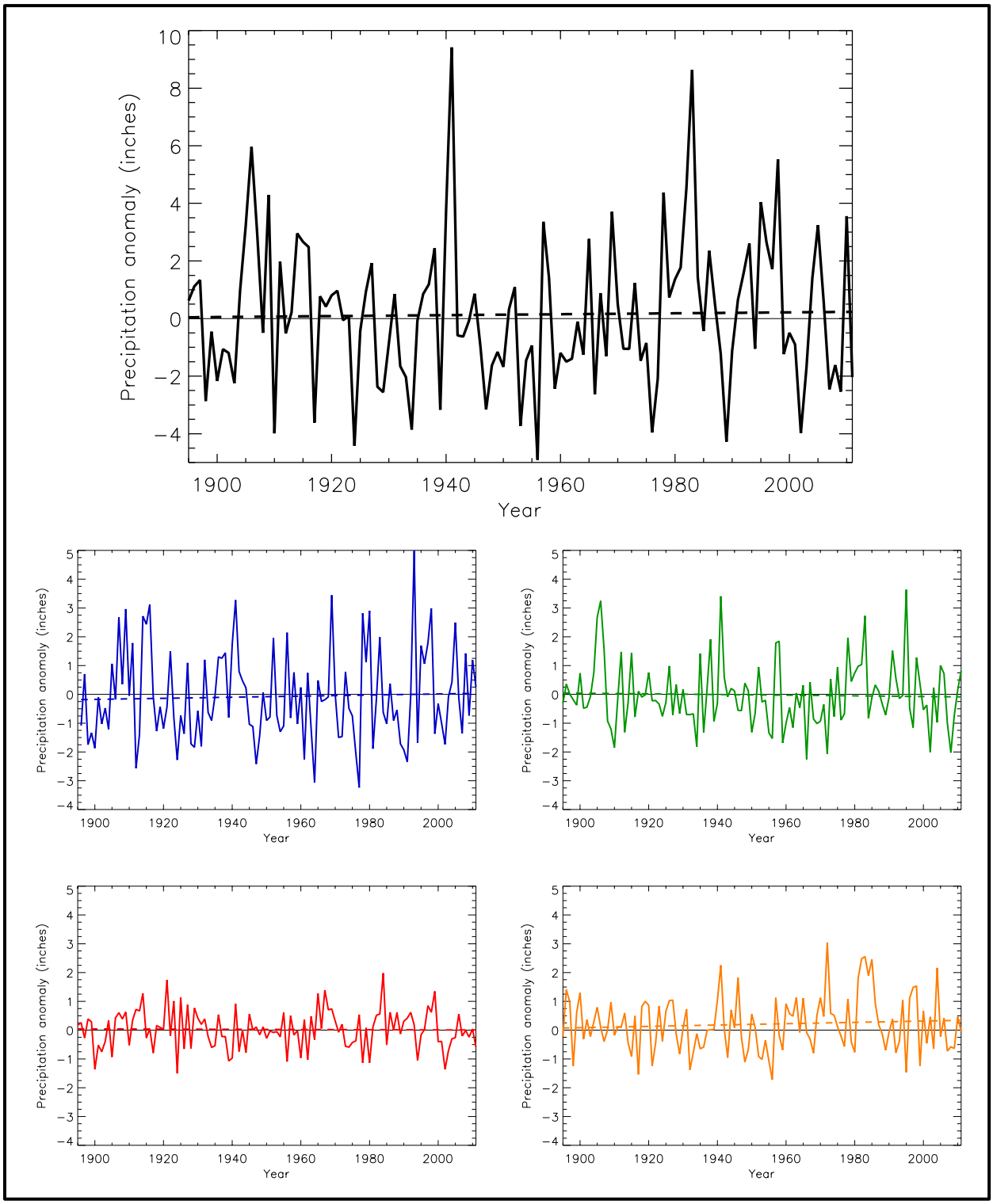

Figure 8. Precipitation anomaly (deviations from the 1895-2011 average, inches) for annual (black), winter (blue), spring (green), summer (red), and fall (orange), for the Southwest U.S. Dashed lines indicate the best fit by minimizing the chi-square error statistic. Based on a new gridded version of COOP data from the National Climatic Data Center, the CDDv2 data set (R. Vose, personal communication, July 27, 2012). Note that the annual time series is on a unique scale. Trends are not statistically significant for any season.

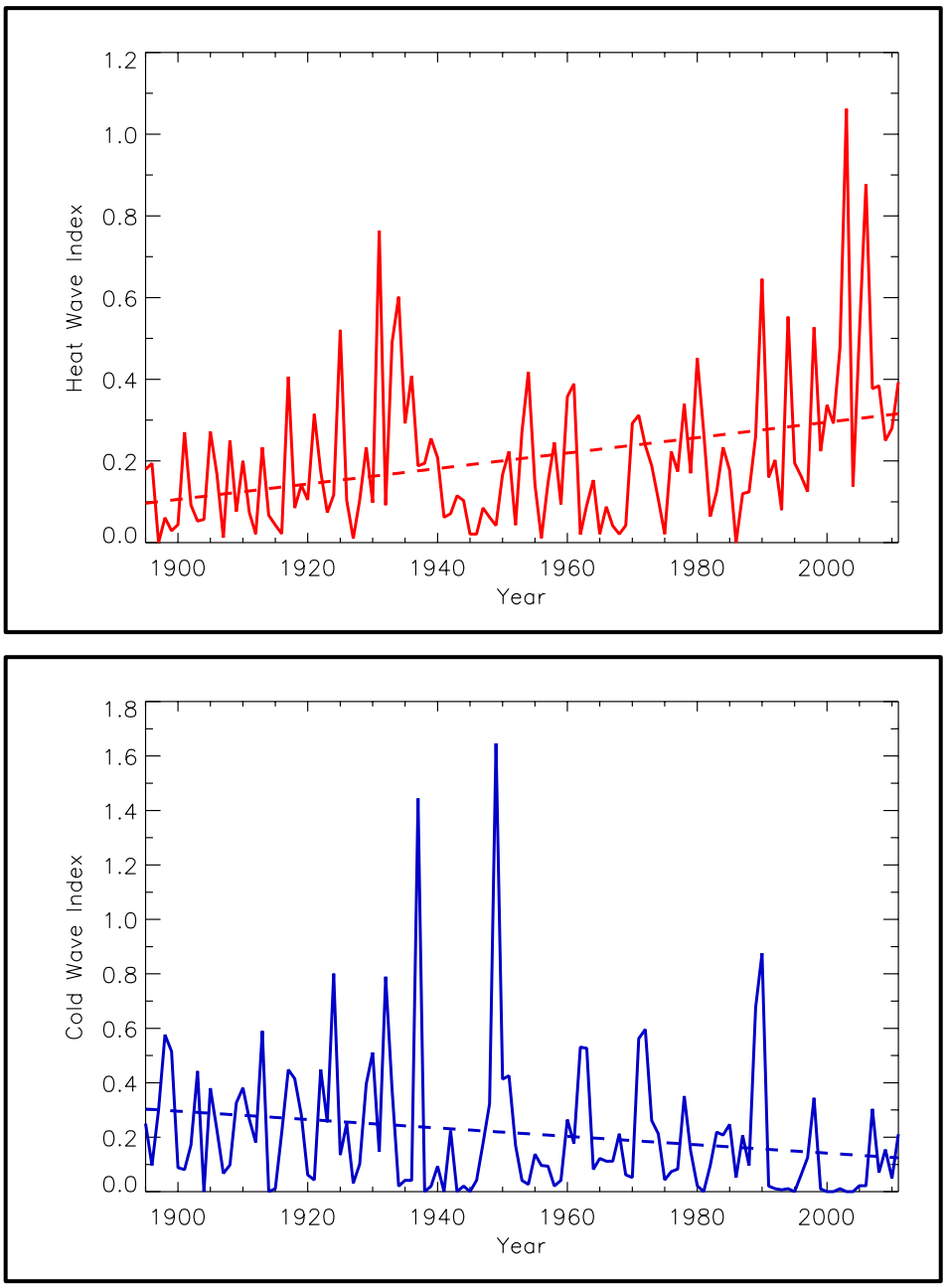

Figure 9. Time series of an index for the occurrence of heat waves (top) and cold waves (bottom), defined as 4-day periods that are hotter and colder, respectively, than the threshold for a 1 in 5-year recurrence, for the Southwest region. The dashed line is a linear fit. Based on daily COOP data from long-term stations in the National Climatic Data Center's Global Historical Climate Network data set. Only stations with less than 10% missing daily temperature data for the period 1895-2011 are used in this analysis. Events are first identified for each individual station by ranking all 4-day period mean temperature values and choosing the highest (heat waves) and lowest (cold waves) non-overlapping N/5 events, where N is the number of years of data for that particular station. Then, event numbers for each year are averaged for all stations in each 1x1° grid box. Finally, a regional average is determined by averaging the values for the individual grid boxes. This regional average is the index. There is a statistically significant upward trend in heat waves. The most intense heat waves occurred in the 1930s and 2000s.There is a statistically significant downward trend in cold waves and the number of intense cold wave events has been low during the last 15 years.

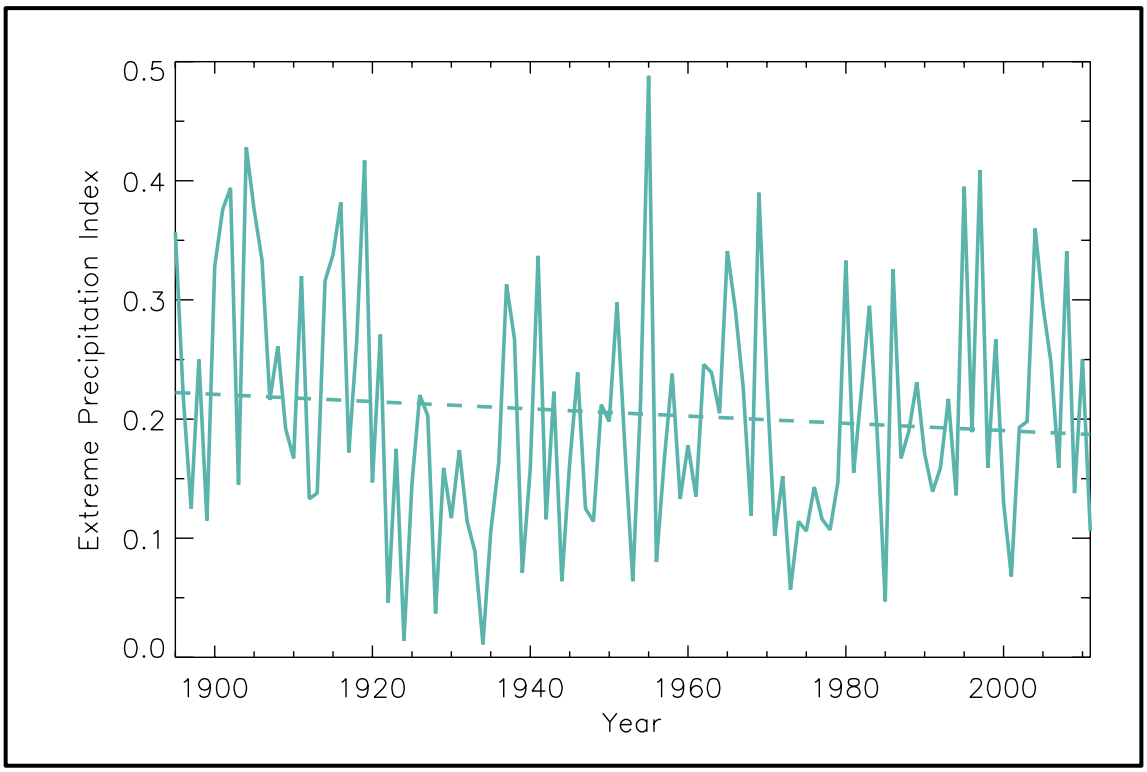

Figure 10. Time series of extreme precipitation index for the occurrence of 1-day, 1 in 5-year extreme precipitation, for the Southwest region. The dashed line is a linear fit. Based on daily COOP data from long-term stations in the National Climatic Data Center's Global Historical Climate Network data set. Only stations with less than 10% missing daily precipitation data for the period 1895-2011 are used in this analysis. Events are first identified for each individual station by ranking all daily precipitation values and choosing the top N/5 events, where N is the number of years of data for that particular station. Then, event numbers for each year are averaged for all stations in each 1x1° grid box. Finally, a regional average is determined by averaging the values for the individual grid boxes. This regional average is the extreme precipitation index. The overall trend is not statistically significant.

2.4.4. Extreme Precipitation

There are many different metrics that have been used in research studies to examine temporal changes in extreme precipitation. Here, we define the threshold for an extreme event based on a recurrence interval. This type of definition is commonly used for design applications, for example, in the design of runoff control structures. The analysis was performed using daily COOP data from long-term stations for a range of recurrence intervals, from one to twenty years. The results were not very sensitive to the exact choice. Results are presented for the five-year threshold, as an intermediate value. The duration of the extreme event is another choice for a metric. A range of durations was analyzed, from one to ten days, but the results were also not very sensitive to the choice. Results are presented (Fig. 10) for 1-day duration events, which is the shortest duration possible because of the daily time resolution of the COOP data.

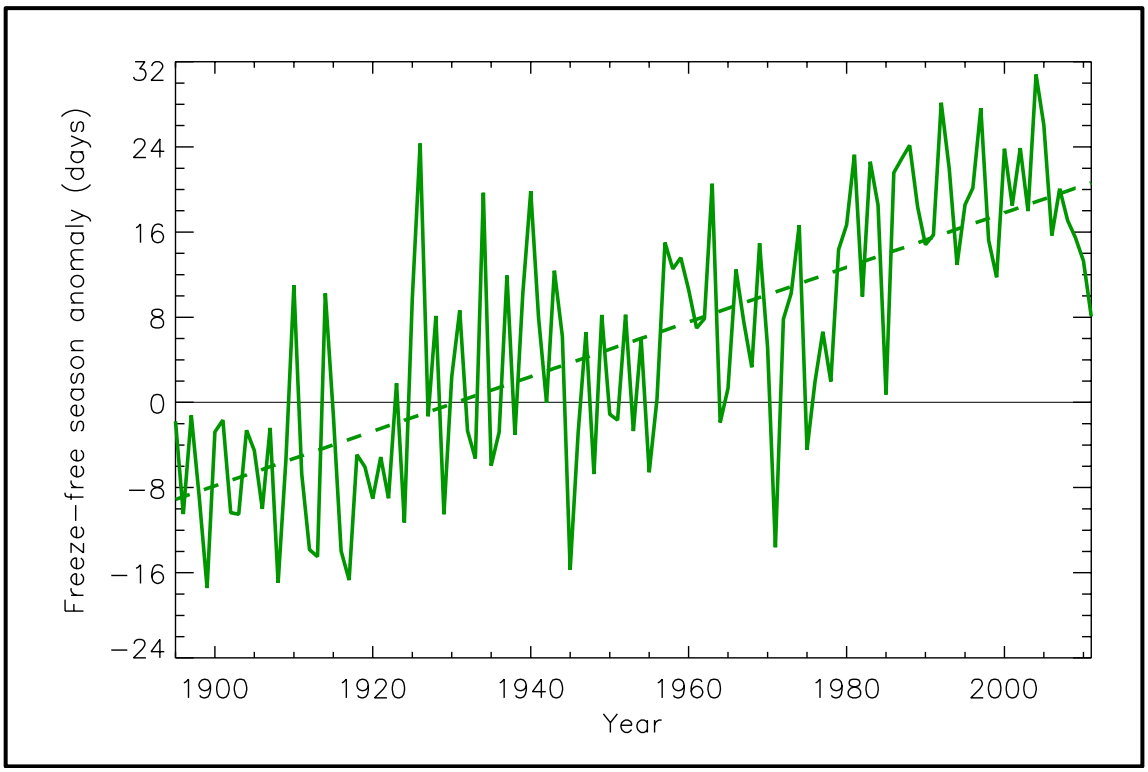

Figure 11. Freeze-free season anomalies shown as number of days per year. Length of the freeze-free season is defined as the period between the last occurrence of 32°F in the spring and first occurrence of 32°F in the fall. The dashed line is a linear fit. Based on daily COOP data from long-term stations in the National Climatic Data Center's Global Historical Climate Network data set. Only stations with less than 10% missing daily temperature data for the period 1895-2010 are used in this analysis. Freeze events are first identified for each individual station. Then, event dates for each year are averaged for 1x1° grid boxes. Finally, a regional average is determined by averaging the values for the individual grid boxes. There has been a statistically significant increase in freeze-free season length over the entire time period.

Unlike many areas of the United States, there has not been an overall trend in the frequency of extreme precipitation events in the Southwest. For example, the number of 1-day-duration and 5-year return interval events (based on the entire time series) was high early in the 20th century and very low in the 1920s and 1930s. Since then, there have been decadal-scale fluctuations, but the number of occurrences has generally been between the high and low extreme values experienced early in the 20th century.

2.4.5. Freeze-Free Season

Figure 11 shows a time series of freeze-free season length, calculated using daily COOP data from long-term stations. The freeze-free season length has increased substantially and now averages about two weeks longer than during the 1960s and 1970s and a whole month longer than in the early part of the 20th century. The last spring freeze has been occurring earlier and the first fall frost has been occurring later. The change in the timing of the last spring freeze has been somewhat greater than the timing change for the first fall frost. Over the entire time period of 1895-2011 there is a statistically significant upward trend in freeze-free season length.

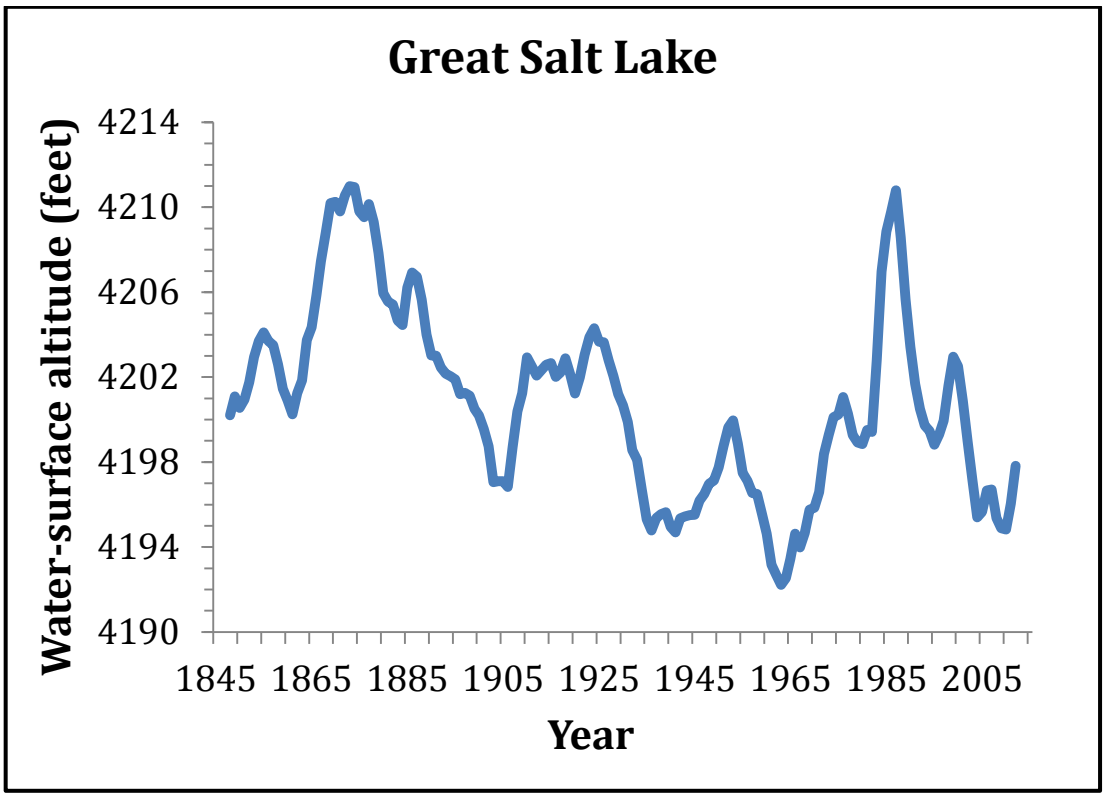

Figure 12. Great Salt Lake elevation, estimated and observed, from USGS. Data from Utah Department of Natural Resources (2012).

2.4.6. Lake Levels

Variations in lake levels, if the lakes are carefully chosen, can provide important insights into climate variations. The levels of natural lakes that are not heavily used for irrigation or other consumptive purposes will vary in an integrated response to precipitation, snowfall, temperature, and other variables that affect evaporation.

The Great Salt Lake is a particularly valuable source of information on climate variations because its brackish waters are not suitable for irrigation. Thus, its variations in levels contain a large component of climate variations. The variations in the level of Great Salt Lake have been observed since the earliest settlers (Fig. 12). Note that precipitation is related to the slope of the curve rather than the level itself. Evaporation does not vary as much from year to year as does streamflow input, which is mainly from the Wasatch Mountains and the Uinta Range to the east.

2.4.7. Paleohistory

A number of long-lived tree species exist in the region. Meko et al. (2007) have formulated a 1200-year reconstruction of Colorado River streamflow at the important Lees Ferry gauge downstream from Glen Canyon Dam (Fig. 13). The Colorado River Compact of 1922 allocated water to the states based (unknowingly) on one of the wettest periods in history, and the region has been wrestling with the consequences ever since. Furthermore, this record shows numerous extended periods (decades) of low flow as a natural feature of this basin.

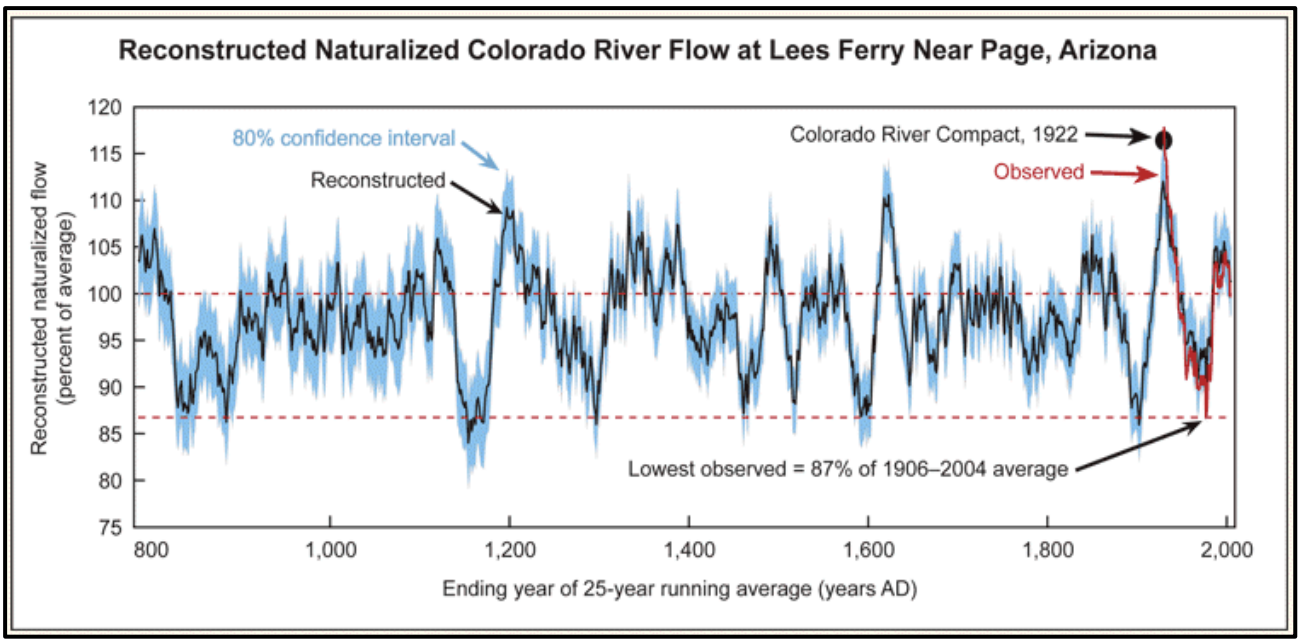

Figure 13. Reconstructed Colorado River flow based on tree ring evidence from Meko et al. (2007), and re-plotted (Guido 2009) by the Climate Assessment for the Southwest (CLIMAS). Republished with permission of the American Geophysical Union, adapted from Meko et al. (2007); permission conveyed through Copyright Clearance Center, Inc.

2.4.8. Santa Ana Winds

Santa Ana wind characteristics exhibit year-to-year and decade-to-decade variability. There has been little success in establishing unambiguous relationships of their occurrence to large-scale climate patterns (e.g., ENSO, other ocean conditions, atmospheric circulation indices). Santa Ana winds occur at "weather" time scales (a few days) and for study require models that resolve to this level. Conil and Hall (2006) showed that Santa Ana conditions occur 2-5 days per month from October through March. Hughes et al. (2009) report a significant decrease from 1959-2001 in the number of seasonal (Oct-Apr) days with Santa Ana events, using a fine-scale model (6 km resolution) driven by the European reanalysis ERA-40. However, the observed time series of Raphael (2003) do not show discernible trends in number of days per year. It may be that these apparent discrepancies arise from methodological differences, data periods, and analytical techniques, and that they can be reconciled.

Miller and Schlegel (2006) found that climate models do produce such events and with approximately the right frequency and seasonality. They used two models and two emission scenarios, and event criteria of high pressure gradient and in one case also low humidity (for one model for which that was available). The annual number of events appears to remain within about 10 percent of current occurrence rate well into the current century. Miller and Schlegel (2006) tentatively conclude that the Santa Ana season may in the future extend somewhat later into winter and early spring than now. One conclusion that does seem robust is that because of overall warming, the events themselves are likely to bring higher temperatures, and therefore also lower relative humidity, so that fire potential with each event would be increased from temperature effects alone.

3. FUTURE REGIONAL CLIMATE SCENARIOS

As noted above, the physical climate framework for the 2013 NCA report is based on climate model simulations of the future using the high (A2) and low (B1) SRES emissions scenarios. The resulting climate conditions are to be viewed as scenarios, not forecasts, and there are no explicit or implicit assumptions about the probability of occurrence of either scenario.

3.1. Description of Data Sources

This summary of future regional climate scenarios is based on the following model data sets:

- **Coupled Model Intercomparison Project phase 3 (CMIP3)** – Fifteen coupled Atmosphere-Ocean General Circulation Models (AOGCMs) from the World Climate Research Programme (WCRP) CMIP3 multi-model dataset (PCMDI 2012), as identified in the 2009 NCA report (Karl et al. 2009), were used (see Table 2). The spatial resolution of the great majority of these model simulations was 2-3° (a grid point spacing of approximately 100-200 miles), with a few slightly greater or smaller. All model data were re-gridded to a common resolution before processing (see below). The simulations from all of these models include:

  a) Simulations of the 20th century using best estimates of the temporal variations in external forcing factors (such as greenhouse gas concentrations, solar output, volcanic aerosol concentrations); and

  b) Simulations of the 21st century assuming changing greenhouse gas concentrations following both the A2 and B1 emissions scenarios. One of the fifteen models did not have a B1 simulation.

  These model simulations also serve as the basis for the following downscaled data set.

- **Downscaled CMIP3 (Daily_CMIP3)** – These temperature and precipitation data are at 1/8° (~8.6 miles latitude and ~6.0-7.5 miles longitude) resolution. The CMIP3 model data were initially downscaled on a monthly timescale using the bias-corrected spatial disaggregation (BCSD) method, for the period of 1961-2100. The starting point for this downscaling was an observationally-based gridded data set produced by Maurer et al. (2002). The climate model output was adjusted for biases through a comparison between this observational gridded data set and the model's simulation of the 20th century. Then, high-resolution gridded data for the future were obtained by applying change factors calculated as the difference between the model's present and future simulations (the so-called "delta" method).

  Daily statistically-downscaled data were then created by randomly sampling historical months and adjusting the values using the "delta" method (Hayhoe et al. 2004; 2008). Eight models with complete data for 1961-2100 were available and used in the Daily_CMIP3 analyses (Table 2).

- **North American Regional Climate Change Assessment Program (NARCCAP)** – This multi-institutional program is producing regional climate model (RCM) simulations in a coordinated experimental approach (NARCCAP 2012). At the time that this data analysis was initiated, simulations were available for 9 different combinations of an RCM driven by a general circulation model (GCM); during the development of these documents, two additional simulations became available and were incorporated into selected products. These 11 combinations involved four different GCMs and six different RCMs (see Table 3). The mean temperature and precipitation maps include all 11 combinations. For calculations and graphics

involving the distribution of NARCCAP models, analyses of only the original 9 model combinations were used. For graphics of the number of days exceeding thresholds and the number of degree days, the values were obtained from the Northeast Regional Climate Center, where only 8 of the model combinations were analyzed.

Each GCM-RCM combination performed simulations for the periods of 1971-2000, 1979-2004 and 2041-2070 for the high (A2) emissions scenario only. These simulations are at a resolution of approximately 50 km (~30 miles), covering much of North America and adjacent ocean areas. The simulations for 1971-2000 and 2041-2070 are "driven" (time-dependent conditions on the lateral boundaries of the domain of the RCM are provided) by global climate model simulations. The 1979-2004 simulations are driven by the NCEP/DOE Reanalysis II data set, which is an estimate of the actual time-dependent state of the atmosphere using a model that incorporates observations; thus the resulting simulations are the RCM's representation of historical observations. From this 1979-2004 simulation, the interval of 1980-2000 was selected for analysis.

Table 2. Listing of the 15 models used for the CMIP3 simulations (left column). The 8 models used in the daily statistically-downscaled (Daily_CMIP3) analyses are indicated (right column).

CMIP3 Models	**Daily_CMIP3**
CCSM3	X
CGCM3.1 (T47)	X
CNRM-CM3	
CSIRO-Mk3.0	
ECHAM5/MPI-OM	X
ECHO-G	X
GFDL-CM2.0	
GFDL-CM2.1	
INM-CM3.0	
IPSL-CM4	X
MIROC3.2 (medres)	X
MRI-CGCM2.3.2	X
PCM	X
UKMO-HadCM3	
UKMO-HadGEM1[2]	

[2] Simulations from this model are for the A2 scenario only.

Table 3. Combinations of the 4 GCMs and 6 RCMs that make up the 11 NARCCAP dynamically-downscaled model simulations.

		GCMs			
		CCSM3	CGCM3.1	GFDL-CM2.1	UKMO-HadCM3
RCMs	CRCM	X	X		
	ECPC			X[3]	
	HRM3			X[4]	X
	MM5I	X			X[3]
	RCM3		X	X	
	WRFG	X	X		

3.2. Analyses

Analyses are provided for the periods of 2021-2050, 2041-2070, and 2070-2099, with changes calculated with respect to an historical climate reference period (either 1971-1999, 1971-2000, or 1980-2000). These future periods will sometimes be denoted in the text by their midpoints of 2035, 2055, and 2085, respectively.

As noted above, three different intervals are used as the reference period for the historical climatology. Although a uniform reference period would be ideal, there were variations in data availability and in the needs of the author teams. For the NARCCAP maps of mean temperature and precipitation, the 1971-2000 period was used as the reference because that represents the full historical simulation period. The 1971-1999 period (rather than 1971-2000) was used as the reference for CMIP3 maps because some of the CMIP3 models' 20th century simulations ended in 1999, but we wanted to keep the same starting date of 1971 for both CMIP3 and NARCCAP mean temperature and precipitation maps. The 1980-2000 period was used as the historical reference for some of the NARCCAP maps (days over thresholds and degree days) because this is the analyzed period of the reanalysis-driven simulation, and we were requested to provide maps of the actual values of these variables for both the historical period and the future period, and not just a difference map. A U.S.-wide climatology based on actual observations was not readily available for all of these variables, and we chose to use the reanalysis-driven model simulation as an alternative. Since the reanalysis data set approximates observations, the reanalysis-driven RCM simulation will be free from biases arising from a driving GCM. To produce the future climatology map of actual values, we added the (future minus historical) differences to the 1980-2000 map values. For consistency then, the differences between future and present were calculated using the 1980-2000 subset of the 1971-2000 GCM-driven simulation.

Three different types of analyses are represented, described as follows:

[3] Data from this model combination were not used for simulations of the number of days exceeding thresholds or degree days.

[4] Data from these model combinations were not used for simulations of the number of days exceeding thresholds or degree days, or calculations and graphics involving the distribution of NARCCAP models.

- **Multi-model mean maps** – Model simulations of future climate conditions typically exhibit considerable model-to-model variability. In most cases, the future climate scenario information is presented as multi-model mean maps. To produce these, each model's data is first re-gridded to a common grid of approximately 2.8° latitude (~190 miles) by 2.8° longitude (~130-170 miles). Then, each grid point value is calculated as the mean of all available model values at that grid point. Finally, the mean grid point values are mapped. This type of analysis weights all models equally. Although an equal weighting does not incorporate known differences among models in their fidelity in reproducing various climatic conditions, a number of research studies have found that the multi-model mean with equal weighting is superior to any single model in reproducing the present-day climate (Overland et al. 2011). In most cases, the multi-model mean maps include information about the variability of the model simulations. In addition, there are several graphs that show the variability of individual model results. These should be examined to gain an awareness of the magnitude of the uncertainties in each scenario's future values.
- **Spatially-averaged products** – To produce these, all the grid point values within the Southwest region boundaries are averaged and represented as a single value. This is useful for general comparisons of different models, periods, and data sources. Because of the spatial aggregation, this product may not be suitable for many types of impacts analyses.
- **Probability density functions (pdfs)** – These are used here to illustrate the differences among models. To produce these, spatially-averaged values are calculated for each model simulation. Then, the distribution of these spatially-averaged values is displayed. This product provides an estimate of the uncertainty of future changes in a tabular form. As noted above, this information should be used as a complement to the multi-model mean maps.

3.3. Mean Temperature

Figure 14 shows the spatial distribution of multi-model mean simulated differences in average annual temperature for the three future time periods (2035, 2055, 2085) relative to the model reference period of 1971-1999, for both emissions scenarios, for the 14 (B1) or 15 (A2) CMIP3 models. The statistical significance regarding the change in temperature between each future time period and the model reference period was determined using a 2-sample *t*-test assuming unequal variances for those two samples. For each period (present and future climate), the mean and standard deviation were calculated using the 29 or 30 annual values. These were then used to calculate *t*. In order to assess the agreement between models, the following three categories were determined for each grid point, similar to that described in Tebaldi et al. (2011):

- *Category 1*: If less than 50% of the models indicate a statistically significant change then the multi-model mean is shown in color. Model results are in general agreement that simulated changes are within historical variations;
- *Category 2*: If more than 50% of the models indicate a statistically significant change, and less than 67% of the significant models agree on the sign of the change, then the grid points are masked out, indicating that the models are in disagreement about the direction of change;
- *Category 3*: If more than 50% of the models indicate a statistically significant change, and more than 67% of the significant models agree on the sign of the change, then the multi-model mean is shown in color with hatching. Model results are in agreement that simulated changes are statistically significant and in a particular direction.

It can be seen from Fig. 14 that all three periods indicate an increase in temperature with respect to the reference period, which is a continuation of the upward trend in mean temperature in the region over the last century. Spatial variations are relatively small, especially for the low (B1) emissions scenario. Changes along the coastal areas are slightly smaller than inland areas. Also, the warming tends to be slightly larger in the north, especially in the states of Nevada, Utah, and Colorado. This is consistent with global analyses that show relatively gradual spatial changes on a global scale (Meehl et al. 2007), a probable consequence of the generally high instantaneous spatial coherence of temperature and the smoothing effect of multi-model averaging. Temperature changes are simulated to increase for each future time period, and the differences between the A2 and B1 scenarios are also simulated to increase over time. For 2035, both A2 and B1 simulated values range between 1.5 and 3.5°F. For 2055, warming in B1 ranges over 2.5-4.5°F and for A2, they range from 2.5 to 5.5°F. Simulated temperature increases by 2085 are larger still, with a 3.5-5.5°F range for B1 and a 5.5-8.5°F range for A2. The CMIP3 models indicate that temperature changes across the Southwest U.S., for all three future time periods and both emissions scenarios, are statistically significant. The models also agree on the sign of change, with all grid points satisfying category 3 above, i.e. the models are in agreement on temperature increases throughout the region for each future time period and scenario.

Figure 15 shows the multi-model mean simulated annual and seasonal 30-year average temperature changes between 2041-2070 and 1971-2000 for the high (A2) emissions scenario, for 11 NARCCAP regional climate model simulations. The annual temperature changes are simulated to be quite uniform and in the range of 4-5°F, except for the Pacific coastal areas where the warming is less than 4°F. The seasonal changes show more spatial variability. Winter differences are simulated to range from 2.5 to 4.5°F, with the greatest warming occurring in the interior north. Springtime differences are similar in magnitude to the winter season; however the warmest area is located not in the north of the region, but rather in western New Mexico. Summer shows the greatest warming, ranging from 4 to 6.5°F, with maximum values in the northeast of the region. Warming in the fall ranges between 3.5 and 5.5°F, with the greatest warming occurring in the plains east of the Rocky Mountains. The agreement between models was again assessed using the three categories described in Fig. 14. The models agree on the sign of change, with all grid points satisfying category 3, annually, and for all seasons.

Figure 16 shows the simulated change in annual mean temperature for each future time period with respect to 1971-1999, for both emissions scenarios, averaged over the entire Southwest region for the 14 (B1) or 15 (A2) CMIP3 models. In addition, values for 9 of the NARCCAP simulations and the 4 GCMs used to drive the NARCCAP experiment are shown for 2055 (A2 scenario only) with respect to 1971-2000. Both the multi-model mean and individual model values are shown. For the high (A2) emissions scenario, the CMIP3 models simulate average temperature increases of 2.9°F by 2035, 4.7°F by 2055, and nearly 8°F by 2085. The increases for the low (B1) emissions scenario are nearly as large in 2035 at around 2.5°F, but by 2085 the increase of 4.6°F is over 3°F smaller than in the A2 scenario. For 2055, the average temperature change simulated by the NARCCAP models (4.4°F) is comparable to the mean of the CMIP3 GCMs for the A2 scenario.

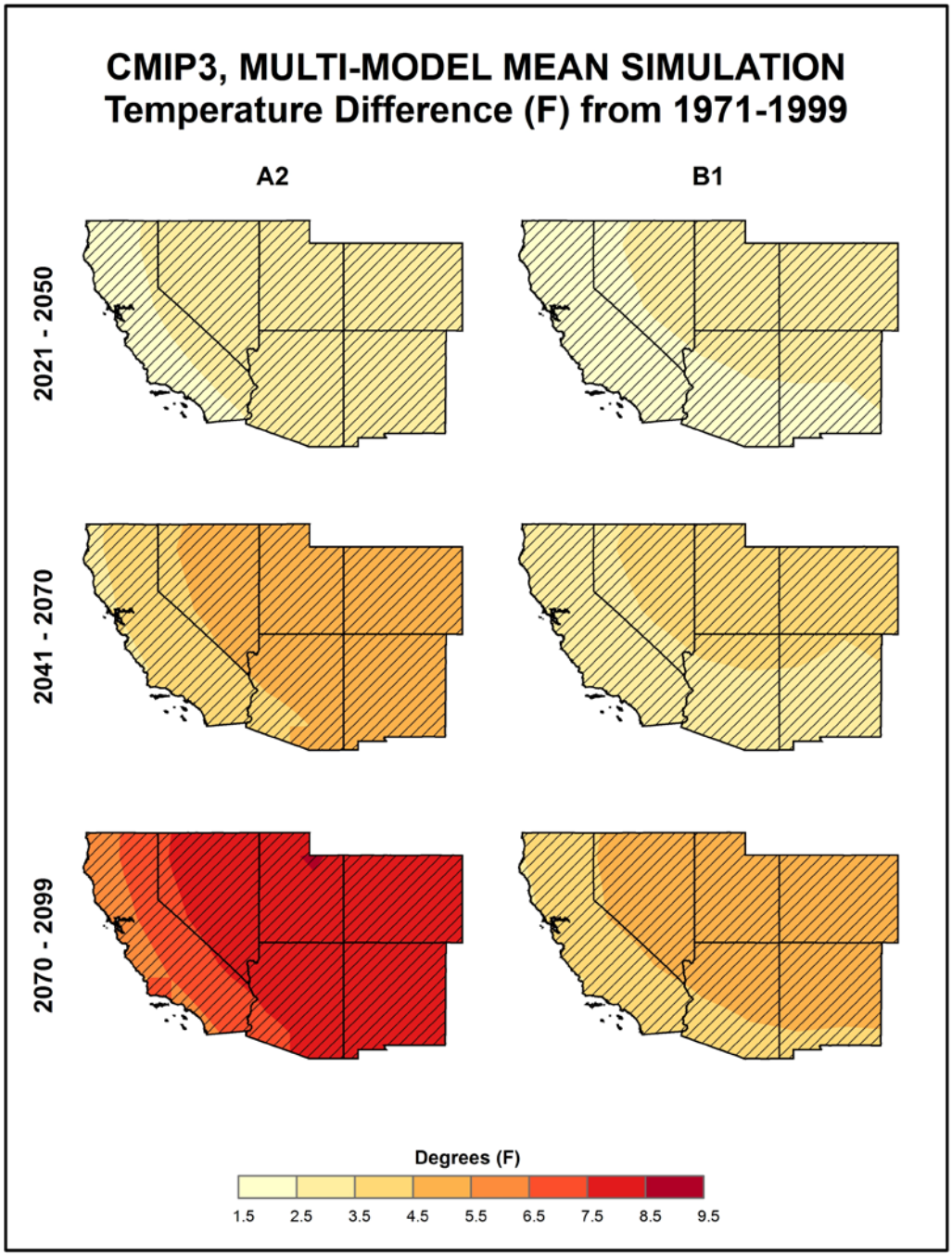

Figure 14. Simulated difference in annual mean temperature (°F) for the Southwest region, for each future time period (2021-2050, 2041-2070, and 2070-2099) with respect to the reference period of 1971-1999. These are multi-model means for the high (A2) and low (B1) emissions scenarios from the 14 (B1) or 15 (A2) CMIP3 global climate simulations. Color with hatching (category 3) indicates that more than 50% of the models show a statistically significant change in temperature, and more than 67% agree on the sign of the change (see text). Temperature changes increase throughout the 21st century, more rapidly for the high emissions scenario.

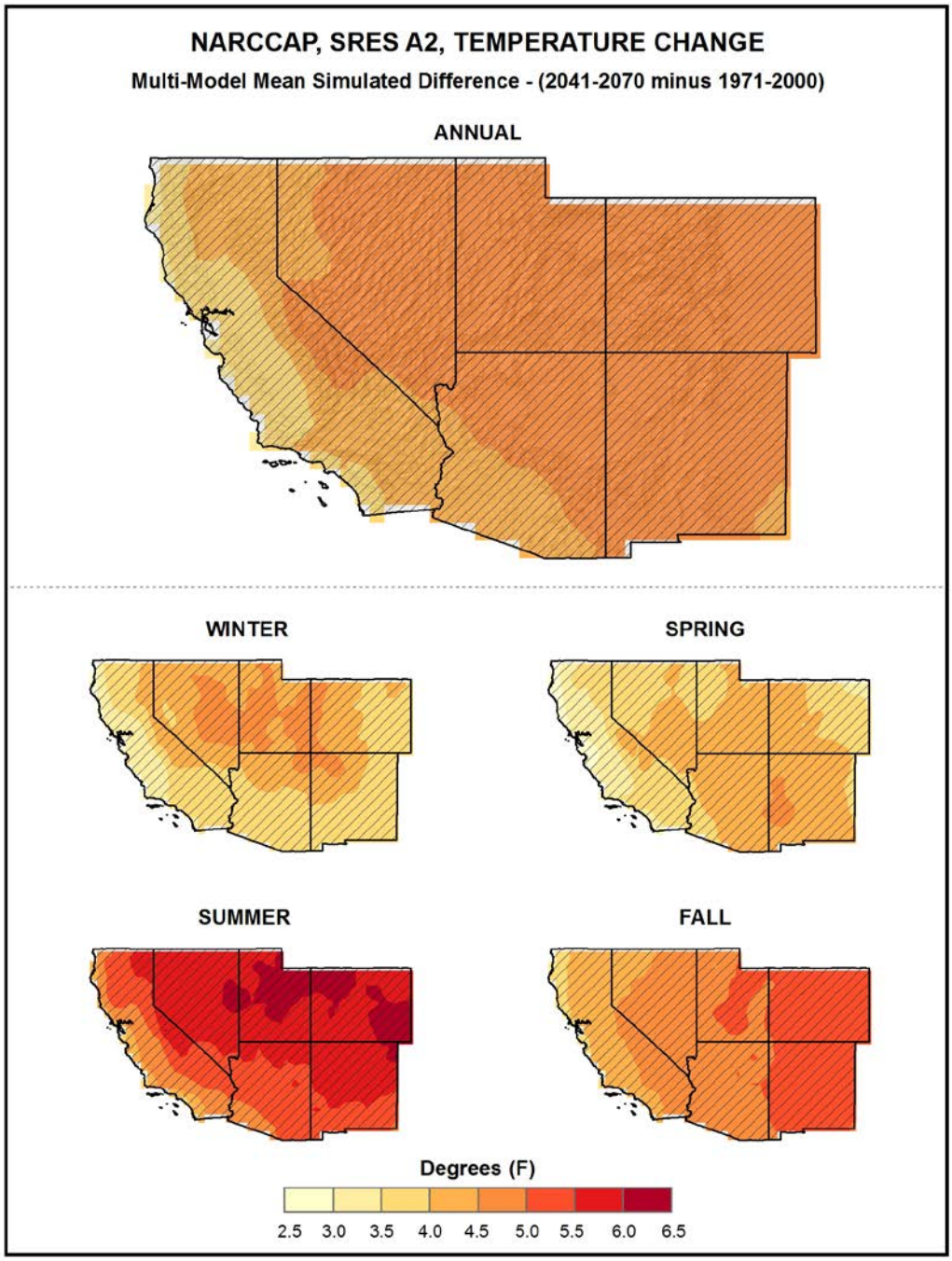

Figure 15. Simulated difference in annual and seasonal mean temperature (°F) for the Southwest region, for 2041-2070 with respect to the reference period of 1971-2000. These are multi-model means from 11 NARCCAP regional climate simulations for the high (A2) emissions scenario. Color with hatching (category 3) indicates that more than 50% of the models show a statistically significant change in temperature, and more than 67% agree on the sign of the change (see text). Note that the color scale is different from that of Fig. 14. Annual temperature changes for the NARCCAP simulations are similar to those for the CMIP3 global models (Fig. 14, middle left panel). Seasonal changes are greatest in summer.

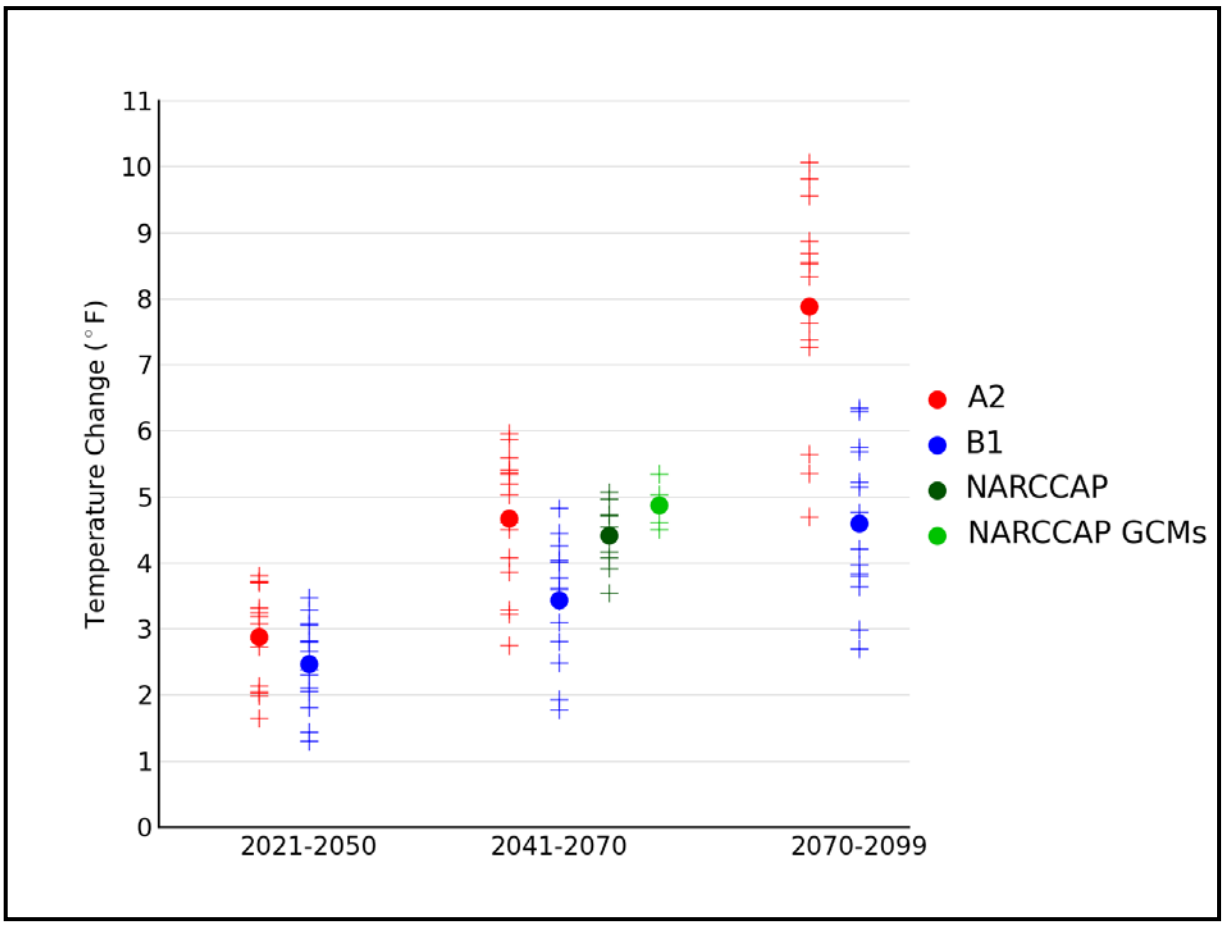

Figure 16. Simulated annual mean temperature change (°F) for the Southwest region, for each future time period (2021-2050, 2041-2070, and 2070-2099) with respect to the reference period of 1971-1999 for the CMIP3 models and 1971-2000 for the NARCCAP models. Values are given for the high (A2) and low (B1) emissions scenarios for the 14 (B1) or 15 (A2) CMIP3 models. Also shown for 2041-2070 (high emissions scenario only) are values for 9 NARCCAP models, as well as for the 4 GCMs used to drive the NARCCAP simulations. The small plus signs indicate each individual model and the circles depict the multi-model means. The range of model-simulated changes is large compared to the mean differences between A2 and B1 in the early and middle 21st century. By the end of the 21st century, the difference between A2 and B1 is comparable to the range of B1 simulations.

A key overall feature is that the simulated temperature changes are similar in value for the high and low emissions scenarios for 2035, but largely different for 2085. This indicates that early in the 21st century, the multi-model mean temperature changes are relatively insensitive to the emissions pathway, whereas late 21st century changes are quite sensitive to the emissions pathway. This arises because atmospheric CO_2 concentrations resulting from the two different emissions scenarios do not considerably diverge from one another until around 2050 (see Fig. 1). It can also be seen from Fig. 16 that the range of individual model changes is quite large, with considerable overlap between the A2 and B1 results, even for 2085. The range of temperature changes for the GCMs used to drive the NARCCAP simulations is small relative to the range for all CMIP3 models. This may be largely responsible for the relatively small range of the NARCCAP models.

Figure 17 shows the simulated change in seasonal mean temperature for each future time period with respect to 1971-1999 for the high (A2) emissions scenario, averaged over the entire Southwest region for the 15 CMIP3 models. Again, both the multi-model mean and individual model values are shown. Temperature increases are simulated to be largest in the summertime, with means 3.5°F in 2035, 5.6°F in 2055, and 8.9°F in 2085. Wintertime is simulated to have the least amount of warming, ranging from 2.5°F in 2035 to 6.8°F in 2085. The range of temperature changes for the individual models increases with each time period and is large relative to the differences between seasons.

The distribution of simulated changes in annual mean temperature for each future time period with respect to 1971-1999 for both emissions scenarios among the 14 (B1) or 15 (A2) CMIP3 models is shown in Table 4. Temperature changes simulated by the individual models vary from the lowest value of 1.3°F (in 2035 for the B1 scenario) to the highest value of 10.1°F (in 2085 for the A2 scenario). Although the inter-model range of temperature changes (i.e. the difference between the highest and lowest model values) is seen to increase for each future time period, the interquartile range (the difference between the 75th and 25th percentiles) varies between 0.9 and 1.8°F across the three time periods. The NARCCAP simulated temperature changes have a smaller range than the comparable CMIP3 simulations, varying from 3.5°F to 5.1°F.

Table 4. Distribution of the simulated change in annual mean temperature (°F) from the 14 (B1) or 15 (A2) CMIP3 models for the Southwest region. The lowest, 25th percentile, median, 75th percentile and highest values are given for the high (A2) and low (B1) emissions scenarios, and for each future time period (2021-2050, 2041-2070, and 2070-2099) with respect to the reference period of 1971-1999. Also shown are values from the distribution of 9 NARCCAP models for 2041-2070, A2 only, with respect to 1971-2000.

Scenario	Period	Lowest	25th Percentile	Median	75th Percentile	Highest
A2	2021-2050	1.7	2.1	3.1	3.5	3.8
	2041-2070	2.8	4.0	5.0	5.4	6.0
	2070-2099	4.7	7.3	8.3	8.8	10.1
	NARCCAP (2041-2070)	*3.5*	*4.1*	*4.5*	*4.7*	*5.1*
B1	2021-2050	1.3	2.1	2.5	3.0	3.5
	2041-2070	1.8	2.9	3.6	4.0	4.8
	2070-2099	2.7	3.8	4.5	5.6	6.3

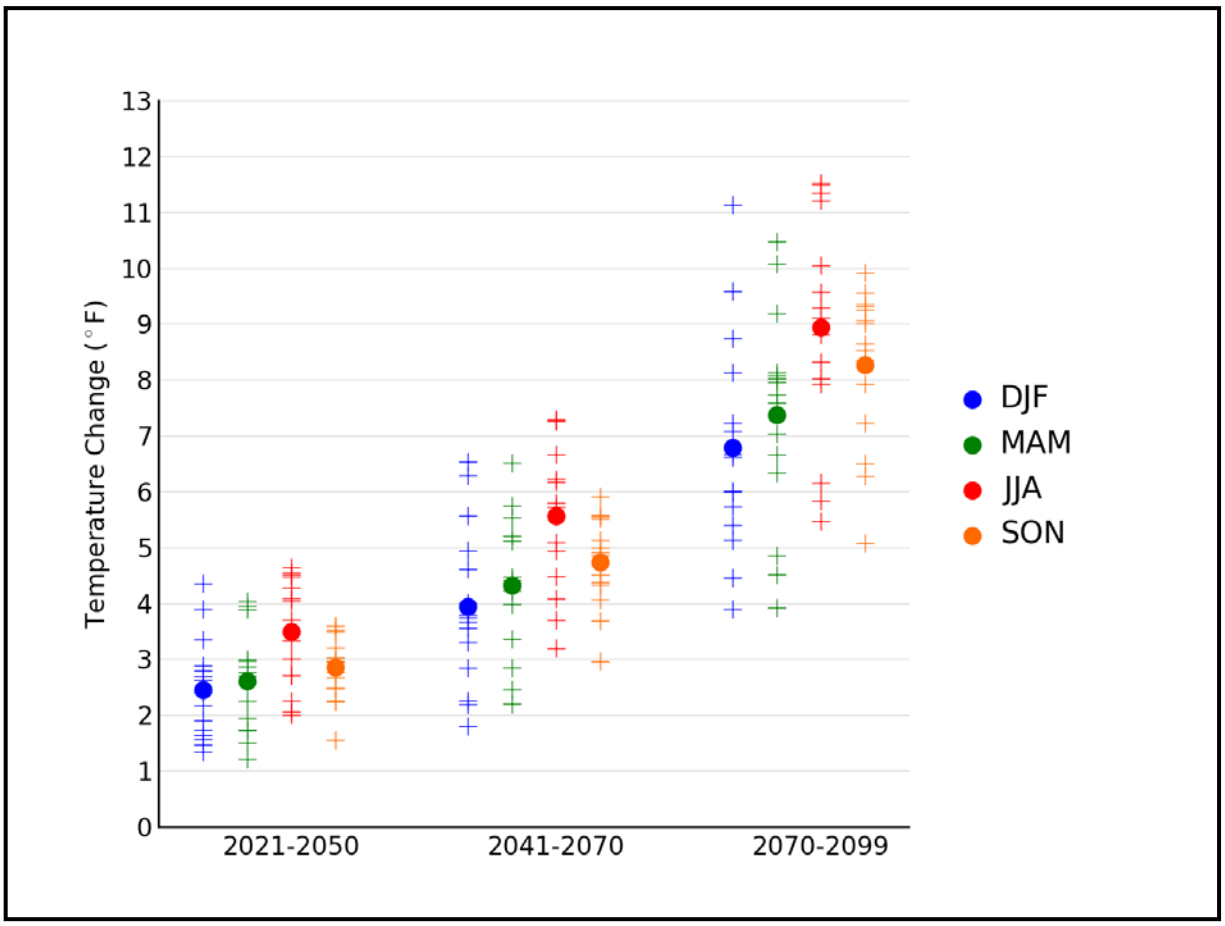

Figure 17. Simulated seasonal mean temperature change (°F) for the Southwest region, for each future time period (2021-2050, 2041-2070, and 2070-2099) with respect to the reference period of 1971-1999. Values are given for all 15 CMIP3 models for the high (A2) emissions scenario. The small plus signs indicate each individual model and the circles depict the multi-model means. Seasons are indicated as follows: winter (DJF, December-January-February), spring (MAM, March-April-May), summer (JJA, June-July-August), and fall (SON, September-October-November). The range of individual model-simulated changes is large compared to the differences among seasons and comparable to the differences between periods.

This table also illustrates the overall uncertainty arising from the combination of model differences and emission pathway. For 2035, the simulated changes range from 1.3°F to 3.8°F and are almost entirely due to differences in the individual models. By 2085, the range of simulated changes has increased to 2.7°F to 10.1°F, with roughly equal contributions to the range from model differences and emission pathway uncertainties.

3.4. Extreme Temperature

A number of metrics of extreme temperatures were calculated from the NARCCAP dynamically-downscaled and CMIP3 daily statistically-downscaled (Daily_CMIP3) data sets. Maps of a few select variables and a table summarizing all of the results follow. Each figure of NARCCAP data includes three map panels and the calculations used in each panel require some explanation. One panel (top) shows the difference between the 2055 period (2041-2070) simulation for the high (A2) emissions scenario and the 1980-2000 subset of the 1971-2000 simulation driven by the GCM. Since biases in the RCM simulations can arise from biases either in the driving global climate model or in the RCM, these two simulations include both sources of biases. It is usually assumed that such biases will be similar for historical and future periods. When taking the difference of these, the biases should at least partially cancel. As noted above, we were requested to include actual values of the variables, not just the future minus historical differences. We decided that the best model representation of the present-day values is the 1980-2000 simulation because it is driven by reanalysis data (NOAA 2012b) and thus will not include biases from a driving global climate model (although the reanalysis data used to drive the RCM is not a perfect representation of the actual state of the atmosphere). Any biases should be largely from the RCM. Thus, the lower left panel in the following figures shows the actual values from the 1980-2000 simulation. The lower right panel shows the actual values for the future period, calculated by adding the differences (the 2041-2070 simulation minus the 1980-2000 subset of the 1971-2000 simulation) to the 1980-2000 simulation. If our assumption that the differencing of present and future at least partially cancels out model biases is true, then the predominant source of biases in the future values in the lower right hand panel is from the RCM simulation of the present-day, 1980-2000. The agreement among models was once again assessed using the three categories described in Fig. 14.

The selection of threshold temperatures to calculate extremes metrics is somewhat arbitrary because impacts-relevant thresholds are highly variable due to the very diverse climate of the U.S., with the exception of the freezing temperature, which is a universal physical threshold. In terms of high temperature thresholds, the values of 90°F, 95°F, and 100°F have been utilized in various studies of heat stress, although it is obvious that these thresholds have very different implications for the impacts on northern, cooler regions compared to southern, warmer regions. The threshold of 95°F has physiological relevance for maize production because the efficiency of pollination drops above that threshold. The low temperature thresholds of 10°F and 0°F also have varying relevance on impacts related to the background climate of a region. Fortunately, our analysis results are not qualitatively sensitive to the chosen thresholds. Thus, the results for these somewhat arbitrary choices nevertheless provide general guidance into scenarios of future changes.

Figure 18 shows the spatial distribution of the multi-model mean change in the average annual number of days with a maximum temperature exceeding 95°F between 2055 and the model reference period of 1980-2000, for the high (A2) emissions scenario, for 8 NARCCAP regional climate model simulations. The largest simulated increases of more than 25 days occur in southern

and eastern areas where the number of occurrences in the historical period is highest, and are more than 30 in some areas of Arizona and New Mexico. The smallest increases of less than 5 days occur in the highest elevation areas where the general increase in temperature is not large enough to markedly increase the chances for such warm days. The NARCCAP models indicate that the changes in the number of 95°F days across the majority of the Southwest are statistically significant. The models also agree on the sign of change, with these grid points satisfying category 3, i.e. the models are in agreement that the number of days above 95°F will increase throughout the region for these scenarios. For areas along the Rocky Mountains, however, the changes are not statistically significant for most models (category 1) because even in this future scenario they remain very rare.

Figure 19 shows the NARCCAP multi-model mean change in the average annual number of days with a minimum temperature of less than 10°F between 2055 and the model reference period of 1980-2000, for the high (A2) emissions scenario. The interior north is simulated to experience a large decrease in the number of days compared to little or no change in southern areas. The largest decreases are simulated to occur in higher elevation areas with some areas decreasing by 25 days or more. The smallest decreases occur in coastal and southern areas, where the number of occurrences in the climatology is very small or zero and these small changes are not statistically significant for parts of California south and west of the Sierra Nevada, as well as southern Arizona. All remaining grid points satisfy category 3, however, with the models indicating that changes are statistically significant. The models also agree on the sign of change, i.e. they are in agreement that the number of days with a minimum temperature of less than 10°F will decrease throughout the region under this scenario.

Figure 20 shows the NARCCAP multi-model mean change in the average annual number of days with a minimum temperature of less than 32°F between 2055 and the model reference period of 1980-2000, for the high (A2) emissions scenario. Model simulated decreases are largest (decreases of more than 40 days) in the high elevation parts of the region. The least amount of change is simulated along the coast as well as in southern California and Arizona, where the number of freezes in the historical period is low. The NARCCAP models indicate that the changes in the number of days below freezing across the Southwest are statistically significant. The models also agree on the sign of change, with all grid points satisfying category 3, i.e. the models are in agreement that the number of days below 32°F will decrease throughout the region under this scenario.

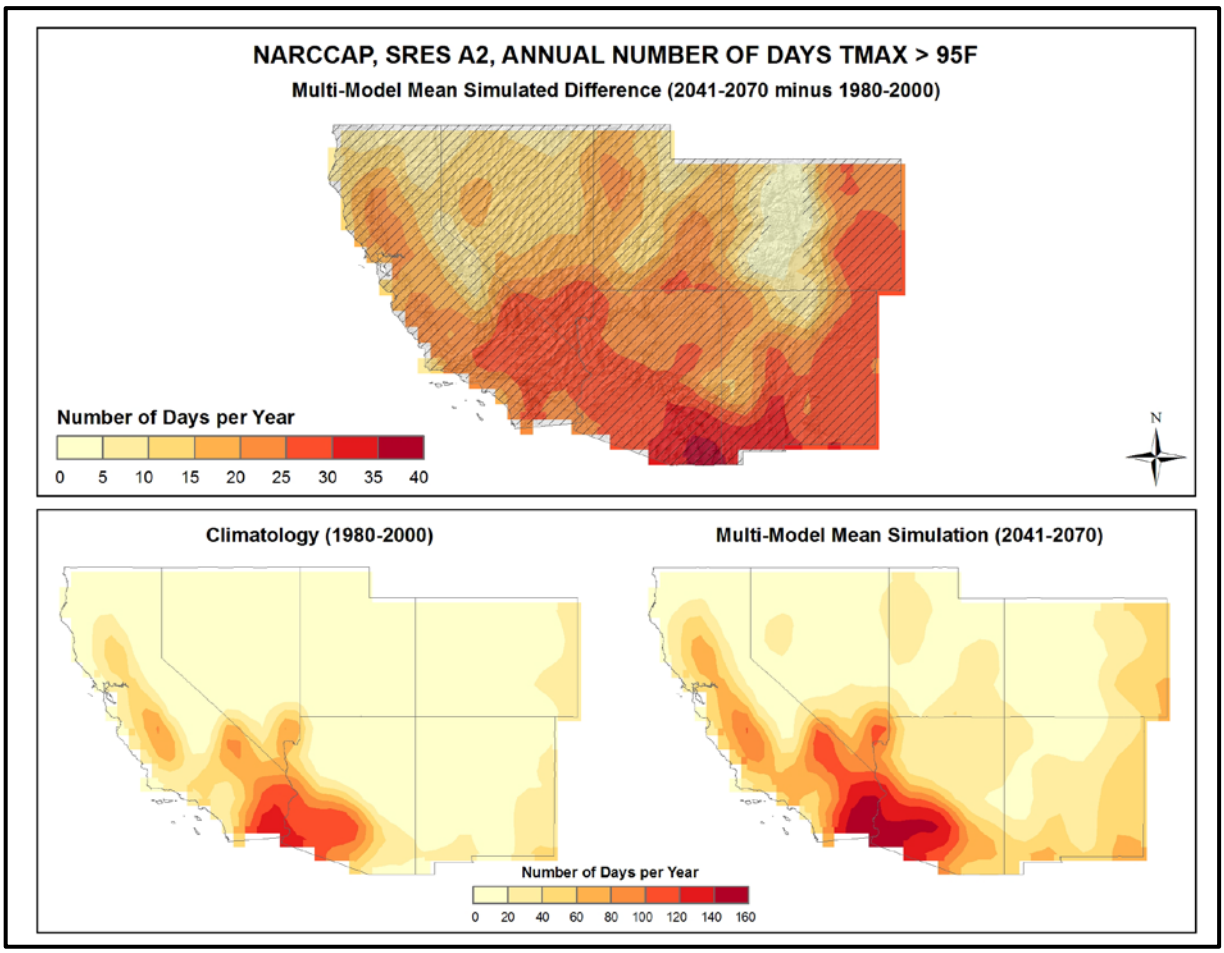

Figure 18. Simulated difference in the mean annual number of days with a maximum temperature greater than 95°F (T_{max} > 95°F) for the Southwest region, for the 2041-2070 time period with respect to the reference period of 1980-2000 (top). Color only (category 1) indicates that less than 50% of the models show a statistically significant change in the number of days. Color with hatching (category 3) indicates that more than 50% of the models show a statistically significant change in the number of days, and more than 67% agree on the sign of the change (see text). Mean annual number of days with T_{max} > 95°F for the 1980-2000 reference period (bottom left). Simulated mean annual number of days with T_{max} > 95°F for the 2041-2070 future time period (bottom right). These are multi-model means from 8 NARCCAP regional climate simulations for the high (A2) emissions scenario. Note that top and bottom color scales are different. The changes are upward everywhere. Increases are smallest at high elevations and largest in the far south of the region.

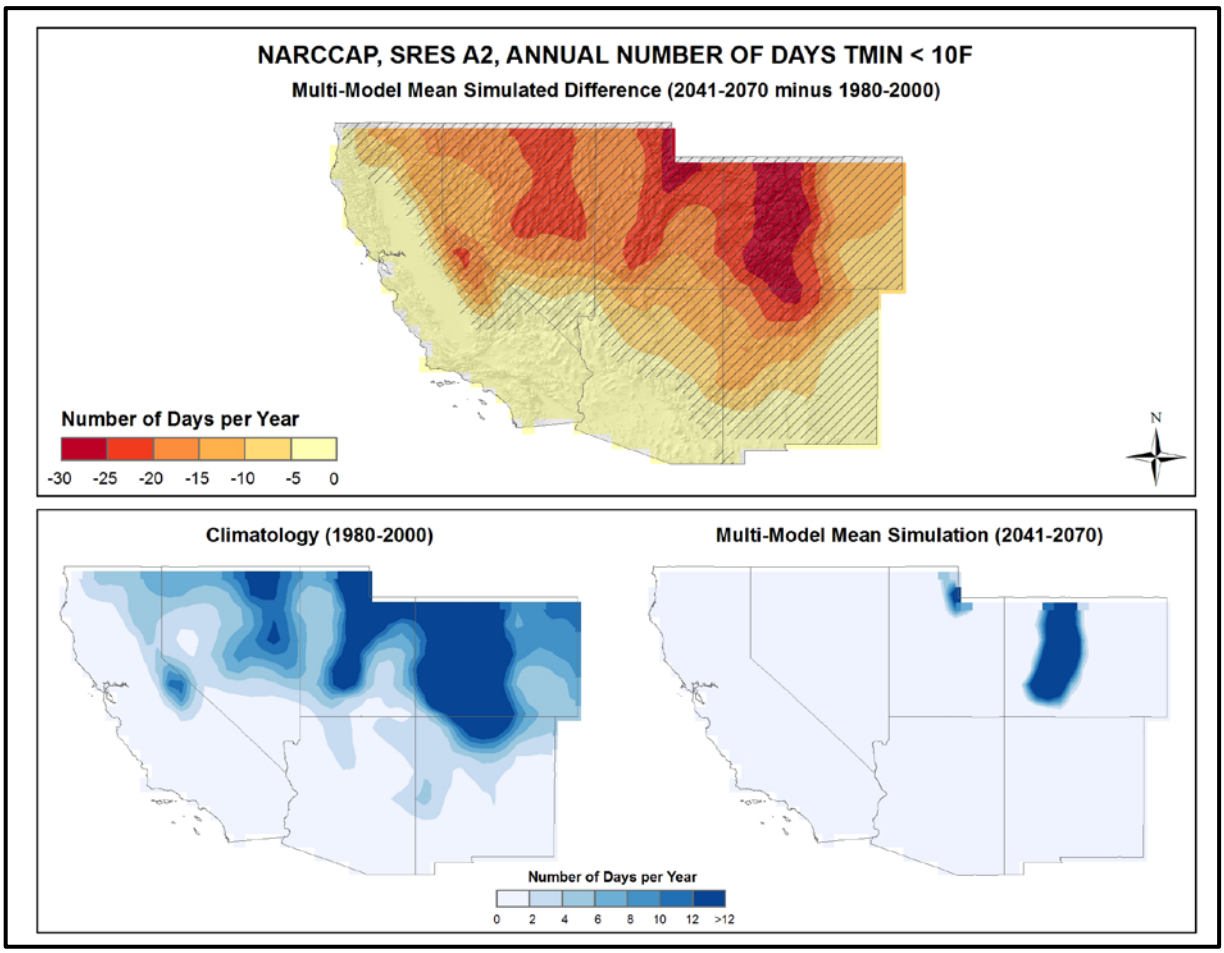

Figure 19. Simulated difference in the mean annual number of days with a minimum temperature less than 10°F (T_{min} < 10°F) for the Southwest region, for the 2041-2070 time period with respect to the reference period of 1980-2000 (top). Color only (category 1) indicates that less than 50% of the models show a statistically significant change in the number of days. Color with hatching (category 3) indicates that more than 50% of the models show a statistically significant change in the number of days, and more than 67% agree on the sign of the change (see text). Mean annual number of days with T_{min} < 10°F for the 1980-2000 reference period (bottom left). Simulated mean annual number of days with T_{min} < 10°F for the 2041-2070 future time period (bottom right). These are multi-model means from 8 NARCCAP regional climate simulations for the high (A2) emissions scenario. Decreases are largest in the northeast and at high elevations and are smallest in the south and west, in a pattern similar to the present-day climatology.

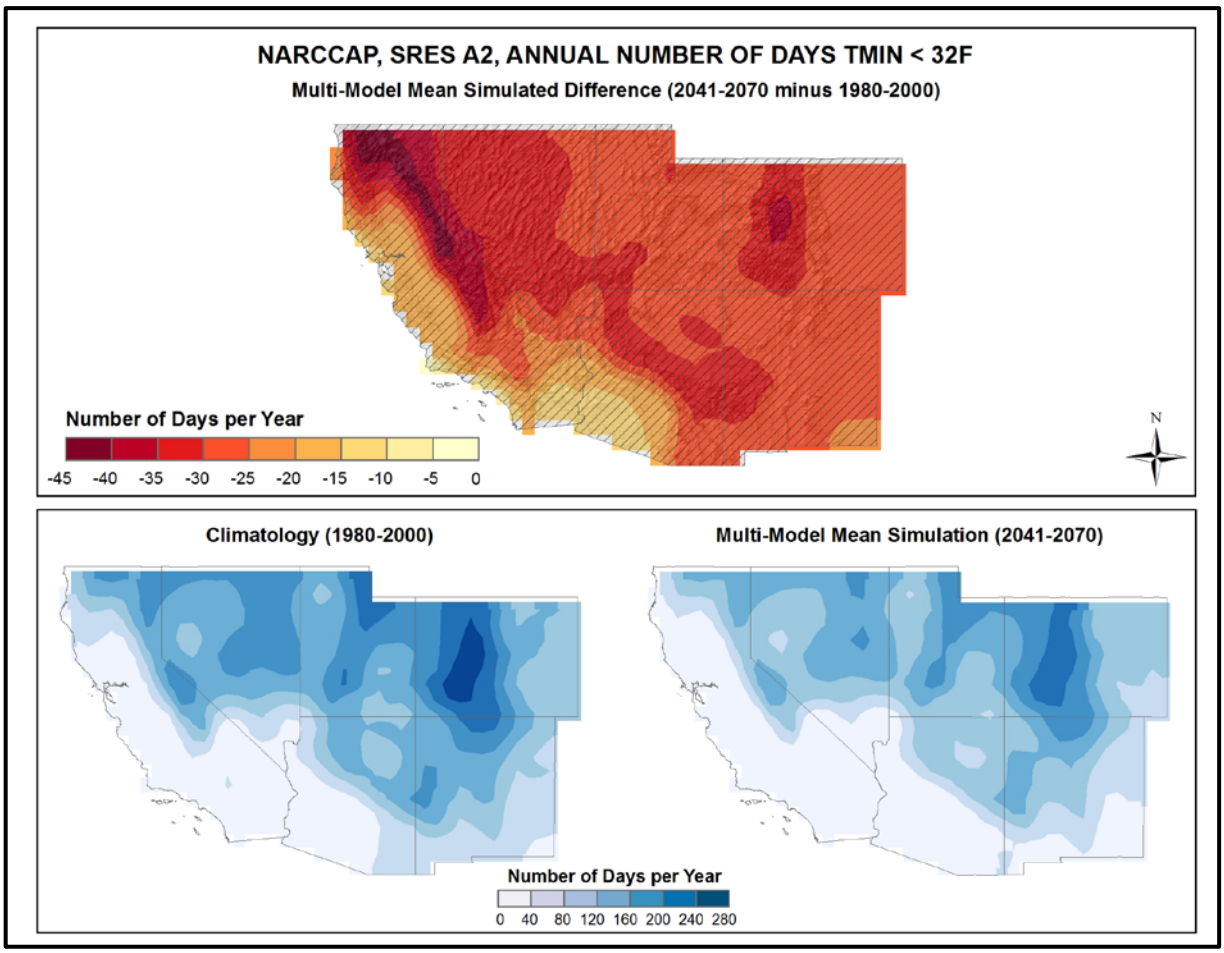

Figure 20. Simulated difference in the mean annual number of days with a minimum temperature less than 32°F (T_{min} < 32°F) for the Southwest region, for the 2041-2070 time period with respect to the reference period of 1980-2000 (top). Color with hatching (category 3) indicates that more than 50% of the models show a statistically significant change in the number of days, and more than 67% agree on the sign of the change (see text). Mean annual number of days with T_{min} < 32°F for the 1980-2000 reference period (bottom left). Simulated mean annual number of days with T_{min} < 32°F for the 2041-2070 future time period (bottom right). These are multi-model means from 8 NARCCAP regional climate simulations for the high (A2) emissions scenario. Changes are downward everywhere. Decreases are largest in high elevation areas and smallest along the coast, as well as southern California and Arizona.

Consecutive warm days can have large impacts on a geographic area and its population and are analyzed here as one metric of heat waves, which have been seen to increase in recent years in the Southwest. Figure 21 shows the NARCCAP multi-model mean change in the average annual maximum number of consecutive days with maximum temperatures exceeding 95°F between 2055 and the model reference period of 1980-2000, for the high (A2) emissions scenario. The pattern is similar to that of the change in the total number of days exceeding 95°F. In interior southern areas, the average annual longest string of days with such high temperatures is simulated to increase by 20 days or more. In most other areas outside of high elevation areas, the increases are generally in the range of 8-16 days. All grid points again satisfy category 3, with the models indicating that the changes in the number of consecutive days over 95°F across the Southwest are statistically significant. The models also agree on the sign of change, i.e. the models are in agreement that the number of consecutive days above 95°F will increase throughout the region under this scenario. The only exception is for areas along the Rocky Mountains, where changes are not simulated to be statistically significant (category 1).

3.5. Other Temperature Variables

The spatial distribution of the NARCCAP multi-model mean change in the average length of the freeze-free season between 2055 and the model reference period of 1980-2000, for the high (A2) emissions scenario, is shown in Fig. 22. The freeze-free season is defined as the period of time between the last spring frost (a daily minimum temperature of less than 32°F) and the first fall frost. This metric has increased significantly over the past century, a trend that is simulated to continue, with increases of at least 20 more days in the annual freeze-free season across most of the region by 2055. The largest simulated increases are in the interior of California, with values of greater than 35 days. Other areas show increases on the order of 3-4 weeks. All grid points satisfy category 3, with the models indicating that the changes in the length of the freeze-free season across the Southwest are statistically significant. The models also agree on the sign of change, i.e. the models are in agreement that the freeze-free season length will increase throughout the region under this scenario.

Cooling and heating degree days are accumulative metrics related to energy use, more specifically regarding the cooling and heating of buildings, with a base temperature of 65°F, assumed to be the threshold below which heating is required and above which cooling is required. Heating degree days provide a measure of the extent (in degrees), and duration (in days), that the daily mean temperature is below the base temperature. Cooling degree days measure the extent and duration that the daily mean temperature is above the base temperature.

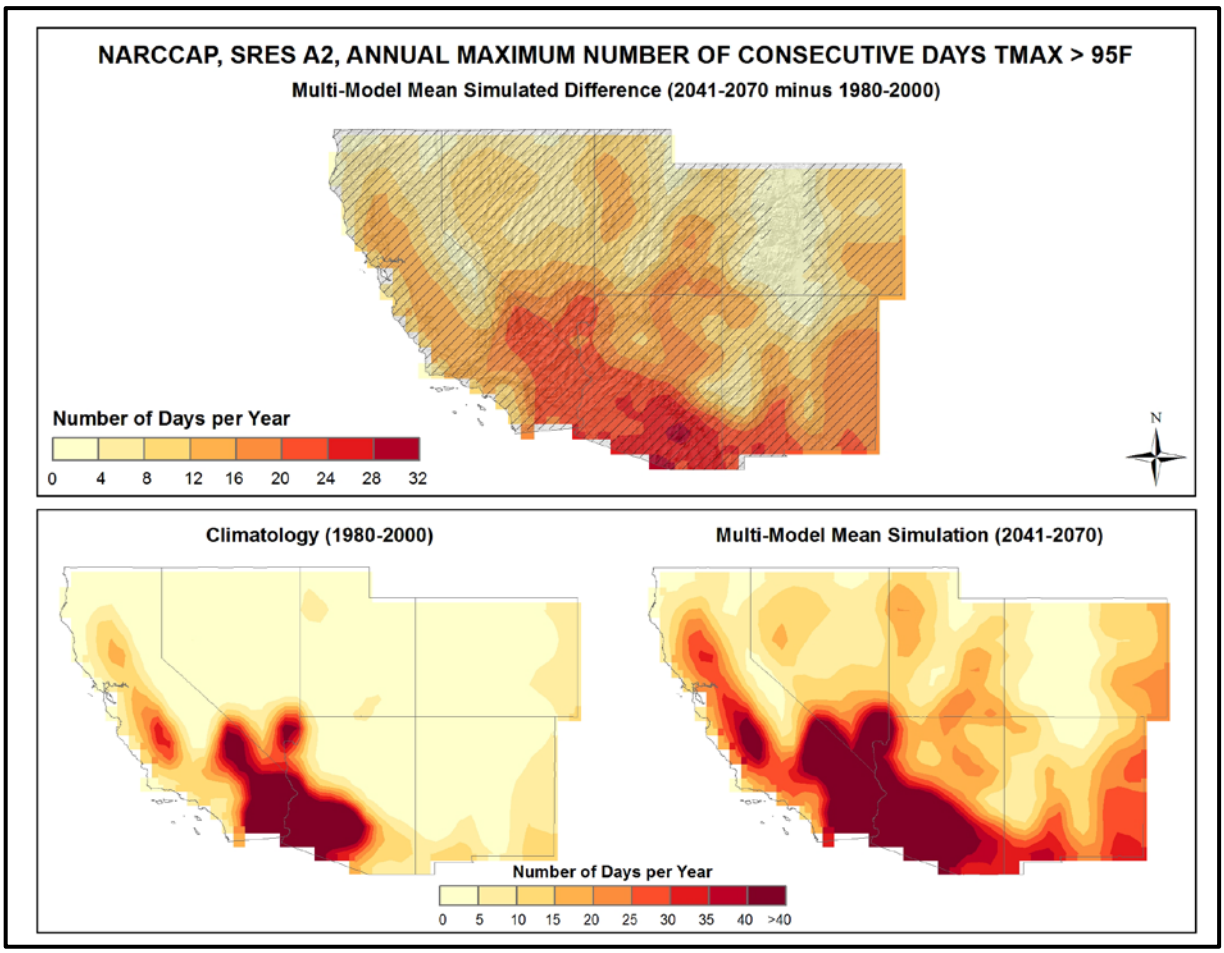

Figure 21. Simulated difference in the mean annual maximum number of consecutive days with a maximum temperature greater than 95°F (T_{max} > 95°F) for the Southwest region, for the 2041-2070 time period with respect to the reference period of 1980-2000 (top). Color only (category 1) indicates that less than 50% of the models show a statistically significant change in the number of consecutive days. Color with hatching (category 3) indicates that more than 50% of the models show a statistically significant change in the number of consecutive days, and more than 67% agree on the sign of the change (see text). Mean annual maximum number of consecutive days with T_{max} > 95°F for the 1980-2000 reference period (bottom left). Simulated mean annual maximum number of consecutive days with T_{max} > 95°F for the 2041-2070 future time period (bottom right). These are multi-model means from 8 NARCCAP regional climate simulations for the high (A2) emissions scenario. Note that top and bottom color scales are different. Increases are largest in the south and smallest in areas of high elevation, with a pattern similar to the present-day climatology.

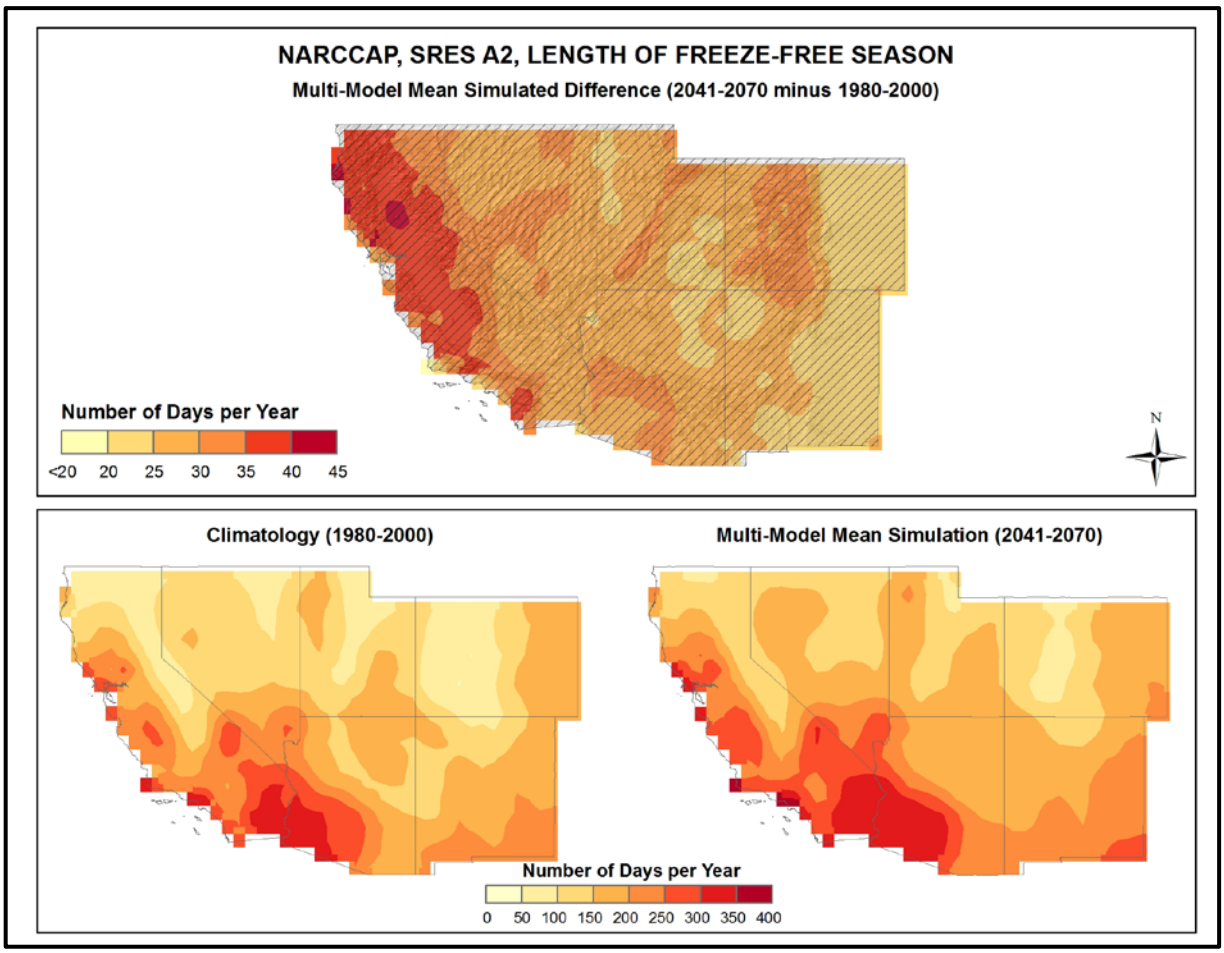

Figure 22. Simulated difference in the mean annual length of the freeze-free season for the Southwest region, for the 2041-2070 time period with respect to the reference period of 1980-2000 (top). Color with hatching (category 3) indicates that more than 50% of the models show a statistically significant change in in the length of the freeze-free season, and more than 67% agree on the sign of the change (see text). Annual mean length of the freeze-free season for the 1980-2000 reference period (bottom left). Simulated mean annual length of the freeze-free season for the 2041-2070 future time period (bottom right). These are multi-model means from 8 NARCCAP regional climate simulations for the high (A2) emissions scenario. Note that top and bottom color scales are different. The length of the freeze-freeze season is simulated to increase throughout the region, with the greatest changes in the west.

Figure 23 shows the NARCCAP multi-model mean change in the average annual number of cooling degree days between 2055 and the model reference period of 1980-2000, for the high (A2) emissions scenario. In general, the simulated changes are quite closely related to mean temperature with the warmest (coolest) areas showing the largest (smallest) changes. The hottest areas, such as southern California and Arizona, are simulated to have the largest increase of up to 1,000 cooling degree days (CDDs) per year. Areas with the highest elevations, including the Rockies and parts of the Sierra Nevada, have the smallest simulated increases of 200 CDDs or less. The models indicate that the changes in cooling degree days across the Southwest are statistically significant. The models also agree on the sign of change, with all grid points satisfying category 3, i.e. the models are in agreement that the number of CDDs will increase throughout the region under this scenario.

The NARCCAP multi-model mean change in the average annual number of heating degree days between 2055 and the model reference period of 1980-2000, for the high (A2) emissions scenario, is shown in Fig. 24. A decrease of at least 700 heating degree days (HDDs) per year is simulated for the majority of the region, with the exception of parts of central and southern California and southern Arizona, where changes are as low as 500 HDDs. The largest changes occur in higher elevation areas, where decreases of up to 1,900 HDDs are simulated. The models once again indicate that the changes across the Southwest are statistically significant. All grid points satisfy category 3, with the models also agreeing on the sign of change, i.e. the models are in agreement that the number of HDDs will decrease throughout the region under this scenario.

3.6. Tabular Summary of Selected Temperature Variables

The mean changes for select temperature-based variables derived from 8 NARCCAP simulations for 2055 with respect to the model reference period of 1971-2000, for the high (A2) emissions scenario, are summarized in Table 5. These were determined by first calculating the derived variable at each grid point. The spatially-averaged value of the variable was then calculated for the reference and future periods. Finally, the difference or ratio between the two periods was calculated from the spatially-averaged values. In addition, these same variables were calculated from the 8 CMIP3 daily statistically-downscaled data set (Daily_CMIP3) simulations for comparison.

For the NARCCAP simulations, the multi-model mean freeze-free period over the Southwest region is simulated to increase by 30 days, comparable to the 31 days calculated for the CMIP3 daily statistically-downscaled data. The number of days with daily maximum temperatures greater than 90°F, 95°F, and 100°F are simulated to increase by 24, 20, and 15 days, respectively, for the NARCCAP models. For the Daily_CMIP3 data, corresponding increases are 31, 24, and 14 days, with values decreasing by a greater amount as the thresholds become more extreme.

The number of days with minimum temperatures of less than 32°F, 10°F, and 0°F are simulated to decrease by 29, 11, and 5 days, respectively, for the NARCCAP models. Corresponding values for the Daily_CMIP3 simulations are comparable decreases of 29, 8, and 3 days.

The multi-model mean annual maximum number of consecutive days exceeding 95°F and 100°F are simulated to increase by 82% and 103% respectively for the NARCCAP data. These increases are greater for the Daily_CMIP3 simulations, with values of 114% for the 95°F threshold, and 158% for the 100°F threshold.

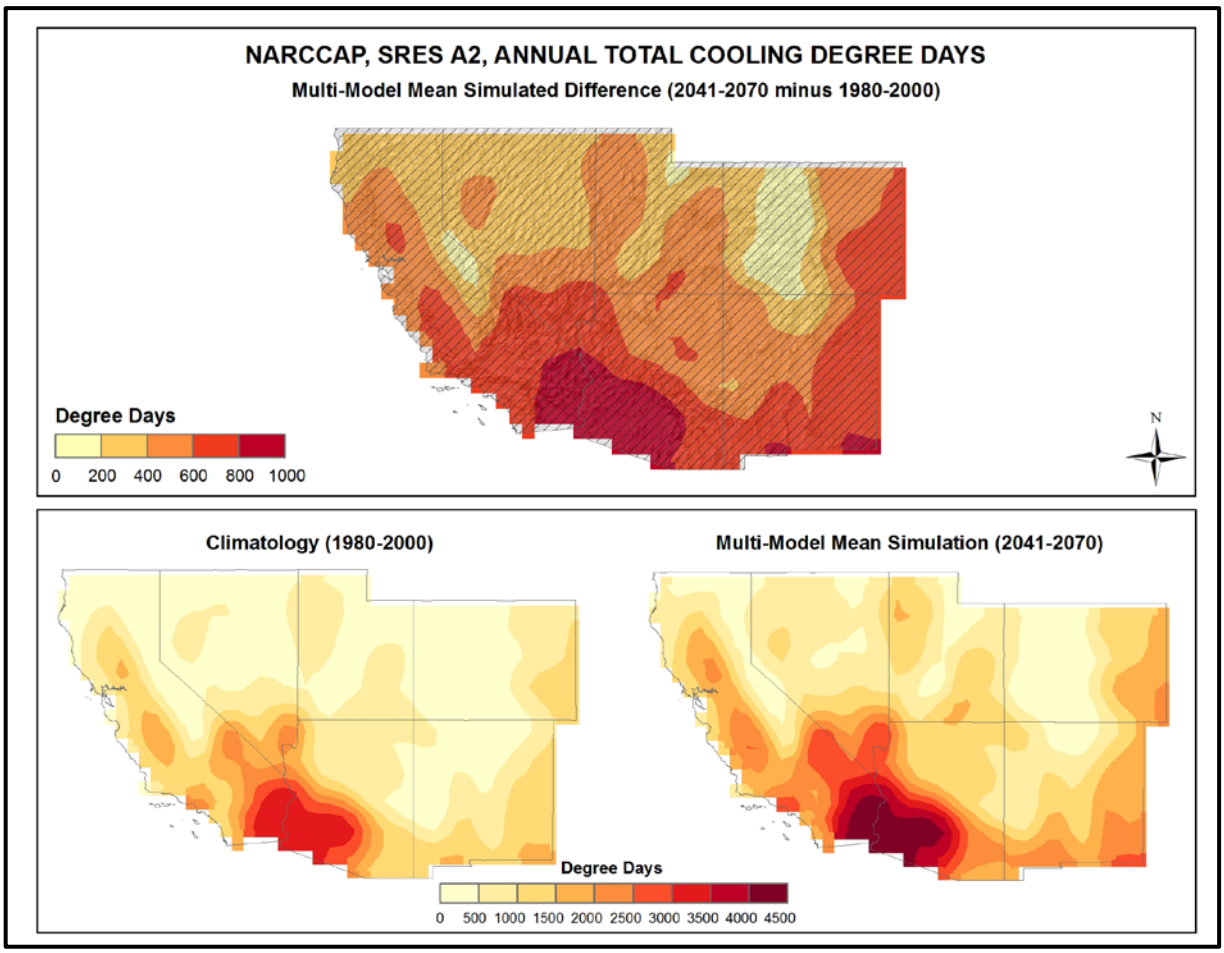

Figure 23. Simulated difference in the mean annual number of cooling degree days for the Southwest region, for the 2041-2070 time period with respect to the reference period of 1980-2000 (top). Color with hatching (category 3) indicates that more than 50% of the models show a statistically significant change in the number of cooling degree days, and more than 67% agree on the sign of the change (see text). Mean annual number of cooling degree days for the 1980-2000 reference period (bottom left). Simulated mean annual number of cooling degree days for the 2041-2070 future time period (bottom right). These are multi-model means from 8 NARCCAP regional climate simulations for the high (A2) emissions scenario. Note that top and bottom color scales are different. There are increases everywhere with the changes becoming larger from north to south.

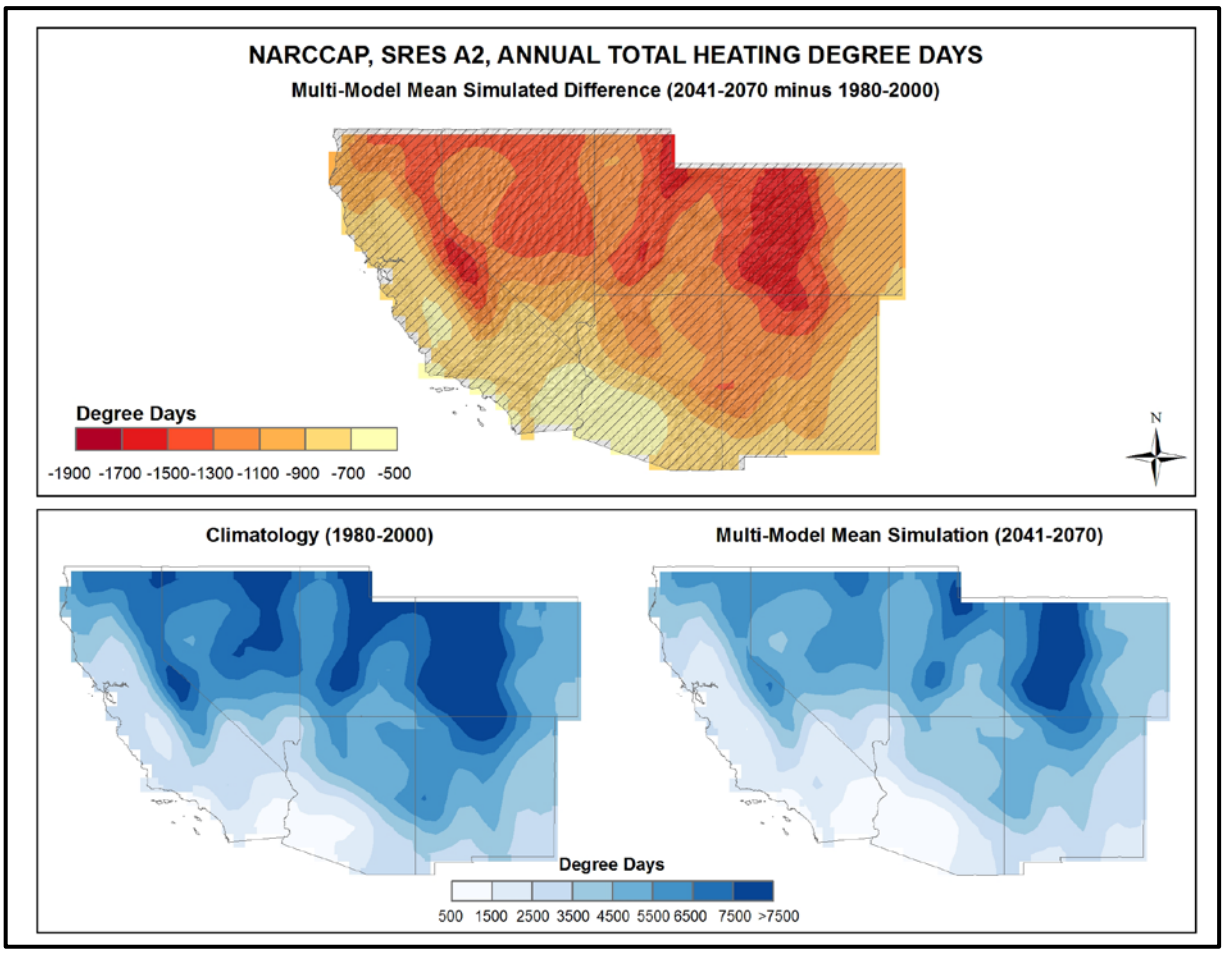

Figure 24. Simulated difference in the mean annual number of heating degree days for the Southwest region, for the 2041-2070 time period with respect to the reference period of 1980-2000 (top). Color with hatching (category 3) indicates that more than 50% of the models show a statistically significant change in the number of heating degree days, and more than 67% agree on the sign of the change (see text). Mean annual number of heating degree days for the 1980-2000 reference period (bottom left). Simulated mean annual number of heating degree days for the 2041-2070 future time period (bottom right). These are multi-model means from 8 NARCCAP regional climate simulations for the high (A2) emissions scenario. There are decreases everywhere with the largest changes in high elevation areas.

Table 5. Multi-model means and standard deviations of the simulated annual mean change in select temperature variables from 8 NARCCAP simulations for the Southwest region. Multi-model means from the 8 Daily_CMIP3 simulations are also shown for comparison. Analyses are for the 2041-2070 time period with respect to the reference period of 1971-2000, for the high (A2) emissions scenario.

Temperature Variable	NARCCAP Mean	NARCCAP Standard Deviation	Daily_CMIP3 Mean
Freeze-free period	+30 days	3 days	+31 days
#days T_{max} > 90°F	+24 days	4 days	+31 days
#days T_{max} > 95°F	+20 days	7 days	+24 days
#days T_{max} > 100°F	+15 days	9 days	+14 days
#days T_{min} < 32°F	-29 days	3 days	-29 days
#days T_{min} < 10°F	-11 days	5 days	-8 days
#days T_{min} < 0°F	-5 days	3 days	-3 days
Consecutive #days > 95°F	+82%	44%	+114%
Consecutive #days > 100°F	+103%	74%	+158%
Heating degree days	-18%	1%	-19%
Cooling degree days	+64%	19%	+65%
Growing degree days (base 50°F)	+34%	5%	+34%

Table 5 indicates that that, for the high (A2) emissions scenario, the number of heating degree days are simulated by the NARCCAP simulations to decrease by 18% (19% for Daily_CMIP3), while the number of cooling degree days are simulated to increase by 64% (65% for Daily_CMIP3). The number of growing degree days (base 50°F) are also comparable for both data sets, increasing by 34% for both NARCCAP and Daily_CMIP3.

3.7. Mean Precipitation

Figure 25 shows the spatial distribution of multi-model mean simulated differences in average annual precipitation for the three future time periods (2035, 2055, 2085) with respect to 1971-1999, for both emissions scenarios, for the 14 (B1) or 15 (A2) CMIP3 models. Generally, there is a north-south gradient in precipitation changes. The far southern regions show the largest decreases while the far northern areas show slight increases. This gradient increases in magnitude as the time progresses for the high (A2) emissions scenario. The gradient in the low (B1) emissions scenario is the strongest for 2055, but drops off by 2085. The largest north-south differences are for the A2 scenario in 2085, varying from an increase of 2% in the far north to a decrease of 12% in the far southwest. The agreement between models was once again assessed using the three categories described in Fig. 14. It can be seen that for the 2035 time period the changes in precipitation are not significant for most models (category 1) over all grid points. This means that most models are in agreement that any changes will be smaller than the normal year-to-year variations that occur. For the high emissions scenario in 2055, most models indicate changes that are larger than these normal variations (category 3) in the southeastern part of the region. For the low emissions scenario, the models again show changes that are not statistically significant. Significant changes are indicated by most models in 2085 for the high emissions scenario across a large part of the region, however, the models are in disagreement about the sign of the changes (category 2) in the northern third of the area.

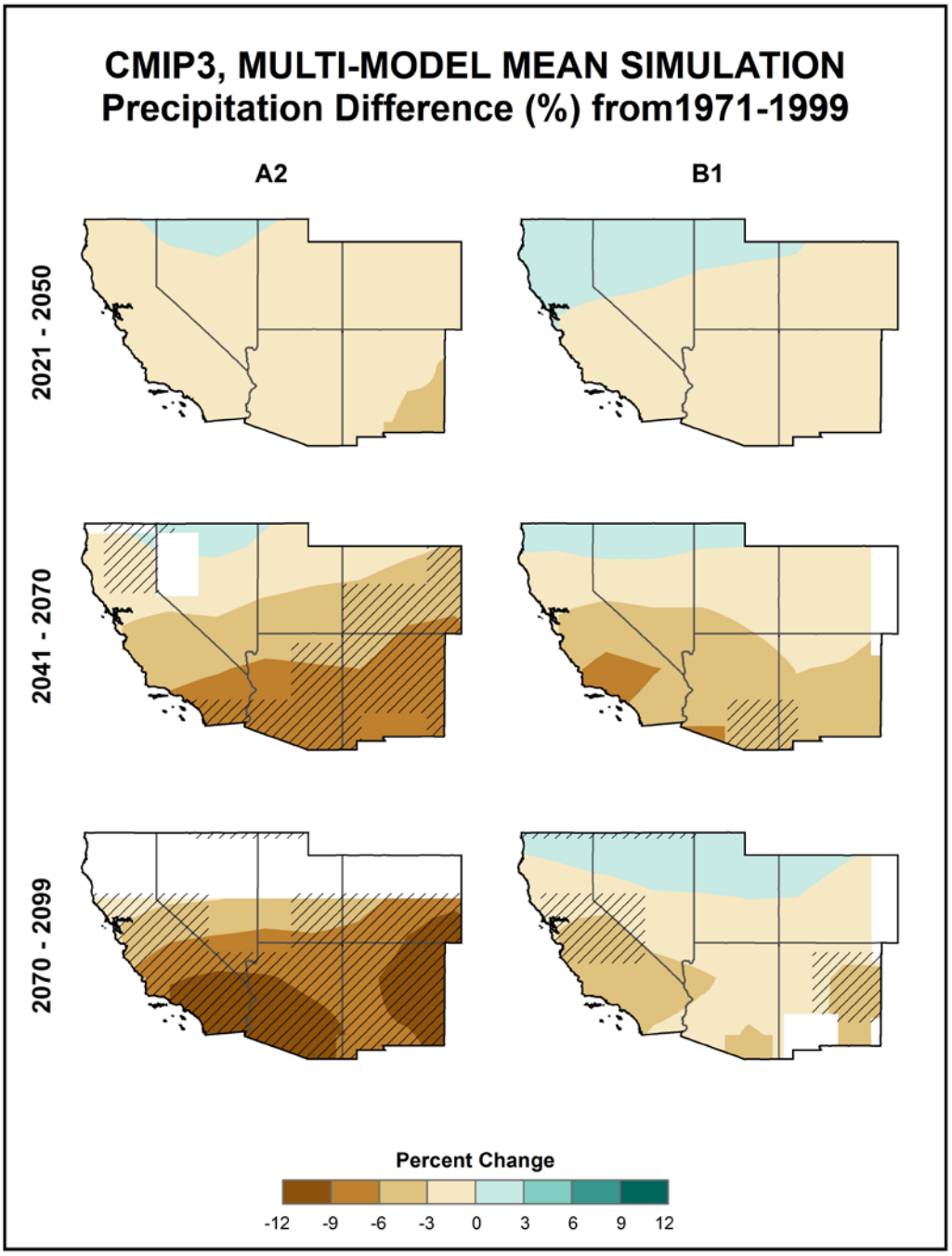

Figure 25. Simulated difference in annual mean precipitation (%) for the Southwest region, for each future time period (2021-2050, 2041-2070, and 2070-2099) with respect to the reference period of 1971-1999. These are multi-model means for the high (A2) and low (B1) emissions scenarios from the 14 (B1) or 15 (A2) CMIP3 global climate simulations. Color only (category 1) indicates that less than 50% of the models show a statistically significant change in precipitation. Color with hatching (category 3) indicates that more than 50% of the models show a statistically significant change in precipitation, and more than 67% agree on the sign of the change. Whited out areas (category 2) indicate that more than 50% of the models show a statistically significant change in precipitation, but less than 67% agree of the sign of the change (see text). Generally, the models simulate increases in the far north, but decreases in the majority of the region.

Table 6 shows the distribution of simulated changes in annual mean precipitation for each future time period with respect to 1971-1999, for both emissions scenarios, among the 14 (B1) or 15 (A2) CMIP3 models. The distribution of 9 NARCCAP simulations (for 2055, high (A2) emissions scenario only) is also shown for comparison, with respect to 1971-2000. Historically, there has been no discernible trend in annual precipitation, and for all three time periods and both scenarios, the CMIP3 model simulations indicate both increases and decreases in precipitation. Most of the median values are negative, but small (3% or less). The inter-model range of changes in precipitation (i.e. the difference between the highest and lowest model values) varies from 13 to 28%. For example, in the A2 scenario the precipitation change for 2055 varies from a low of -17% to a high of +7%. The NARCCAP values range from -13% to -2% (for A2, 2055). The interquartile range (the difference between the 75th and 25th percentiles) of precipitation changes across all the GCMs is less than 13%.

Table 6. Distribution of the simulated change in annual mean precipitation (%) from the 14 (B1) or 15 (A2) CMIP3 models for the Southwest region. The lowest, 25th percentile, median, 75th percentile and highest values are given for the high (A2) and low (B1) emissions scenarios, and for each future time period (2021-2050, 2041-2070, and 2070-2099) with respect to the reference period of 1971-1999. Also shown are values from the distribution of 9 NARCCAP models for 2041-2070, A2 only, with respect to 1971-2000.

Scenario	**Period**	**Lowest**	**25th Percentile**	**Median**	**75th Percentile**	**Highest**
A2	2021-2050	-10	-3	-2	2	5
	2041-2070	-17	-6	-3	1	7
	2070-2099	-20	-10	-3	3	8
	NARCCAP (2041-2070)	*-13*	*-7*	*-3*	*-3*	*-2*
B1	2021-2050	-10	-3	1	3	7
	2041-2070	-10	-3	-2	0	3
	2070-2099	-10	-5	-2	1	10

Figure 26 shows the multi-model mean annual and seasonal 30-year average precipitation change between 2041-2070 and 1971-2000 for the high (A2) emissions scenario, for 11 NARCCAP regional climate model simulations. The annual changes are mostly downward with the largest decreases occurring over the Sierra Nevada and southern parts of Arizona and New Mexico. The exception is in parts of Nevada and Utah, which see simulated increases of up to 6%. Winter (the wettest season) has the smallest variability, ranging from -10 to greater than +15%. Spring changes are mostly downward with the largest decreases simulated in parts of California, Arizona, and New Mexico. The largest variability occurs in summer, ranging from decreases of more than 15% to increases of more than 15%. Simulated fall changes are mostly downward, but smaller in magnitude. The agreement between models was again assessed using the three categories described in Fig. 14. It can be seen that annually, and for all seasons, the simulated changes in precipitation are not statistically significant for most models over the majority of grid points (category 1). The models are in agreement (category 3), however, for some southern parts of the region for the spring simulation, for scattered areas in the north and east for summer, and for a small region of southern California for fall. The models are in disagreement about the sign of the change (category 2) for a few small areas in southern California for the summer and fall seasons.

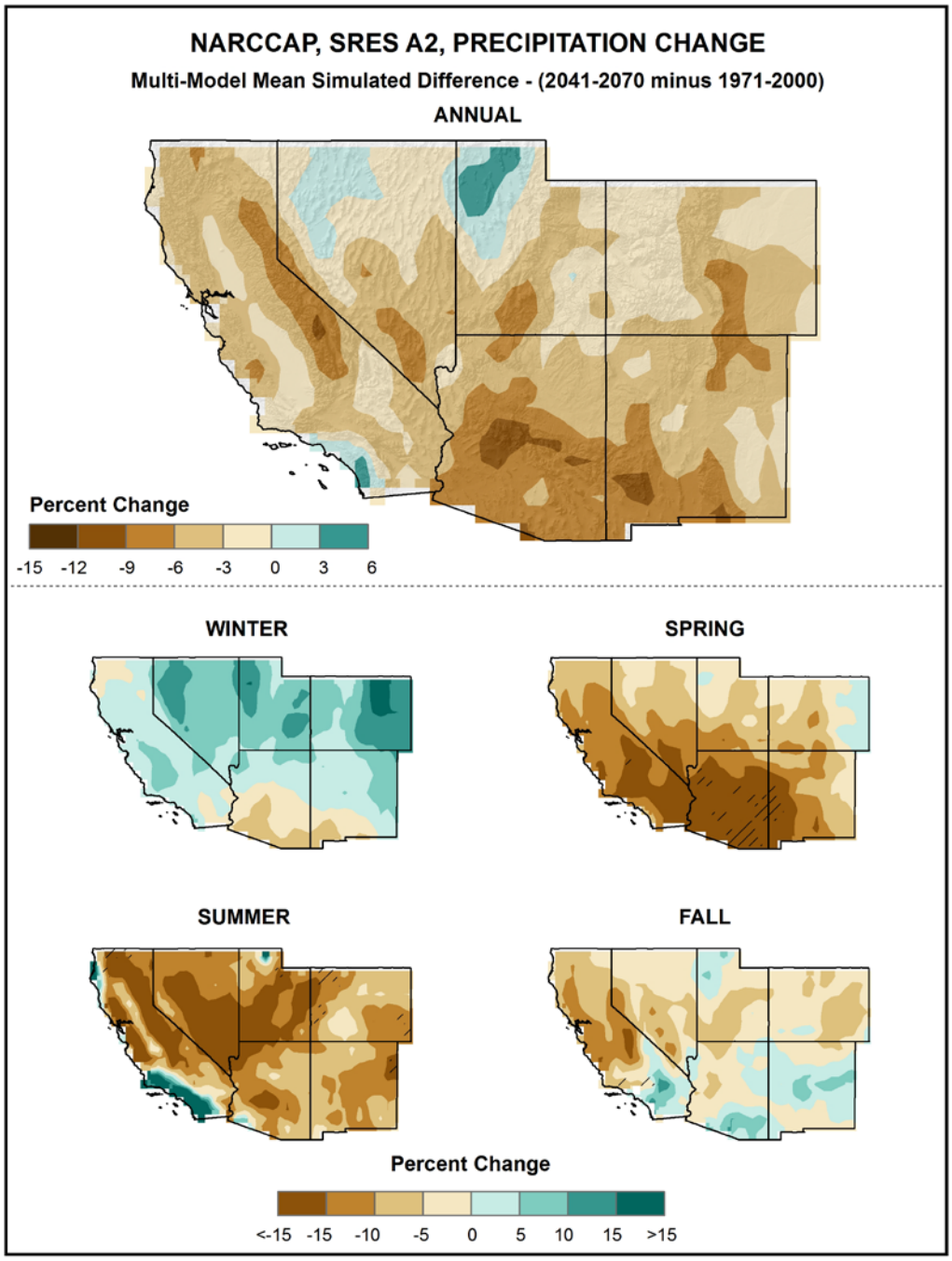

Figure 26. Simulated difference in annual and seasonal mean precipitation (%) for the Southwest region, for 2041-2070 with respect to the reference period of 1971-2000. These are multi-model means from 11 NARCCAP regional climate simulations for the high (A2) emissions scenario. Color only (category 1) indicates that less than 50% of the models show a statistically significant change in precipitation. Color with hatching (category 3) indicates that more than 50% of the models show a statistically significant change in precipitation, and more than 67% agree on the sign of the change. Whited out areas (category 2) indicate that more than 50% of the models show a statistically significant change in precipitation, but less than 67% agree of the sign of the change (see text). Note that top and bottom color scales are unique, and different from that of Fig. 25. The annual change is upward in the far north and downward throughout the remainder of the region. Changes are mostly upward in winter, and downward in spring, summer, and fall.

Table 7 shows the distribution of simulated changes in seasonal mean precipitation among the 14 (B1) or 15 (A2) CMIP3 models between 2070-2099 and 1971-1999, for both emissions scenarios, with each model's values averaged over the entire region. On a seasonal basis, the range of region-averaged model-simulated changes is quite large. For example, in the high (A2) emissions scenario, the change in summer precipitation varies from a decrease of 44% to an increase of 20%. A majority of the models simulate increases in winter precipitation. In the other three seasons, most of the models simulate decreases. In the spring, all but one model simulate decreases. In both the summer and fall, a few models simulate sizeable increases in precipitation. In the low (B1) emissions scenario, the range of changes in precipitation is generally smaller. The central feature of the results in Table 7 is the large uncertainty in seasonal precipitation changes.

Table 7. Distribution of the simulated change in seasonal mean precipitation (%) from the 14 (B1) or 15 (A2) CMIP3 models for the Southwest region. The lowest, 25th percentile, median, 75th percentile and highest values are given for the high (A2) and low (B1) emissions scenarios, and for the 2070-2099 time period with respect to the reference period of 1971-1999.

Scenario	Period	Season	Lowest	25th Percentile	Median	75th Percentile	Highest
A2	2070-2099	DJF	-19	-8	3	8	31
		MAM	-36	-29	-12	-10	2
		JJA	-44	-13	-9	3	20
		SON	-21	-8	-1	-1	38
B1	2070-2099	DJF	-12	-6	2	5	17
		MAM	-27	-9	-7	-1	11
		JJA	-16	-7	0	3	18
		SON	-24	-4	-2	6	13

Figure 27 shows the simulated change in annual mean precipitation for each future time period with respect to1971-1999, for both emissions scenarios, averaged over the entire Southwest region for the 14 (B1) or 15 (A2) CMIP3 models. In addition, averages for 9 of the NARCCAP simulations (relative to 1971-2000) and the 4 GCMs used in the NARCCAP experiment are shown for 2055 (A2 scenario only). Both the multi-model mean and individual model values are shown. All the multi-model mean simulated changes are downward, although the values are rather small overall. For the high (A2) emissions scenario, the CMIP3 models simulate average decreases of 2% in 2035, 4% by 2055, and about 5% by 2085. The decreases for the low (B1) emissions scenario are smaller, reaching a decrease of 1% by 2085. The mean of the NARCCAP simulations is slightly larger in magnitude than the mean of the CMIP3 GCMs or the mean of the 4 GCMs used in the NARCCAP experiment. The range of individual model changes in Fig. 27 is large compared to the differences in the multi-model means, as also illustrated in Table 6. In fact, for both emissions scenarios, the individual model range is much larger than the differences in the CMIP3 multi-model means between time periods.

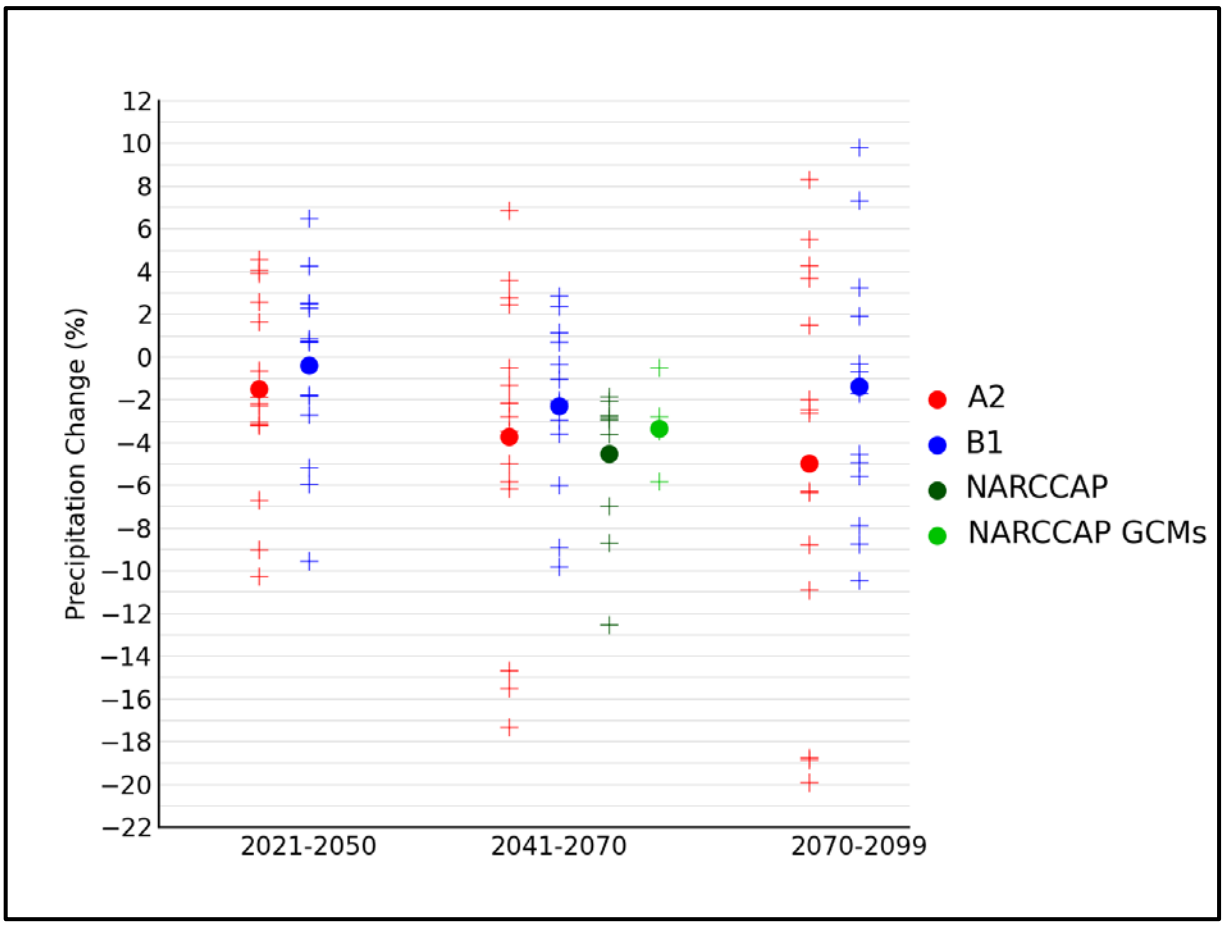

Figure 27. Simulated annual mean precipitation change (%) for the Southwest region, for each future time period (2021-2050, 2041-2070, and 2070-2099) with respect to the reference period of 1971-1999. Values are given for the high (A2) and low (B1) emissions scenarios for the 14 (B1) or 15 (A2) CMIP3 models. Also shown for 2041-2070 (high emissions scenario only) are values for 9 NARCCAP models, as well as for the 4 GCMs used to drive the NARCCAP simulations. The small plus signs indicate each individual model and the circles depict the multi-model means. The range of model-simulated changes is very large compared to the mean changes and to differences between the A2 and B1 scenarios.

Figure 28 shows the simulated change in seasonal mean precipitation for each future time period with respect to 1971-1999, for the high (A2) emissions scenario, averaged over the entire Southwest region for the individual 15 CMIP3 models, as well as the NARCCAP models for 2055, relative to 1971-2000. Again, both the multi-model mean and individual model values are shown. The simulated multi-model mean decreases are largest in the spring, ranging from -6% in 2035 to -17% in 2085. The NARCCAP models, which are displayed for 2055, indicate changes close to the same as the CMIP3 models. As was the case for the annual totals in Fig. 27, the model ranges in Fig. 28 are large compared to the multi-model mean differences. This illustrates the large uncertainty in the precipitation estimates using these simulations.

3.8. Extreme Precipitation

Figure 29 shows the spatial distribution of the multi-model mean change in the average annual number of days with precipitation exceeding 1 inch, for 8 NARCCAP regional climate model simulations. Again this is the difference between the period of 2041-2070 and the 1980-2000 reference period, for the high (A2) emissions scenario. In addition to this difference map, maps of the model simulations of the actual values for historical conditions (NARCCAP models driven by the NCEP Reanalysis II) and for the future are also displayed for comparison. Most areas exhibit simulated increases, the greatest being in parts of northern Nevada, Utah and western Colorado, where changes of up to 130% are simulated. Some areas experience decreases, such as eastern Colorado, Arizona, and the Sierra Nevada. It can be seen that changes in days with precipitation exceeding 1 inch are not statistically significant for most models (category 1) over the majority of the region. This means that most models are in agreement that any changes will be smaller than the normal year-to-year variations that occur under this scenario. In areas where the largest increases are simulated, however, most models indicate changes in days with precipitation of more than 1 inch that are larger than these normal variations (category 3). In a few small areas in southern Arizona the models are in disagreement about the sign of the changes (category 2).

Consecutive days with little or no precipitation can have large impacts on a region. Figure 30 shows the NARCCAP multi-model mean change in the average annual maximum number of consecutive days with precipitation less than 0.1 inches (3 mm) between 2055 and the model reference period of 1980-2000, for the high (A2) emissions scenario. Areas that are already prone to little precipitation are simulated to see an increase of days with little or no precipitation, up to 25 days per year in parts of Nevada, Arizona, and California. Most other areas are simulated to see increases of up to 15 days. There are some areas in Colorado with simulated decreases in days, but these values are very small. In the northeast of the region, as well as parts of central California, changes in the number of consecutive days with precipitation of less than 0.1 inches are not statistically significant for most models (category 1). However, for the majority of the Southwest region, most models indicate statistically significant changes (category 3) under this scenario.

3.9. Tabular Summary of Selected Precipitation Variables

The mean changes for select precipitation-based variables derived from 8 NARCCAP simulations for 2055 with respect to the model reference period of 1971-2000, for the high (A2) emissions scenario, are summarized in Table 8. The same variables from the 8 CMIP3 statistically-downscaled (Daily_CMIP3) simulations are also shown for comparison. These spatially-averaged values were calculated as described for Table 5.

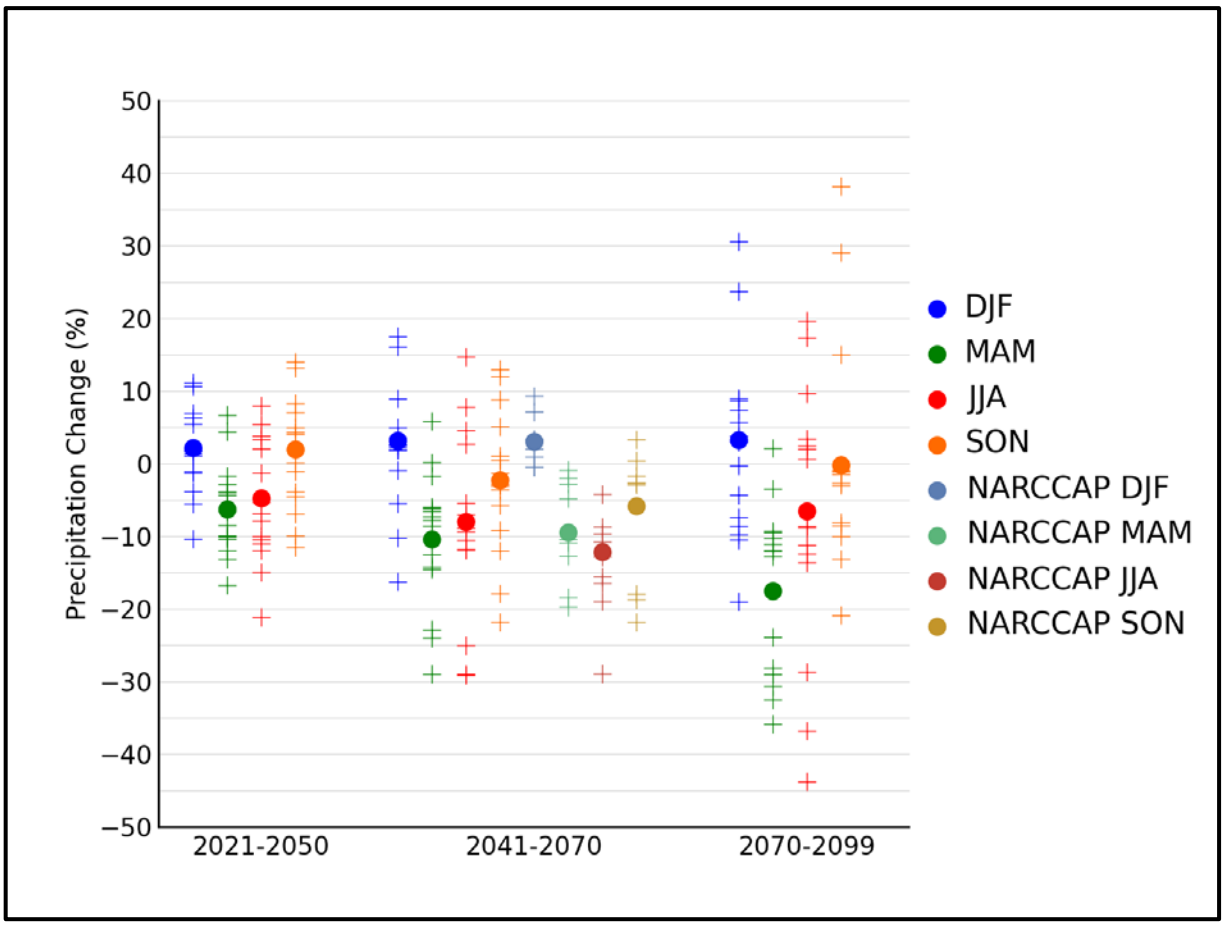

Figure 28. Simulated seasonal mean precipitation change (%) for the Southwest region, for each future time period (2021-2050, 2041-2070, and 2070-2099) with respect to the reference period of 1971-1999. Values are given for all 15 CMIP3 models for the high (A2) emissions scenario. Also shown are values (relative to 1971-2000) for 9 NARCCAP models for 2041-2070. The small plus signs indicate each individual model and the circles depict the multi-model means. Seasons are indicated as follows: winter (DJF, December-January-February), spring (MAM, March-April-May), summer (JJA, June-July-August), and fall (SON, September-October-November). The range of model-simulated changes is large compared to the mean changes and to differences between the seasons.

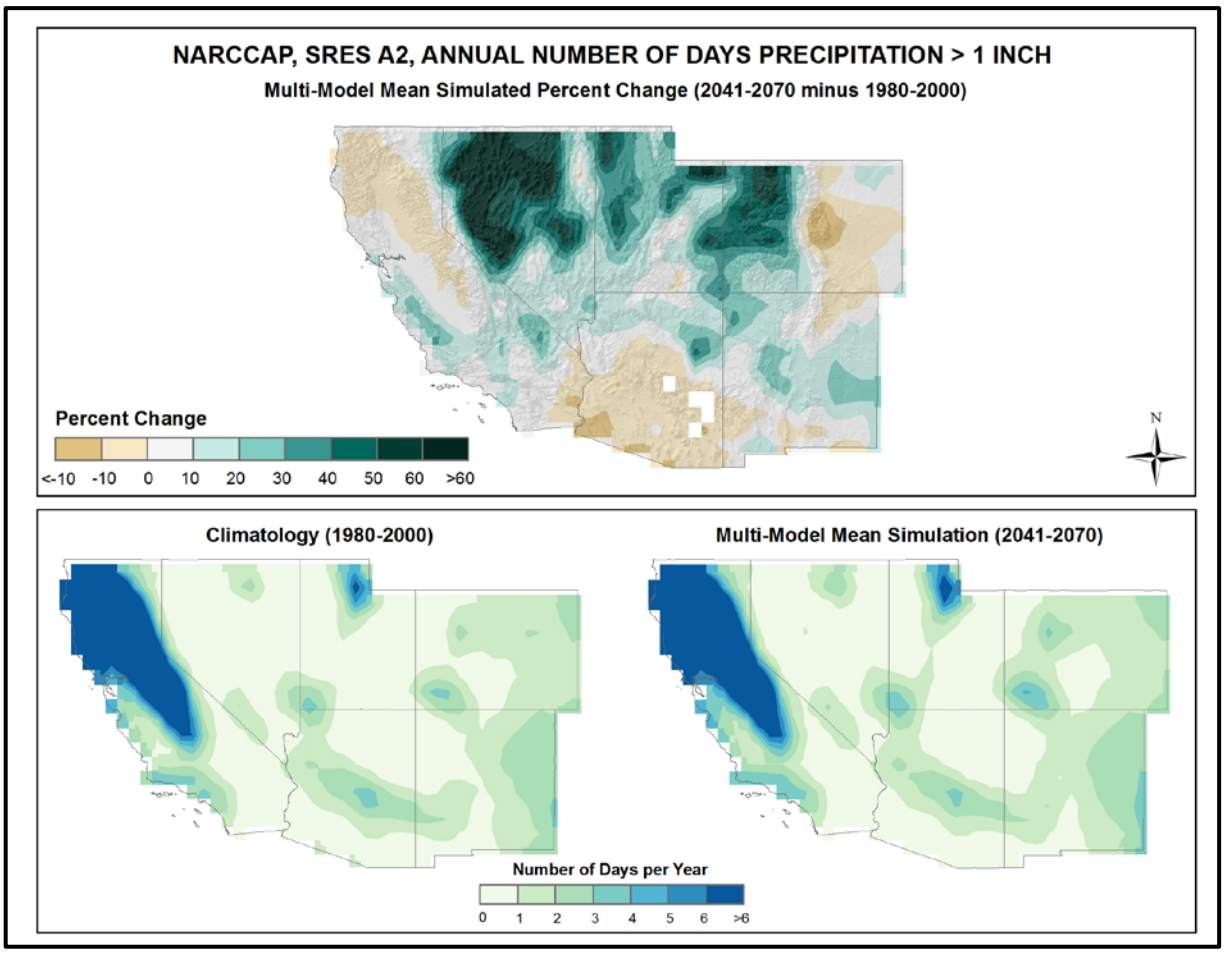

Figure 29. Simulated percentage difference in the mean annual number of days with precipitation of greater than one inch for the Southwest region, for the 2041-2070 time period with respect to the reference period of 1980-2000 (top). Color only (category 1) indicates that less than 50% of the models show a statistically significant change in the number of days. Color with hatching (category 3) indicates that more than 50% of the models show a statistically significant change in the number of days, and more than 67% agree on the sign of the change. Whited out areas (category 2) indicate that more than 50% of the models show a statistically significant change in the number of days, but less than 67% agree of the sign of the change (see text). Mean annual number of days with precipitation of greater than one inch for the 1980-2000 reference period (bottom left). Simulated mean annual number of days with precipitation of greater than one inch for the 2041-2070 future time period (bottom right). These are multi-model means from 8 NARCCAP regional climate simulations for the high (A2) emissions scenario. The models simulate decreases in the south, northeast, and northwest, with increases across the remainder of the region.

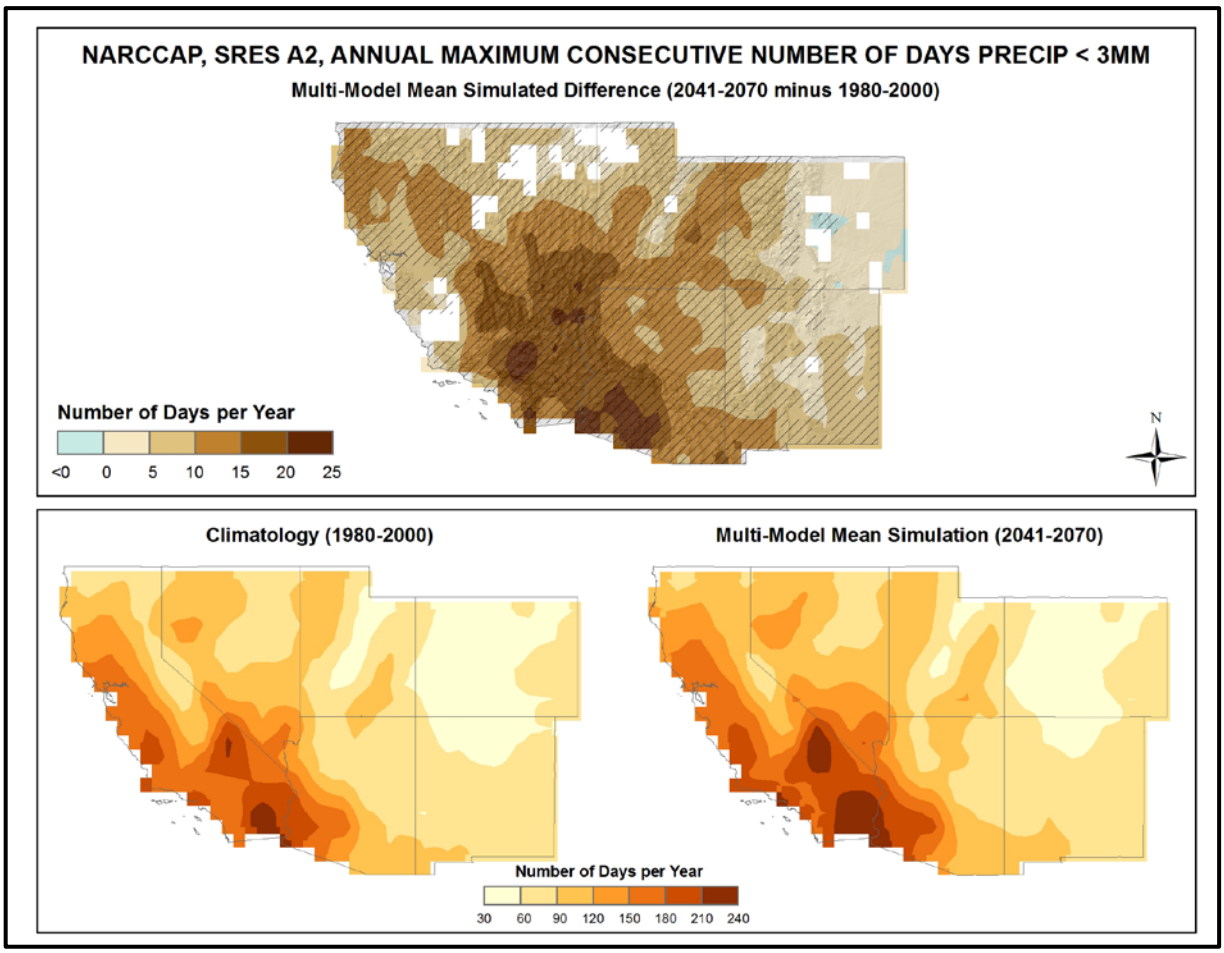

Figure 30. Simulated difference in the mean annual maximum number of consecutive days with precipitation of less than 0.1 inches/3 mm for the Southwest region, for the 2041-2070 time period with respect to the reference period of 1980-2000 (top). Color only (category 1) indicates that less than 50% of the models show a statistically significant change in the number of consecutive days. Color with hatching (category 3) indicates that more than 50% of the models show a statistically significant change in the number of consecutive days, and more than 67% agree on the sign of the change. Whited out areas (category 2) indicate that more than 50% of the models show a statistically significant change in the number of days, but less than 67% agree of the sign of the change (see text). Mean annual maximum number of consecutive days with precipitation of less than 0.1 inches/3 mm for the 1980-2000 reference period (bottom left). Simulated mean annual maximum number of consecutive days with precipitation of less than 0.1 inches/3 mm for the 2041-2070 future time period (bottom right). These are multi-model means from 8 NARCCAP regional climate simulations for the high (A2) emissions scenario. The models simulate increases over the majority of the region, with the greatest changes in the south.

Table 8. Multi-model means and standard deviations of the simulated mean annual change in select precipitation variables from 8 NARCCAP simulations for the Southwest region. Multi-model means from the 8 Daily_CMIP3 simulations are also shown for comparison. Analyses are for the 2041-2070 time period with respect to the reference period of 1971-2000, for the high (A2) emissions scenario.

Precipitation Variable	NARCCAP Mean	NARCCAP Standard Deviation	Daily_CMIP3 Mean
#days > 1 inch	+3%	9%	+12%
#days > 2 inches	+11%	8%	+22%
#days > 3 inches	+20%	10%	+32%
#days > 4 inches	+33%	21%	+44%
Consecutive #days < 0.1 inches	+10 days	+5 days	+8 days

For the NARCCAP data, the multi-model mean number of days with precipitation exceeding 1, 2, 3, and 4 inches are simulated to increase for the high (A2) emissions scenario, with changes of between +3% for a threshold of 1 inch and +33% for 4 inches. Similar to the temperature variables in Table 5, greater increases are seen in Table 8 for the more extreme thresholds. The multi-model means from the CMIP3 statistically-downscaled simulations are higher than their NARCCAP counterparts. The average annual maximum number of consecutive days with precipitation less than 0.1 inches is simulated to increase by 10 days. The corresponding Daily_CMIP3 simulations indicate a comparable increase of 8 days.

3.10. Comparison Between Model Simulations and Observations

In this section, some selected comparisons between CMIP3 model simulations and observations are presented. These are limited to annual and seasonal temperature and precipitation. The model simulations of the 20th century that are shown herein are based on estimated historical forcings of the climate system, including such factors as greenhouse gases, volcanic eruptions, solar variations, and aerosols. Also shown are the simulations of the 21st century for the high (A2) emissions scenario.

In these comparisons, both model and observational data are expressed as deviations from the 1901-1960 average. As explained in Section 2.4 (Climatic Trends), acceleration of the anthropogenic forcing occurs shortly after 1960. Thus, for the purposes of comparing net warming between periods of different anthropogenic forcing, 1960 is a rational choice for the ending date of a reference period. It is not practical to choose a beginning date earlier than about 1900 because many model simulations begin in 1900 or 1901 and the uncertainties in the observational time series increase substantially prior to 1900. Therefore, the choice of 1901-1960 as the reference period is well suited for this purpose (comparing the net warming between periods of different anthropogenic forcing). However, there are some uncertainties in the suitability of the 1901-1960 reference period for this purpose. Firstly, there is greater uncertainty in the natural climate forcings (e.g., solar variations) during this time period than in the latter half of the 20th century. If there are sizeable errors in the estimated natural forcings used in climate models, then the simulations will be affected; this type of error does not represent a model deficiency. Secondly, the 1930s “Dust Bowl” era is included in this period. The excessive temperatures experienced then, particularly during the summers, are believed to be caused partially by poor land management through its effects on the surface energy budget. Climate models do not incorporate land management changes and there is no

expectation that models should simulate the effects of such. Thirdly, there are certain climate oscillations that occur over several decades. These oscillations have important effects on regional temperatures. A 60-year period is too short to sample entire cycles of some of these, and thus only represents a partial sampling of the true baseline climate.

Figure 31 shows observed (using the same data set as shown in Fig. 5) and simulated decadal mean annual temperature changes for the Southwest U.S. from 1900 to 2100, expressed as deviations from the 1901-1960 average. The observed rate of warming is similar to that of the models, with temperature values being contained within the envelope of 20th century modeled temperatures for the entire period.

For the spring and summer seasons (Fig. 32), observed temperatures for the 1930s are higher than any model simulation. The observed spring cooling from the 1930s to the 1970s is not in the envelope of the model simulations. For the summer and fall seasons, the observed temperatures are lower than most model simulations during the 1970s to 90s. The winter season contains the widest range of observational temperatures, being lower than any model simulation in the 1910s/20s and higher in the 1950s. However, the overall warming for the entire observational record is within the range of model simulations for all seasons.

The 21st century portions of the time series indicate that the simulated future warming is much larger than the observed and simulated temperature changes for the 20th century.

Observed and model-simulated decadal mean precipitation changes (using the same data set as shown in Fig. 8) can be seen in Fig. 33 for annual and Fig. 34 for seasonal values. The observed variability is generally greater than the model simulations. This leads to a number of individual observed decadal values being outside the envelope of the model simulations. This is particularly true of spring and fall where there are a few very large observed anomalies that are well outside the envelope of the model simulations. The 21st century portions of the time series show increased variability among the model simulations. It can be seen that the majority of the models simulate an overall decrease in precipitation annually, as well as for the spring and fall seasons.

The CMIP3 archive contains a total of 74 simulations of the 20th century, 40 simulations of the 21st century for the high (A2) emissions scenario, and 32 simulations of the 21st century for the low (B1) emissions scenario from a total of 23 different models (many models performed multiple simulations for these periods). An exploratory analysis of the entire archive was performed, limited to temperature and to the year as a whole. As before, the data were processed using 1901-1960 as the reference period to calculate anomalies.

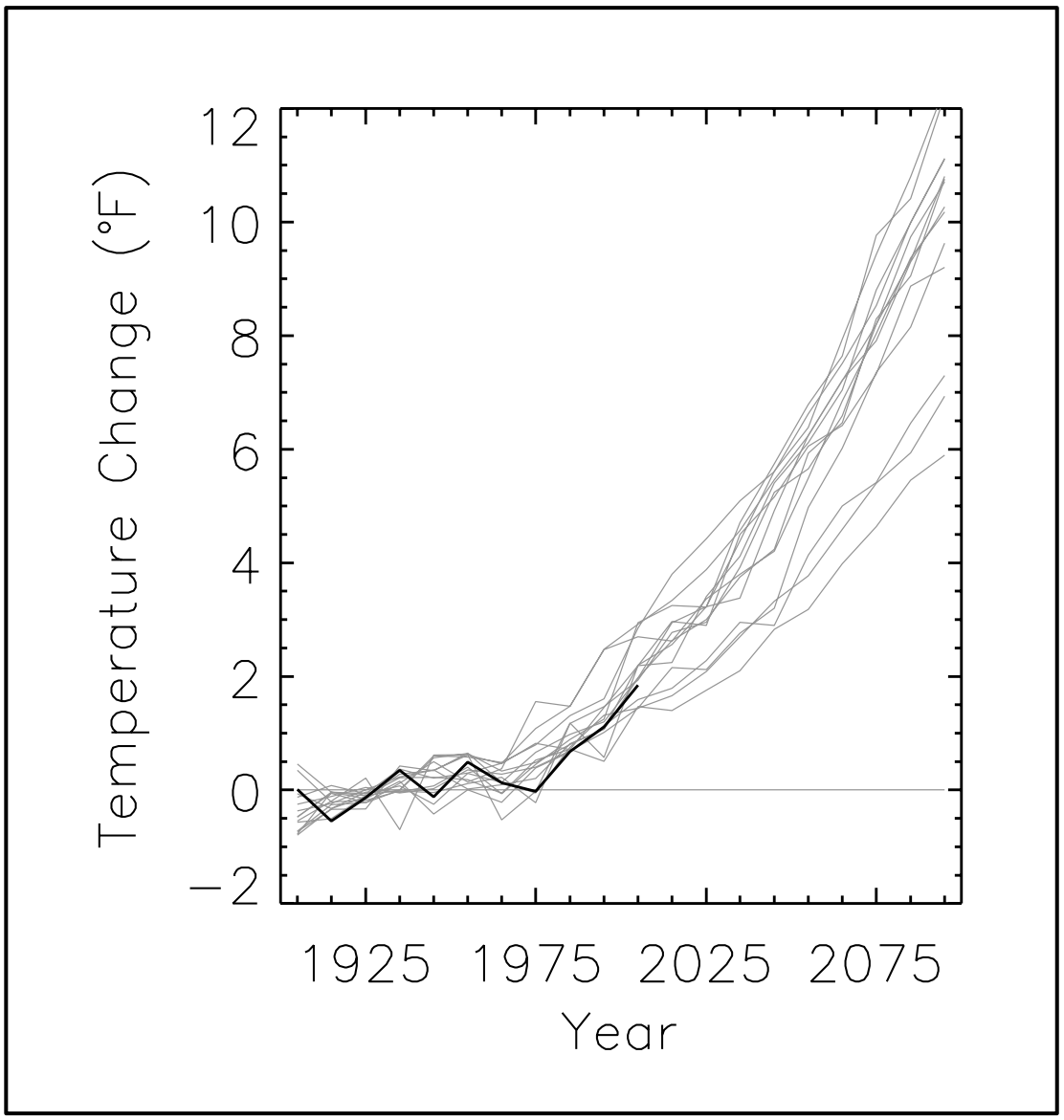

Figure 31. Observed decadal mean annual temperature change (deviations from the 1901-1960 average, °F) for the Southwest U.S. (black line Based on a new gridded version of COOP data from the National Climatic Data Center, the CDDv2 data set (R. Vose, personal communication, July 27, 2012). Gray lines indicate the 20th and 21st century simulations from 15 CMIP3 models, for the high (A2) emissions scenario. The observed rate of warming is within the envelope of model simulations.

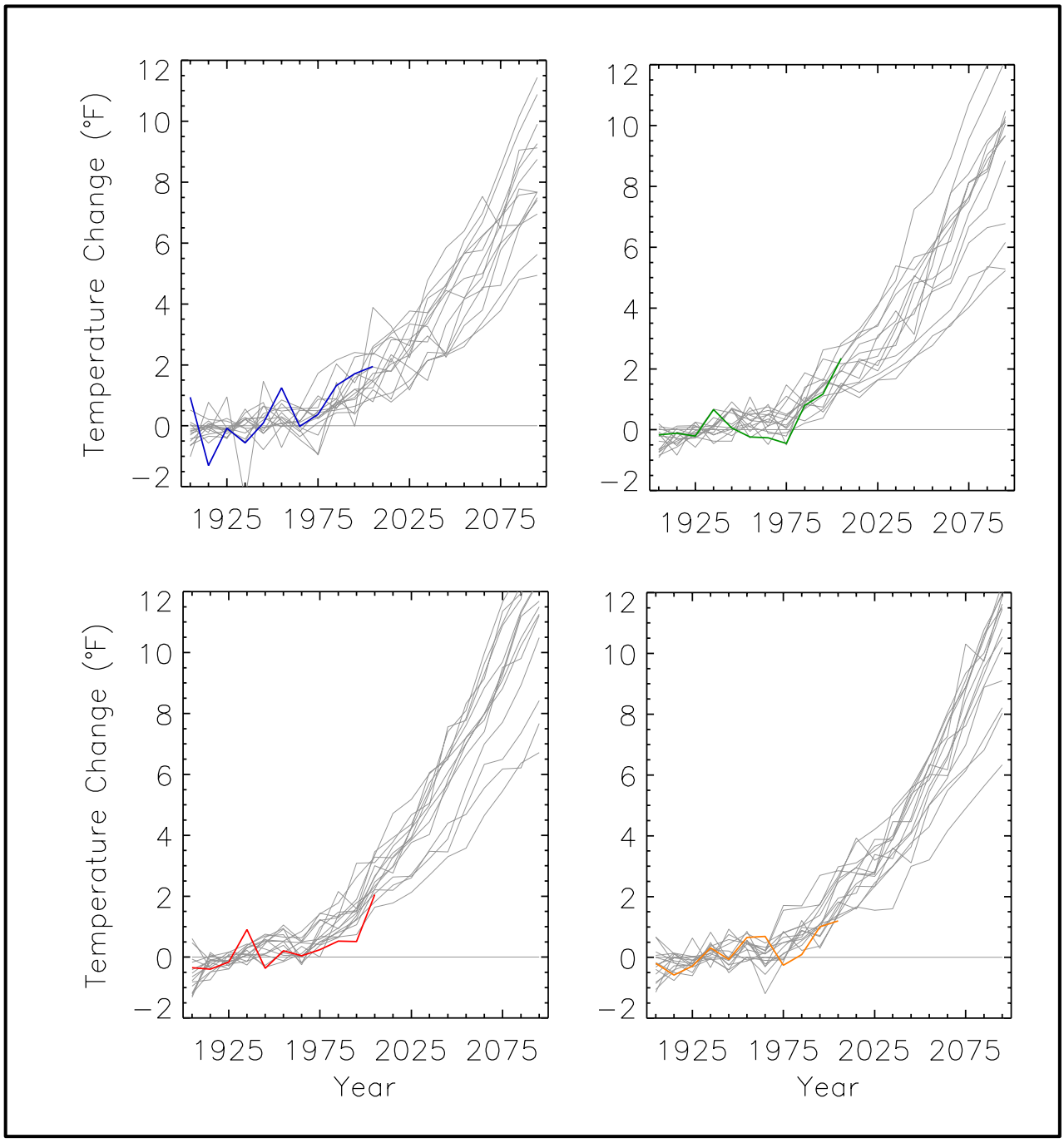

Figure 32. Observed decadal mean temperature change (deviations from the 1901-1960 average, °F) for the Southwest U.S. for winter (top left, blue line), spring (top right, green line), summer (bottom left red line), and fall (bottom right, orange line). Based on a new gridded version of COOP data from the National Climatic Data Center, the CDDv2 data set (R. Vose, personal communication, July 27, 2012). Gray lines indicate 20th and 21st century simulations from 15 CMIP3 models, for the high (A2) emissions scenario. The observed amount of 20th century warming is generally within the envelope of model simulations.

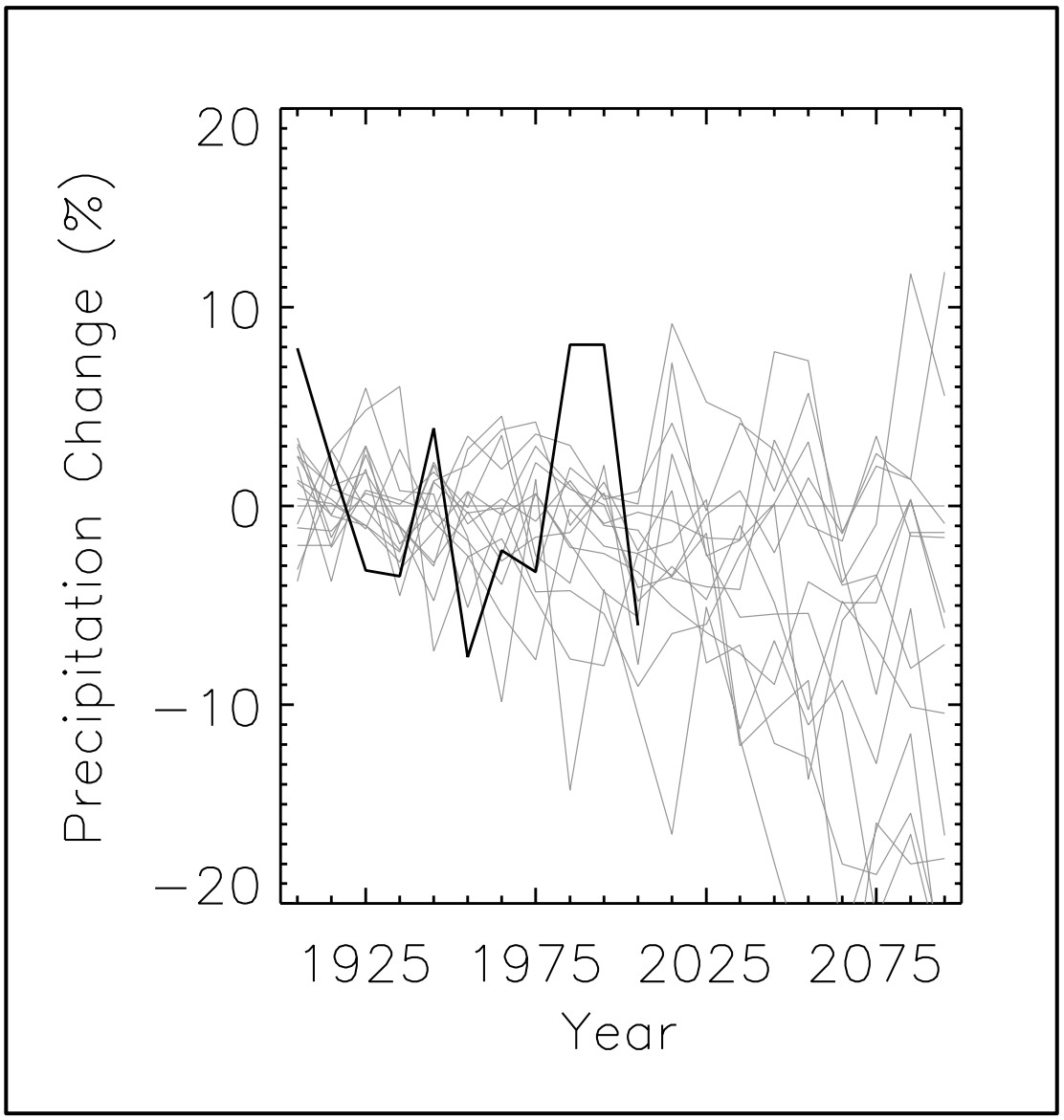

Figure 33. Observed decadal mean annual precipitation change (deviations from the 1901-1960 average, %) for the Southwest U.S. (black line Based on a new gridded version of COOP data from the National Climatic Data Center, the CDDv2 data set (R. Vose, personal communication, July 27, 2012). Gray lines indicate the 20th and 21st century simulations from 15 CMIP3 models, for the high (A2) emissions scenario. Observed precipitation variations show greater variability than the model simulations.

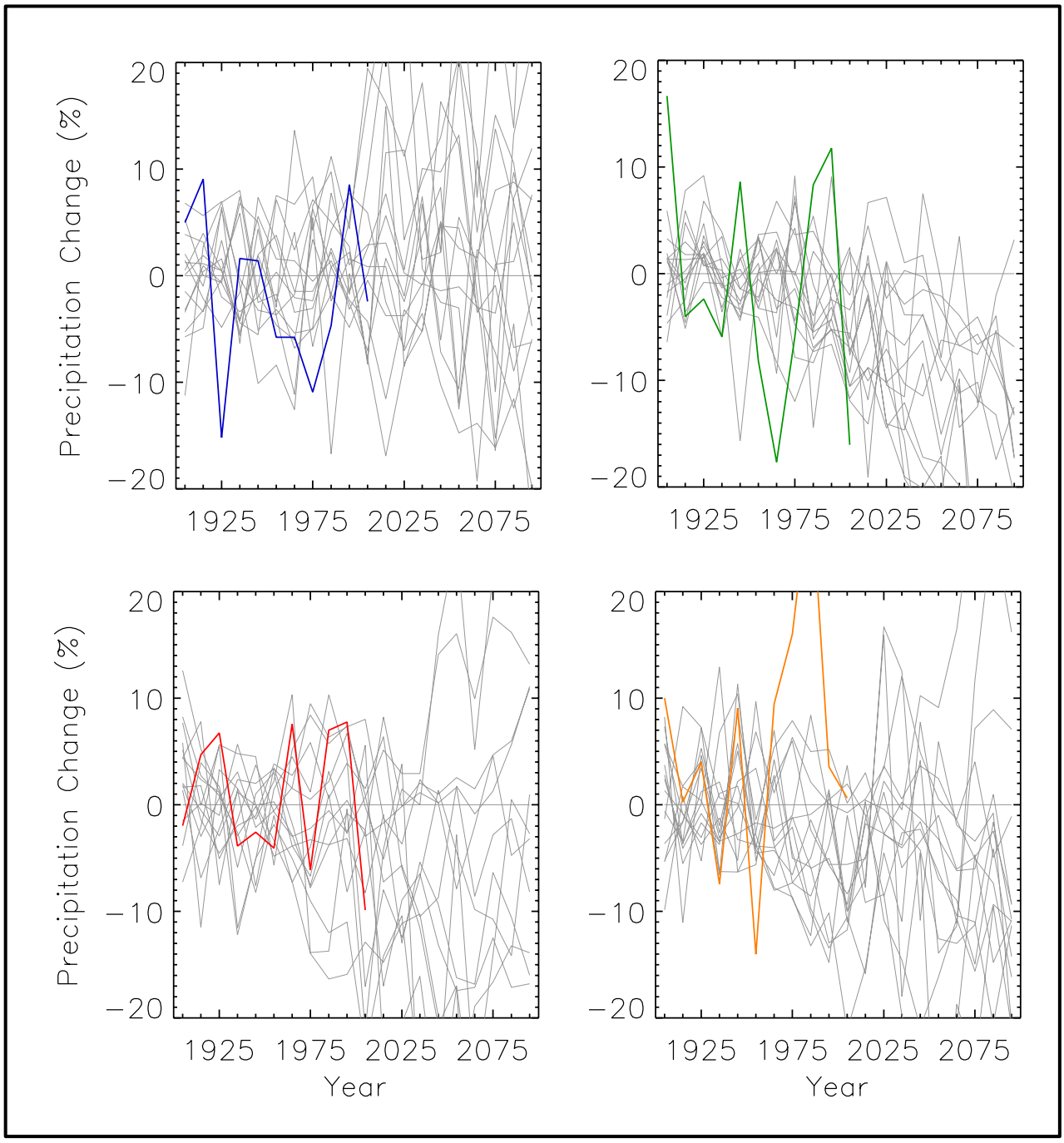

Figure 34. Observed decadal mean precipitation change (deviations from the 1901-1960 average, %) for the Southwest U.S. for winter (top left, blue line), spring (top right, green line), summer (bottom left red line), and fall (bottom right, orange line). Based on a new gridded version of COOP data from the National Climatic Data Center, the CDDv2 data set (R. Vose, personal communication, July 27, 2012). Gray lines indicate 20th and 21st century simulations from 15 CMIP3 models, for the high (A2) emissions scenario. Observed seasonal precipitation variations generally show greater variability than the model simulations for all seasons except summer.

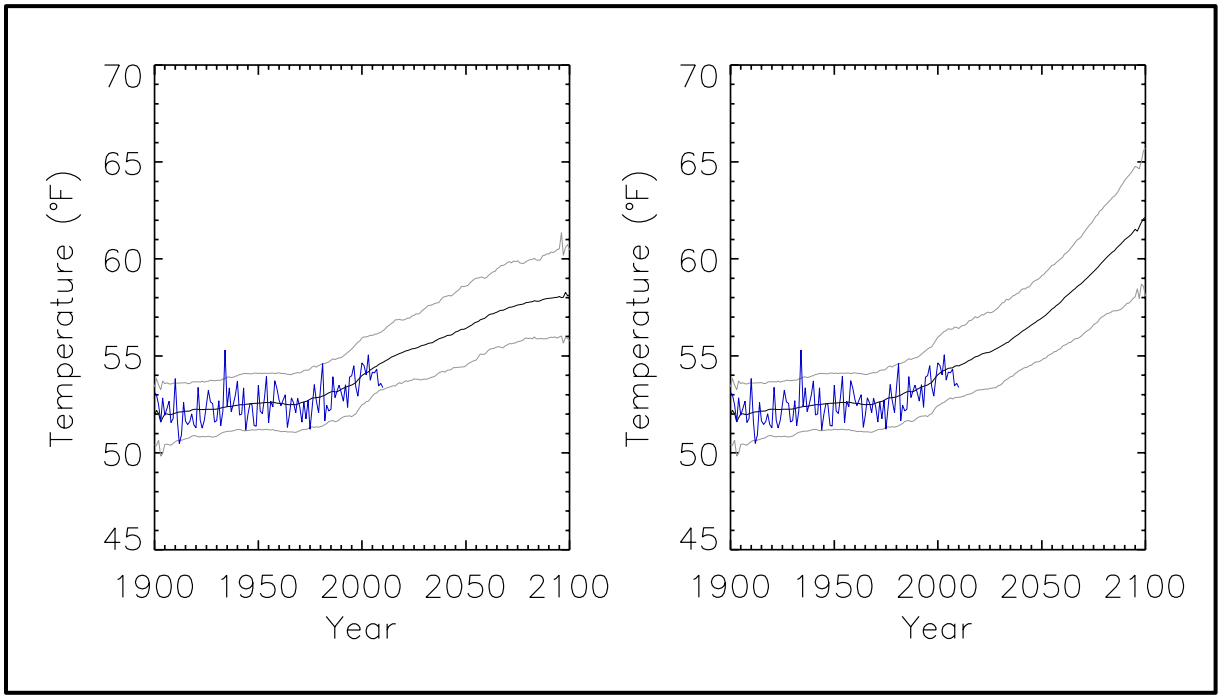

Figure 35. Time series of mean annual temperature for the Southwest region from observations (blue) and from all available CMIP3 global climate model simulations (black and grey). Black represents the mean and grey indicates the 5 and 95% limits of the model simulations. Model mean and percentile limits were calculated for each year separately and then smoothed. Results are shown for the low (B1) emissions scenario (left) and the high (A2) emissions scenario (right). A total of 74 simulations of the 20th century were used. For the 21st century, there were 40 simulations for the high emissions scenario and 32 for the low emissions scenario. For each model simulation, the annual temperature values were first transformed into anomalies by subtracting the simulation's 1901-1960 average from each annual value. Then, the mean bias between model and observations was removed by adding the observed 1901-1960 average to each annual anomaly value from the simulation. For each year, all available model simulations were used to calculate the multi-model mean and the 5th and 95th percentile bounds for that year. Then, the mean and 5th and 95th percentile values were smoothed with a 10-year moving boxcar average.

Figure 35 compares observations of annual temperature with the entire suite of model simulations. For each model, the annual anomalies were first calculated using the 1901-1960 period as the reference. Then the mean 1901-1960 value from the observations was added to each annual anomaly, essentially removing the model mean bias. In this presentation, the multi-model mean and the 5th and 95th percentile bounds of the model simulations are shown. The mean and percentile values were calculated separately for each year. Then, the curves were smoothed with a 10-year moving boxcar average. The observational time series is not smoothed. During the first half of the 20th century, the observed annual values vary around the model mean because that is the common reference period. These values occasionally fall outside the 5th/95th percentile bounds for the model simulations, most notably in 1934. After 1960, the observed values remain within the 5th/95th percentile bounds and vary around the model mean curve. The rate of observed warming after 1960 is similar to that of the multi-model mean, a similar result to that found in Fig. 31 for a subset of the CMIP3 models. One value is below the 5th percentile bound while none are above the 95th percentile bound after 1960.

On decadal time scales, climate variations arising from natural factors can be comparable to or larger than changes arising from anthropogenic forcing. An analysis of change on such time scales was performed by examining the decadal changes simulated by the CMIP3 models with respect to the most recent historical decade of 2001-2010. Figure 36 shows the simulated change in decadal mean values of annual temperature for each future decadal time period with respect to the most recent historical decade of 2001-2010, averaged over the entire Southwest region for the 14 (B1) or 15 (A2) CMIP3 models. For the 2011-2020 decade, the temperature increases are not statistically significant relative to the 2001-2010 decade for most of the models. As the time period increases, more of the individual models simulate statistically significant temperature changes, with all being significant at the 95% confidence level by 2035 for the high emissions scenario (2065 for the low emissions scenario). By this point, all of the model decadal mean values lie outside the 10-90th percentile range of the historical annual temperature anomalies. As also shown in Fig. 31, the model simulations show increased variability over time, with the inter-model range of temperature changes for 2091-2100 being more than double that for 2041-2050 (for the high emissions scenario).

The corresponding simulated change in decadal mean values of annual precipitation can be seen in Fig. 37. Unlike for temperature, many of the model values of precipitation change are not statistically significant in all decades out to 2091-2099. For the high (A2) emissions scenario (Fig. 37, top) positive changes in multi-model mean precipitation are simulated up to the 2041-2050 period, with negative changes indicated after this time. However, for the low (B1) emissions scenario (Fig. 37, bottom) increases in multi-model mean precipitation are simulated for all time periods. Little change in variability is seen over time for either scenario, with a large number of models lying outside the 10-90th percentile range for all time periods.

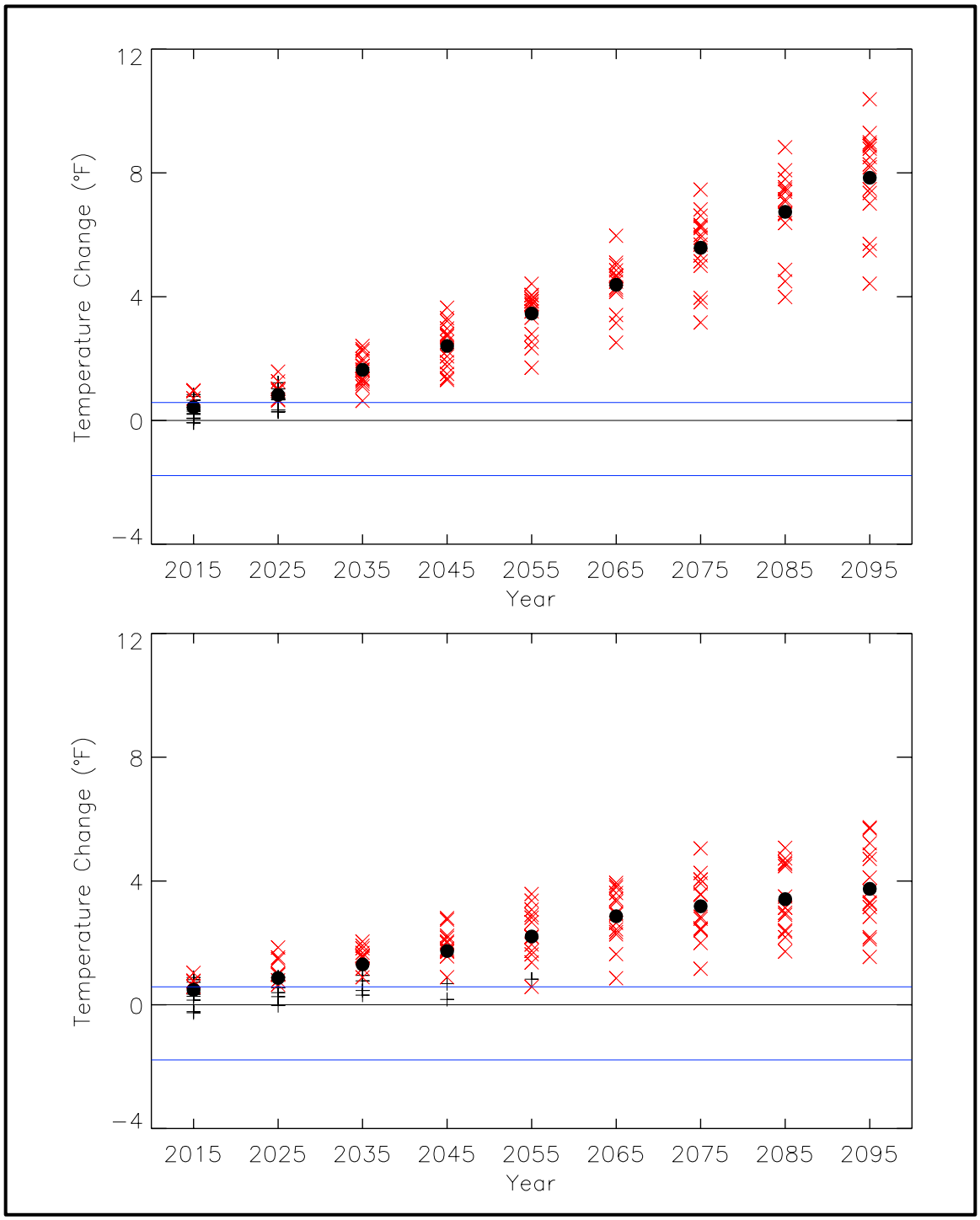

Figure 36. Simulated decadal mean change in annual temperature (°F) for the Southwest U.S. for each future decadal time period (represented by their approximate midpoints, e.g., 2015 = 2011-2020), with respect to the reference period of 2001-2010. Values are given for the high (A2, top) and low (B1, bottom) emissions scenarios for the 14 (B1) or 15 (A2) CMIP3 models. Large circles depict the multi-model means. Each individual model is represented by a black plus sign (+), or a red x if the value is statistically significant at the 95% confidence level. Blue lines indicate the 10th and 90th percentiles of 30 annual anomaly values from 1981-2010. The model simulated warming by 2015 is not statistically significant for most models, but by mid-21st century, all models simulate statistically significant warming.

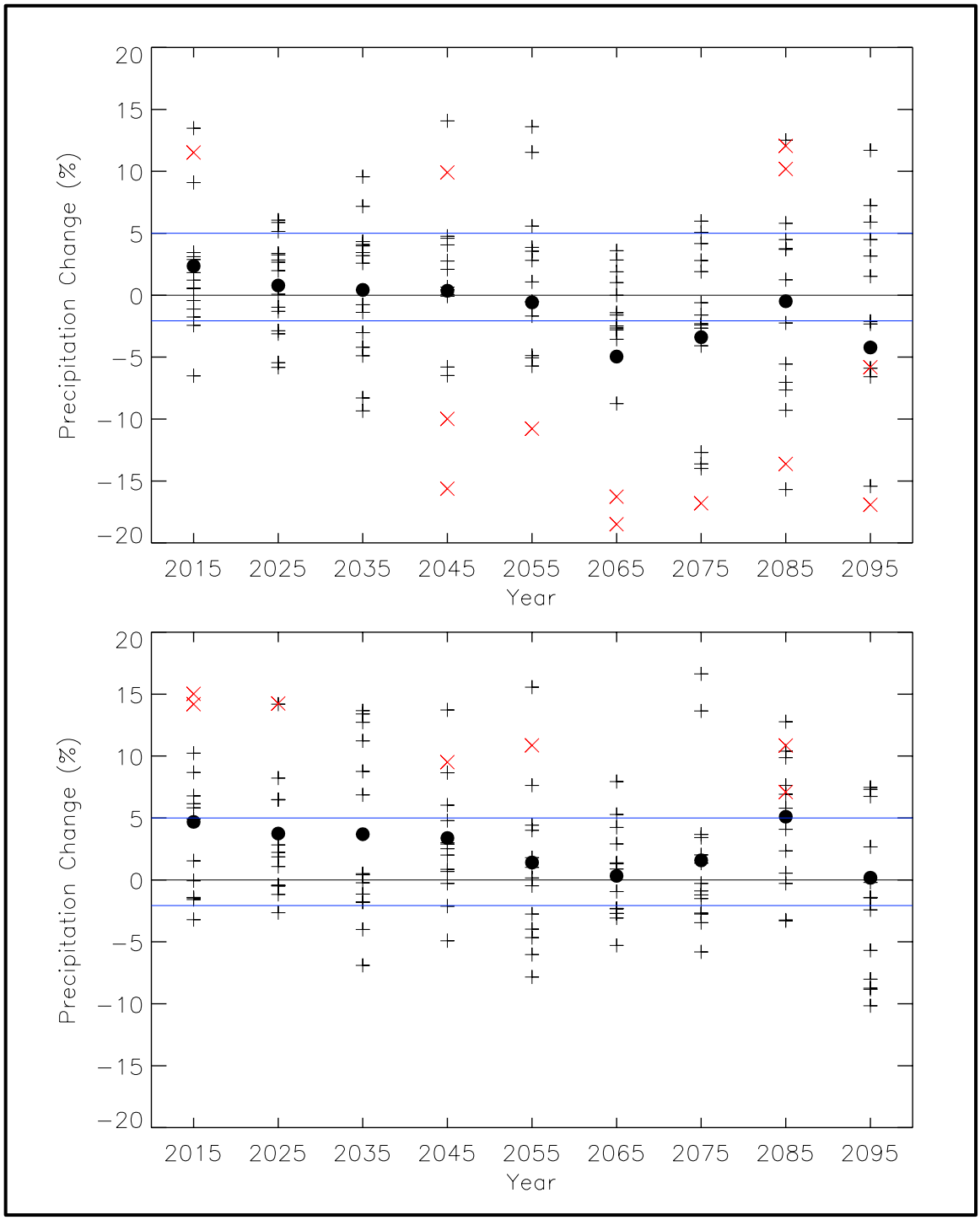

Figure 37. Simulated decadal mean change in annual precipitation (%) for the Southwest U.S. for each future decadal time period (represented by their approximate midpoints, e.g., 2015 = 2011-2020), with respect to the reference period of 2001-2010. Values are given for the high (A2, top) and low (B1, bottom) emissions scenarios for the 14 (B1) or 15 (A2) CMIP3 models. Large circles depict the multi-model means. Each individual model is represented by a black plus sign (+), or a red x if the value is statistically significant at the 95% confidence level. Blue lines indicate the 10th and 90th percentiles of the 30 annual anomaly values from 1981-2010. Many models simulate precipitation changes that are not statistically significant out to the end of the 21st century.

4. SUMMARY

The primary purpose of this document is to provide physical climate information for potential use by the authors of the 2013 National Climate Assessment report. The document contains two major sections. One section summarizes historical conditions in the Southwest U.S. and primarily focuses on trends in temperature and precipitation metrics that are important in the region. The core observational data set used is that of the National Weather Service's Cooperative Observer Network (COOP).

The second section summarizes climate model simulations for two scenarios of the future path of greenhouse gas emissions: the IPCC SRES high (A2) and low (B1) emissions scenarios. These simulations incorporate analyses from multiple sources, the core source being Coupled Model Intercomparison Project 3 (CMIP3) simulations. Additional sources consist of statistically- and dynamically-downscaled data sets, including simulations from the North American Regional Climate Change Assessment Program (NARCCAP). Analyses of the simulated future climate are provided for the periods of 2021-2050, 2041-2070, and 2070-2099), with changes calculated with respect to an historical climate reference period (1971-1999, 1971-2000, or 1980-2000). The resulting climate conditions are to be viewed as scenarios, not forecasts, and there are no explicit or implicit assumptions about the probability of occurrence of either scenario. The basis for these climate scenarios (emissions scenarios and sources of climate information) were considered and approved by the National Climate Assessment Development and Advisory Committee.

Some key characteristics of the historical climate include:

- Climatic phenomena that have major impacts on the Southwest include drought, heat waves, winter storms, and floods.
- Average annual temperature has generally increased over the past 115 years, with a rise in the 1920s and 1930s, a prolonged level period, and a second rise from the mid-1970s to around 2000. Temperatures have leveled since then, and the past 3 years have been cooler than recent averages. Daytime temperatures resemble the mean temperature time series, while nighttime temperatures show a somewhat steadier increase and little evidence of the cool mean temperatures seen in this region in the last 5 years.
- Seasonal patterns are similar to annual patterns, with the recent period of elevated temperatures being most prominent in the spring and summer. Temperature trends are upward and statistically significant (at the 95% level) for each season, as well as the year as a whole, with magnitudes ranging from +0.16 to +0.21°F per decade.
- The region experienced its wettest conditions in the 1980s and 1990s, coinciding with a shift in Pacific climate in 1976, after which El Niño became much more frequent, but has dried in the last decade.
- Precipitation does not exhibit any obvious long-term trends, except for fall, which shows a slight upward trend. Trends are not statistically significant for any season.
- There is an overall downward trend in occurrence of extreme cold periods that is statistically significant. The frequency of extreme heat waves has generally been increasing in recent decades, with a statistically significant upward trend.

- There is not a statistically significant trend in the occurrence of extreme precipitation events in the Southwest.
- Freeze-free season length has increased substantially and now averages about two weeks longer than during the 1960s and 1970s and a whole month longer than in the early part of the 20th century.

The climate characteristics simulated by climate models for the two emissions scenarios have the following key features:

- All three future time periods indicate an increase in temperature. Spatial variations are relatively small, with changes along coastal areas being smaller than inland areas. Warming tends to be slightly larger in the northern portion of the region. CMIP3 models indicate that temperature changes across the Southwest are statistically significant everywhere for all three future time periods and both emissions scenarios.
- Seasonal temperature changes show greater spatial variability. The greatest warming is seen in summer (3.5-6.5°F), with a localized maximum in central Utah.
- Simulated temperature changes are similar in value for the high and low emissions scenarios for early and mid-21st century, but largely different by late in the century.
- The range of model-simulated temperature changes is substantial, indicating substantial uncertainty in the magnitude of warming associated with each scenario. However, in each model simulation, the warming is unequivocal and large compared to historical variations. This is also true for all of the derived temperature variables described below.
- Simulated increases in the average annual number of days with maximum temperatures above 95°F are largest (more than 25 days) in southern and eastern areas (for the A2 scenario at mid-century). In interior southern areas, the average annual longest string of days above 95°F is simulated to increase by 20 days or more. Outside of very high elevation areas, the increases are generally in the range of 4-16 days.
- The interior north of the region is simulated to experience a large decrease (25 days or more) in the annual number of days with a minimum temperature below 10°F; in other areas, the number of such days in the current climate is small and thus changes are also small. Similarly, statistically significant decreases in the annual number of days with a minimum temperature of less than 32°F are simulated everywhere (for the A2 scenario at mid-century).
- The freeze-free period over the Southwest is simulated to increase on average by about a month by 2055, with the largest simulated increases (greater than 35 days) occurring in the interior of California (for the A2 scenario at mid-century).
- The hottest areas, such as southern California and Arizona, are simulated to have the largest increase (up to 1,000) of cooling degree days per year (for the A2 scenario at mid-century), while high elevation areas have the smallest simulated increases (around 200 or less).
- A decrease of at least 700 heating degree days per year is simulated for the entire region, with the exception of central and southern California and southern Arizona (for the A2 scenario at mid-century). The largest changes occur in higher elevation areas.

- The far southern regions show the largest decreases in average annual precipitation, while the far northern areas show slight increases. Statistically significant changes are simulated by most models late in the 21st century and under the high (A2) emissions scenario; however, while the models agree on drying in the south, they are in disagreement about the sign of the changes in the northern part of the region. The range of model-simulated precipitation changes is considerably larger than the multi-model mean change. Thus, there is great uncertainty associated with future precipitation changes in these scenarios.
- Most areas exhibit simulated increases in the average annual number of days with precipitation exceeding 1 inch, though some areas do show decreases (for the A2 scenario at mid-century). The largest increases are simulated to occur in western Colorado, Utah, and northern Nevada, with increases of more than 40%. However, these changes are not statistically significant.
- Areas that are already prone to little precipitation are simulated to see an increase of days with little or no precipitation (less than 0.1 inches) of up to 25 days per year in parts of Nevada, Arizona, and California (for the A2 scenario at mid-century). The decreases are statistically significant over most of the region.
- Most models do not indicate a statistically significant change in temperature (with respect to 2001-2010) for the next decade; however, as the time period increases, a greater number of models simulate statistically significant temperature changes, with all being significant at the 95% confidence level by 2035 (for the high emissions scenario).
- Many of the modeled values of decadal precipitation change are not statistically significant, with respect to 2001-2010, out to 2091-2099.

A comparison of model simulations of the 20th century with observations indicates the following:

- The observed rate of warming is similar to that of the models, with temperature values being contained within the envelope of 20th century modeled temperatures for the entire period. In particular, the observed acceleration of warming beginning in the 1980s is simulated by the models. Simulations of temperature in the 21st century indicate that future warming is much larger than the observed and simulated values for the 20th century.
- Observed variability of decadal mean precipitation is generally greater than the model simulations, leading to a number of individual observed decades being outside the envelope of the model simulations.

5. REFERENCES

AchutaRao, K., and K.R. Sperber, 2002: Simulation of the El Niño Southern Oscillation: Results from the Coupled Model Intercomparison Project. *Clim. Dyn.*, **19,** 191–209.

Arakawa, A., 2004: The cumulus parameterization problem: Past, present, and future. *J. Climate,* **17**, 2493-2525.

Bader D. C., C. Covey, W. J. Gutowski Jr., I. M. Held, K. E. Kunkel, R. L. Miller, R. T. Tokmakian, and M. H. Zhang, 2008: *Climate models: An Assessment of Strengths and Limitations*. U.S. Climate Change Science Program Synthesis and Assessment Product 3.1. Department of Energy, Office of Biological and Environmental Research, 124 pp.

Biondi, F., A. Gershunov, and D. R. Cayan, 2001: North Pacific decadal climate variability since 1661. *J. Climate,* **14,** 5-10.

Brown, D. P., and A. C. Comrie, 2002: Sub- regional seasonal precipitation linkages to SOI and PDO in the Southwest United States. *Atmos. Sci. Lett.*, **3,** 94-102.

Cayan, D. R., K. T. Redmond, and L. G. Riddle, 1999: ENSO and Hydrologic Extremes in the Western United States. *J. Climate,* **12,** 2881-2893.

Dettinger, M. D., F. M. Ralph, T. Das, P. J. Neiman, and D. R. Cayan, 2011: Atmospheric rivers, floods and the water resources of California. *Water,* **3,** 445-478.

Conil, S., and A. Hall, 2006: Local modes of atmospheric variability: A case study of southern California. *J. Climate*, **19**, 4308-4325.

Dettinger, M. D., and Coauthors, 2012: Design and quantification of an extreme winter storm scenario for emergency preparedness and planning exercises in California. *Nat. Hazards,* **60,** 1085-1111.

DRI, cited 2012: WestMap Climate Analysis & Mapping Toolbox. [Available online at http://www.cefa.dri.edu/Westmap/.]

Dufresne, J.-L., and S. Bony. 2008: An assessment of the primary sources of spread of global warming estimates from coupled ocean–atmosphere models. *J. Climate*, **21**, 5135-5144.

Ebbesmeyer, C. C., D. R. Cayan, D. R. McLain, F. H. Nichols, D. H. Peterson, and K. T. Redmond, 1991: 1976 step in the Pacific climate: Forty environmental changes between 1968-1975 and 1977-1984. *Seventh Annual Pacific Climate Workshop,* California Dept. of Water Resources, Interagency Ecological Studies Program Technical Report 26, 115-126.

Fall, S., A. Watts, J. Nielsen-Gammon, E. Jones, D. Niyogi, J. R. Christy, and R. A. Pielke Sr, 2011: Analysis of the impacts of station exposure on the US Historical Climatology Network temperatures and temperature trends. *J. Geophys. Res.*, **116,** D14120.

Gershunov, A., D. R. Cayan, and S. F. Iacobellis, 2009: The Great 2006 Heat Wave over California and Nevada: Signal of an Increasing Trend. *J. Climate,* **22,** 6181-6203.

Grissino-Mayer, H. D., and T. W. Swetnam, 2000: Century scale climate forcing of fire regimes in the American Southwest. *The Holocene*, **10,** 213-220.

Guido, Z., 2009: Past and present climate. *Southwest Climate Outlook, February 2009,* 3-5. [Available online at http://www.climas.arizona.edu/files/climas/pdfs/feature-articles/2009_feb_pastpresentclimate.pdf.]

Gutzler, D., and Coauthors, 2009: Simulations of the 2004 North American monsoon: NAMAP2. *J. Climate*, **22,** 6716-6740.

Hayhoe, K., and Coauthors, 2004: Emission pathways, climate change, and impacts on California. *P. Natl. Acad. Sci. USA*, **101,** 12422-12427.

Hayhoe, K., and Coauthors, 2008: Regional climate change projections for the Northeast USA. *Mitig. Adapt. Strateg. Glob. Change*, **13,** 425-436.

Hayhoe, K. A., 2010: A standardized framework for evaluating the skill of regional climate downscaling techniques. Ph.D. thesis, University of Illinois, 153 pp. [Available online at https://www.ideals.illinois.edu/handle/2142/16044.]

Higgins, W., and D. Gochis, 2007: Synthesis of results from the North American Monsoon Experiment (NAME) process study. *J. Climate*, **20,** 1601-1607.

Hirschboeck, K. K., 1988: Flood Hydroclimatology. *Flood Geomorphology*, V. R. Baker, R. C. Kockel, and P. C. Patton, Eds., John Wiley & Sons, 27–49.

Hubbard, K., and X. Lin, 2006: Reexamination of instrument change effects in the US Historical Climatology Network. *Geophys. Res. Lett.*, **33,** L15710.

Hughes, M., A. Hall, and J. Kim, 2009: *Anthropogenic Reduction of Santa Ana Winds*. California Energy Commission, 19 pp. [Available online at http://www.energy.ca.gov/2009publications/CEC-500-2009-015/CEC-500-2009-015-D.PDF.]

IPCC, 2000: *Special Report on Emissions Scenarios: A Special Report of Working Group III of the Intergovernmental Panel on Climate Change*, N. Nakicenovic, and R. Swart, Eds., Cambridge University Press, 570 pp.

——, 2007: *Climate Change 2007: Synthesis Report. Contribution of Working Groups I, II and III to the Fourth Assessment Report of the Intergovernmental Panel on Climate Change*, Pachauri, R. K, and Reisinger, A., Eds., IPCC, 104 pp.

——, cited 2012: IPCC Data Distribution Centre. [Available online at http://www.ipcc-data.org/ddc_co2.html.]

Jones, P. D., P. Y. Groisman, M. Coughlan, N. Plummer, W. C. Wang, and T. R. Karl, 1990: Assessment of urbanization effects in time series of surface air temperature over land. *Nature*, **347,** 169-172.

Kailes, J.I., 2008: *Southern California Wildfires After Action Report*. Prepared in partnership with the Access to Readiness Coalition, California Foundation for Independent Living Centers, and The Center for Disability Issues and the Health Professions at Western University of Health Sciences, 150 pp. [Available online at www.jik.com/CaliforniaWildfires.pdf.]

Karl, T. R., C. N. Williams Jr, P. J. Young, and W. M. Wendland, 1986: A model to estimate the time of observation bias associated with monthly mean maximum, minimum and mean temperatures for the United States. *J. Appl. Meteorol.*, **25,** 145-160.

Karl, T. R., H. F. Diaz, and G. Kukla, 1988: Urbanization: Its detection and effect in the United States climate record. *J. Climate*, **1,** 1099-1123.

Karl, T. R., J. M. Melillo, and T. C. Peterson, Eds, 2009: *Global Climate Change Impacts in the United States.* Cambridge University Press, 188 pp.

Knowlton, K., and Coauthors, 2009: The 2006 California heat wave: impacts on hospitalizations and emergency department visits. *Environ. Health Persp.*, **117,** 61-67.

Knutti, R., 2010: The end of model democracy? *Climatic Change*, **102,** 395-404.

Krawchuk, M.A., and M.A. Moritz, 2012: *Fire and Climate Change in California.* California Energy Commission. 50 pp. [Available online at http://www.energy.ca.gov/2012publications/CEC-500-2012-026/CEC-500-2012-026.pdf.]

LSU, cited 2012: Climate Trends. [Available online at http://charts.srcc.lsu.edu/trends/.]

Maddox, R. A., L. R. Hoxit, C. F. Chappell, and F. Caracena, 1978: Comparison of meteorological aspects of the Big Thompson and Rapid City flash floods. *Mon. Wea. Rev.*, **106,** 375-389.

Mantua, N. J., S. R. Hare, Y. Zhang, J. M. Wallace, and R. C. Francis, 1997: A Pacific interdecadal climate oscillation with impacts on salmon production. *Bull. Am. Meteorol. Soc.*, **78,** 1069-1080.

Maurer, E. P., A. W. Wood, J. C. Adam, D. P. Lettenmaier, and B. Nijssen, 2002: A long-term hydrologically based dataset of land surface fluxes and states for the conterminous United States. *J. Climate*, **15,** 3237–3251.

McCabe, G. J., M. A. Palecki, and J. L. Betancourt, 2004: Pacific and Atlantic Ocean influences on multidecadal drought frequency in the United States. *P. Natl. Acad. Sci. USA*, **101,** 4136-4141.

Meehl, G. A., W. M. Washington, T. M. L. Wigley, J. M. Arblaster, and A. Dai, 2003: Solar and greenhouse gas forcing and climate response in the twentieth century. *J. Climate*, **16,** 426-444.

Meehl, G. A., and Coauthors, 2007: Global climate projections. *Climate Change 2007: The Physical Basis. Contribution of Working Group I to the Fourth Assessment Report of the Intergovernmental Panel on Climate Change*, Solomon, S., D. Qin, M. Manning, Z. Chen, M. Marquis, K.B. Averyt, M. Tignor, and H.L. Miller, Eds., Cambridge University Press, 747-845.

Meko, D. M., C. A. Woodhouse, C. A. Baisan, T. Knight, J. J. Lukas, M. K. Hughes, and M. W. Salzer, 2007: Medieval Drought in the upper Colorado River Basin. *Geophys. Res. Lett.*, **34,** L10705.

Menne, M. J., C. N. Williams, and R. S. Vose, 2009: The US Historical Climatology Network monthly temperature data, version 2. *Bull. Am. Meteorol. Soc.*, **90,** 993-1007.

Menne, M. J., C. N. Williams, and M. A. Palecki, 2010: On the reliability of the U.S. surface temperature record. *J. Geophys. Res.*, **115,** D11108.

Michaud, J. D., K. K. Hirschboeck, and M. Winchell, 2001: Regional variations in small-basin floods in the United States. *Water Resour. Res.*, **37,** 1405-1416.

Miller, N.L., and N.J. Schlegel, 2006: Climate change projected fire weather sensitivity: California Santa Ana wind occurrence. *Geophys. Res. Lett.*, **33,** L15711.

Monahan, A.H., and A. Dai, 2004: The spatial and temporal structure of ENSO nonlinearity. *J. Climate*, **17,** 3026–3036.

NARCCAP, cited 2012: North American Regional Climate Change Assessment Program. [Available online at http://www.narccap.ucar.edu/.]

National Research Council, 1999: *Improving American River Flood Frequency Analysis.* National Academies Press, 113 pp.

Neiman, P. J., F. M. Ralph, G. A. Wick, J. D. Lundquist, and M. D. Dettinger, 2008: Meteorological characteristics and overland precipitation impacts of atmospheric rivers affecting the west coast of North America based on eight years of SSM/I satellite observations. *J. Hydrometeorol.*, **9,** 22-47.

NOAA, cited 2012a: Cooperative Observer Program. [Available online at http://www.nws.noaa.gov/om/coop/.]

——, cited 2012b: NCEP/DOE AMIP-II Reanalysis. [Available online at http://www.cpc.ncep.noaa.gov/products/wesley/reanalysis2/.]

Norton, C. W., P.-S. Chu, and T. A. Schroeder, 2011: Projecting changes in future heavy rainfall events for Oahu, Hawaii: A statistical downscaling approach. *J. Geophys. Res.*, **116,** D17110.

Null, J., and J. Hulbert, 2007: California Washed Away: The Great Flood of 1862. *Weatherwise*, **60,** 26-30.

NWS, 1993: Cooperative Program Operations. National Weather Service Observing Handbook No. 6, 56 pp. [Available online at http://www.srh.noaa.gov/srh/dad/coop/coophb6.pdf.]

Ostro, B. D., L. A. Roth, R. S. Green, and R. Basu, 2009: Estimating the mortality effect of the July 2006 California heat wave. *Environ. Res.*, **109,** 614-619.

Overland, J. E., M. Wang, N. A. Bond, J. E. Walsh, V. M. Kattsov, and W. L. Chapman, 2011: Considerations in the selection of global climate models for regional climate projections: The Arctic as a case study. *J. Climate*, **24,** 1583-1597.

PCMDI, cited 2012: CMIP3 Climate Model Documentation, References, and Links. [Available online at http://www-pcmdi.llnl.gov/ipcc/model_documentation/ipcc_model_documentation.php.]

Quayle, R. G., D. R. Easterling, T. R. Karl, and P. Y. Hughes, 1991: Effects of recent thermometer changes in the cooperative station network. *Bull. Am. Meteorol. Soc.*, **72,** 1718-1723.

Randall, D.A., and Coauthors, 2007: Climate models and their evaluation. *Climate Change 2007: The Physical Basis. Contribution of Working Group I to the Fourth Assessment Report of the Intergovernmental Panel on Climate Change*, Solomon, S., D. Qin, M. Manning, Z. Chen, M. Marquis, K.B. Averyt, M. Tignor, and H.L. Miller, Eds., Cambridge University Press, 590-662.

Raphael, M.N., 2003: The Santa Ana Winds of California. *Earth Interact.*, **7,** 1-13.

Redmond, K. T., and R. W. Koch, 1991: Surface climate and streamflow variability in the western United States and their relationship to large-scale circulation indices. *Water Resour. Res.*, **27,** 2381-2399.

Redmond, K. T., D. Stahle, M. Therrell, D. Cayan, and M. Dettinger, 2002: 400 Years of California Central Valley precipitation reconstructed from blue oaks. Preprint, *13th AMS Symposium on Global Change and Climate Variations,* Orlando, FL, 20-23.

Redmond, K. T., 2003: Climate variability in the intermontane West: Complex spatial structure associated with topography, and observational issues. *Water and Climate in the Western United States,* W. M. Lewis, Jr., Ed., University Press of Colorado, 29-48.

Tebaldi, C., J. M. Arblaster, and R. Knutti, 2011: Mapping model agreement on future climate projections. *Geophys. Res. Lett.*, **38,** L23701.

U.S. Census Bureau, cited 2011: Metropolitan and Micropolitan Statistical Areas. [Available online at http://www.census.gov/popest/data/metro/totals/2011/.]

Utah Department of Natural Resources, cited 2012: Great Salt Lake Information System. [Available online at http://www.greatsaltlakeinfo.org/.]

Vose, R. S., C. N. Williams, Jr., T. C. Peterson, T. R. Karl, and D. R. Easterling, 2003: An evaluation of the time of observation bias adjustment in the U.S. Historical Climatology Network. *Geophys. Res. Lett.*, **30,** 2046.

Weaver, J. F., E. Gruntfest, and G. M. Levy, 2000: Two floods in Fort Collins, Colorado: Learning from a natural disaster. *Bull. Am. Meteorol. Soc.*, **81,** 2359-2366.

Wilby, R. L., and T. Wigley, 1997: Downscaling general circulation model output: a review of methods and limitations. *Prog. Phys. Geog.*, **21,** 530.

Williams, C. N., M. J. Menne, and P. W. Thorne, 2011: Benchmarking the performance of pairwise homogenization of surface temperatures in the United States. *J. Geophys. Res.*, **52,** 154-163.

Woodhouse, C. A., 2003: A 431-yr reconstruction of western Colorado snowpack from tree rings. *J. Climate*, **16,** 1551-1561.

WRCC, cited 2012: North American Freezing Level Tracker. [Available online at http://www.wrcc.dri.edu/cwd/products/.]

6. ACKNOWLEDGEMENTS

6.1. Regional Climate Trends and Important Climate Factors

Document and graphics support was provided by Brooke Stewart of the Cooperative Institute for Climate and Satellites (CICS), and by Fred Burnett and Clark Lind of TBG Inc. Analysis support was provided by Russell Vose of NOAA's National Climatic Data Center (NCDC).

6.2. Future Regional Climate Scenarios

We acknowledge the modeling groups, the Program for Climate Model Diagnosis and Intercomparison (PCMDI) and the WCRP's Working Group on Coupled Modelling (WGCM) for their roles in making available the WCRP CMIP3 multi-model dataset. Support of this dataset is provided by the Office of Science, U.S. Department of Energy. Analysis of the CMIP3 GCM simulations was provided by Michael Wehner of the Lawrence Berkeley National Laboratory, and by Jay Hnilo of CICS. Analysis of the NARCCAP simulations was provided by Linda Mearns and Seth McGinnis of the National Center for Atmospheric Research, and by Art DeGaetano and William Noon of the Northeast Regional Climate Center. Additional programming and graphical support was provided by Byron Gleason of NCDC, and by Andrew Buddenberg and Jared Rennie of CICS.

A partial listing of reports appears below:

NESDIS 102 **NOAA Operational Sounding Products From Advanced-TOVS Polar Orbiting Environmental Satellites. Anthony L. Reale, August 2001.**

NESDIS 103 **GOES-11 Imager and Sounder Radiance and Product Validations for the GOES-11 Science Test. Jaime M. Daniels and Timothy J. Schmit, August 2001.**

NESDIS 104 **Summary of the NOAA/NESDIS Workshop on Development of a Coordinated Coral Reef Research and Monitoring Program. Jill E. Meyer and H. Lee Dantzler, August 2001.**

NESDIS 105 **Validation of SSM/I and AMSU Derived Tropical Rainfall Potential (TRaP) During the 2001 Atlantic Hurricane Season. Ralph Ferraro, Paul Pellegrino, Sheldon Kusselson, Michael Turk, and Stan Kidder, August 2002.**

NESDIS 106 **Calibration of the Advanced Microwave Sounding Unit-A Radiometers for NOAA-N and NOAA-N=. Tsan Mo, September 2002.**

NESDIS 107 **NOAA Operational Sounding Products for Advanced-TOVS: 2002. Anthony L. Reale, Michael W. Chalfant, Americo S. Allegrino, Franklin H. Tilley, Michael P. Ferguson, and Michael E. Pettey, December 2002.**

NESDIS 108 **Analytic Formulas for the Aliasing of Sea Level Sampled by a Single Exact-Repeat Altimetric Satellite or a Coordinated Constellation of Satellites. Chang-Kou Tai, November 2002.**

NESDIS 109 **Description of the System to Nowcast Salinity, Temperature and Sea nettle (*Chrysaora quinquecirrha*) Presence in Chesapeake Bay Using the Curvilinear Hydrodynamics in3-Dimensions (CH3D) Model. Zhen Li, Thomas F. Gross, and Christopher W. Brown, December 2002.**

NESDIS 110 **An Algorithm for Correction of Navigation Errors in AMSU-A Data. Seiichiro Kigawa and Michael P. Weinreb, December 2002.**

NESDIS 111 **An Algorithm for Correction of Lunar Contamination in AMSU-A Data. Seiichiro Kigawa and Tsan Mo, December 2002.**

NESDIS 112 **Sampling Errors of the Global Mean Sea Level Derived from Topex/Poseidon Altimetry. Chang-Kou Tai and Carl Wagner, December 2002.**

NESDIS 113 **Proceedings of the International GODAR Review Meeting: Abstracts. Sponsors: Intergovernmental Oceanographic Commission, U.S. National Oceanic and Atmospheric Administration, and the European Community, May 2003.**

NESDIS 114 **Satellite Rainfall Estimation Over South America: Evaluation of Two Major Events. Daniel A. Vila, Roderick A. Scofield, Robert J. Kuligowski, and J. Clay Davenport, May 2003.**

NESDIS 115 **Imager and Sounder Radiance and Product Validations for the GOES-12 Science Test. Donald W. Hillger, Timothy J. Schmit, and Jamie M. Daniels, September 2003.**

NESDIS 116 **Microwave Humidity Sounder Calibration Algorithm. Tsan Mo and Kenneth Jarva, October 2004.**

NESDIS 117 **Building Profile Plankton Databases for Climate and EcoSystem Research. Sydney Levitus, Satoshi Sato, Catherine Maillard, Nick Mikhailov, Pat Cadwell, Harry Dooley, June 2005.**

NESDIS 118 **Simultaneous Nadir Overpasses for NOAA-6 to NOAA-17 Satellites from 1980 and 2003 for the Intersatellite Calibration of Radiometers. Changyong Cao, Pubu Ciren, August 2005.**

NESDIS 119 **Calibration and Validation of NOAA 18 Instruments. Fuzhong Weng and Tsan Mo, December 2005.**

NESDIS 120 **The NOAA/NESDIS/ORA Windsat Calibration/Validation Collocation Database. Laurence Connor, February 2006.**

NESDIS 121 **Calibration of the Advanced Microwave Sounding Unit-A Radiometer for METOP-A. Tsan Mo, August 2006.**

NESDIS 122 JCSDA Community Radiative Transfer Model (CRTM). Yong Han, Paul van Delst, Quanhua Liu, Fuzhong Weng, Banghua Yan, Russ Treadon, and John Derber, December 2005.

NESDIS 123 Comparing Two Sets of Noisy Measurements. Lawrence E. Flynn, April 2007.

NESDIS 124 Calibration of the Advanced Microwave Sounding Unit-A for NOAA-N'. Tsan Mo, September 2007.

NESDIS 125 The GOES-13 Science Test: Imager and Sounder Radiance and Product Validations. Donald W. Hillger, Timothy J. Schmit, September 2007.

NESDIS 126 A QA/QC Manual of the Cooperative Summary of the Day Processing System. William E. Angel, January 2008.

NESDIS 127 The Easter Freeze of April 2007: A Climatological Perspective and Assessment of Impacts and Services. Ray Wolf, Jay Lawrimore, April 2008.

NESDIS 128 Influence of the ozone and water vapor on the GOES Aerosol and Smoke Product (GASP) retrieval. Hai Zhang, Raymond Hoff, Kevin McCann, Pubu Ciren, Shobha Kondragunta, and Ana Prados, May 2008.

NESDIS 129 Calibration and Validation of NOAA-19 Instruments. Tsan Mo and Fuzhong Weng, editors, July 2009.

NESDIS 130 Calibration of the Advanced Microwave Sounding Unit-A Radiometer for METOP-B. Tsan Mo, August 2010.

NESDIS 131 The GOES-14 Science Test: Imager and Sounder Radiance and Product Validations. Donald W. Hillger and Timothy J. Schmit, August 2010.

NESDIS 132 Assessing Errors in Altimetric and Other Bathymetry Grids. Karen M. Marks and Walter H.F. Smith, January 2011.

NESDIS 133 The NOAA/NESDIS Near Real Time CrIS Channel Selection for Data Assimilation and Retrieval Purposes. Antonia Gambacorta, Chris Barnet, Walter Wolf, Thomas King, Eric Maddy, Murty Divakarla, Mitch Goldberg, April 2011.

NESDIS 134 Report from the Workshop on Continuity of Earth Radiation Budget (CERB) Observations: Post-CERES Requirements. John J. Bates and Xuepeng Zhao, May 2011.

NESDIS 135 Averaging along-track altimeter data between crossover points onto the midpoint gird: Analytic formulas to describe the resolution and aliasing of the filtered results. Chang-Kou Tai, August 2011.

NESDIS 136 Separating the Standing and Net Traveling Spectral Components in the Zonal-Wavenumber and Frequency Spectra to Better Describe Propagating Features in Satellite Altimetry. Chang-Kou Tai, August 2011.

NESDIS 137 Water Vapor Eye Temperature vs. Tropical Cyclone Intensity. Roger B. Weldon, August 2011.

NESDIS 138 Changes in Tropical Cyclone Behavior Related to Changes in the Upper Air Environment. Roger B. Weldon, August 2011.

NESDIS 139 Computing Applications for Satellite Temperature Datasets: A Performance Evaluation of Graphics Processing Units. Timothy F.R. Burgess and Scott F. Heron, December 2011.

NESDIS 140 Microburst Nowcasting Applications of GOES. Kenneth L. Pryor, September 2011.

NESDIS 141 The GOES-15 Science Test: Imager and Sounder Radiance and Product Validations. Donald W. Hillger and Timothy J. Schmit, November 2011.

NOAA SCIENTIFIC AND TECHNICAL PUBLICATIONS

The National Oceanic and Atmospheric Administration **was established as part of the Department of Commerce on October 3, 1970. The mission responsibilities of NOAA are to assess the socioeconomic impact of natural and technological changes in the environment and to monitor and predict the state of the solid Earth, the oceans and their living resources, the atmosphere, and the space environment of the Earth.**

The major components of NOAA regularly produce various types of scientific and technical information in the following types of publications

PROFESSIONAL PAPERS – Important definitive research results, major techniques, and special investigations.

CONTRACT AND GRANT REPORTS – Reports prepared by contractors or grantees under NOAA sponsorship.

ATLAS – Presentation of analyzed data generally in the form of maps showing distribution of rainfall, chemical and physical conditions of oceans and atmosphere, distribution of fishes and marine mammals, ionospheric conditions, etc.

TECHNICAL SERVICE PUBLICATIONS – Reports containing data, observations, instructions, etc. A partial listing includes data serials; prediction and outlook periodicals; technical manuals, training papers, planning reports, and information serials; and miscellaneous technical publications.

TECHNICAL REPORTS – Journal quality with extensive details, mathematical developments, or data listings.

TECHNICAL MEMORANDUMS – Reports of preliminary, partial, or negative research or technology results, interim instructions, and the like.

U.S. DEPARTMENT OF COMMERCE
National Oceanic and Atmospheric Administration
National Environmental Satellite, Data, and Information Service
Washington, D.C. 20233